# “DEVELOPMENT OF A CONCEPT FOR THE AUTARKIC ENERGY AND WATER SUPPLY OF A HOUSING ESTATE IN AN AREA WITH HIGH AVERAGE SOLAR IRRADIATION”


TECHNISCHE UNIVERSITÄT WIEN

VIENNA UNIVERSITY OF TECHNOLOGY

INSTITUTE FOR THERMODYNAMICS AND ENERGY CONVERSION

**DANIEL PONS STRIGARI**


**MAY 2009**

*TECHNISCHE UNIVERSITÄT WIEN*

*Hinweise für die Abfassung der Master Thesis*

# *MASTER THESIS*

## *"DEVELOPMENT OF A CONCEPT FOR THE AUTARKIC ENERGY AND WATER SUPPLY OF A HOUSING ESTATE IN AN AREA WITH HIGH AVERAGE SOLAR IRRADIATION"*

*ausgeführt am Institut für Termodynamik und Energiewandlung*

*der Technischen Universität Wien*

*unterAnleitung von Ao.Univ. Prof.Dipl.-Ing. Dr.techn Karl PONWEISER*

*durch*

*PONS STRIGARI, Daniel,*

*von "Universidad Carlos III de Madrid"*

---------- ----------

*(Ort, Datum)* *(Unterschrift)*

# TABLE OF CONTENTS

# NOMENCLATURE

| Symbol | Units | Name/Description |
|---|---|---|
| $\dot{Q}u$ | [kJ/hr] | The useful energy gain of the LPC collector |
| $A_c$ | [$m^2$] | The collector area |
| $F_R(\tau\alpha)_n$ | [ ] | The efficiency with which solar radiation is absorbed by the plate and removed by fluid flowing through the collector |
| $I_t$ | [kJ/hr.m2] | The amount of solar radiation incident on the plane of the collector surface |
| $F_R U_L$ | [ ] | The collector loss rate |
| $\Delta T$ | [ºC] | A temperature difference |
| $R_{test}$ | [] | |
| $g_{test}$ | [kg/hr] | The mass flow rate of fluid flowing through the collector under test conditions |
| $C_{p\,fluid}$ | [kJ/kg.K] | The specific heat of the collector fluid |
| $F'U_L$ | [ ] | |
| $R_1$ | [ ] | |
| $N_{series}$ | [-] | The number of collectors in series |
| $N_{paralell}$ | [-] | The number of series collector strings in parallel |
| $\dot{m}_{fluid}$ | [kg/hr] | The mass flow rate of fluid flowing through the collector at any given time |
| $A_{aperture}$ | [$m^2$] | The area formed by the mouth of the parabolic reflector and the length of a single collector tube |
| *IAM* | [0..1] | The Incidence Angle Modifier; a dimensionless parameter that accounts for the collector's change in the transmittance absorptance product when the sun is not normal to the plane of the collector |
| $I_{beam}$ | [kJ/hr.m2] | The amount of beam solar radiation incident on the plane of the collector surface |
| *ConcRat* | [kg/hr] | |
| $T_{in}$ | [ºC] | The temperature of fluid entering the collector array |
| $T_{amb}$ | [ºC] | The ambient dry bulb temperature of the collector's surroundings |
| $T_{out}$ | [ºC] | The temperature of fluid exiting the collector array |
| $T_{max}$ | [ºC] | The maximum (user defined) temperature at which fluid may exit the collector array |
| $\dot{Q}_{dump}$ | [kJ/hr] | The amount of energy that had to be dumped from the outlet fluid stream in order to limit the collector outlet temperature, $T_{out}$ |
| $K_{kat}$ | [ ] | Incidence angle modifier |
| *conc* | [ ] | Collector concentration ratio |
| $Q_{HC}$ | [l/day] | Daily human consumption water flow |
| $Q_{Maint}$ | [l/day] | Daily maintenance water flow |
| $Q_{sp}$ | [l/day] | Daily swimming pool water flow |
| $Q_{ev+filt}$ | [l/day] | Daily evaporation and filtration water flow |
| $Q_{golf}$ | [l/day] | Daily golf course water flow |
| $ED_{desalination}$ | [kWh/day] | Daily electric demand for desalination plant |
| $ED_{AC}$ | [kWh/day] | Daily electric demand for standard air conditioning system |
| $ED_{Hot\_Water}$ | [kWh/day] | Daily electric demand for standard domestic hot water system |
| $h_i$ | [kJ/kg] | Enthalpy in point i |
| $s_i$ | [kJ/kg·K] | Entropy in point i |
| $T_i$ | ºC | Temperature in point i |
| $P_i$ | bar | Pressure in point i |
| $x_i$ | % | Title in point i |
| $x_{is}$ | % | Title in point I isentropic |
| $h_f$ | [kJ/kg] | Enthalpy saturated liquid |
| $h_{fg}$ | [kJ/kg] | Enthalpy of vaporization |
| $\eta_t$ | % | Turbine efficiency |
| $\dot{m}_1$ | [kg/s] | Working fluid flow rate |
| $\dot{W}_{demand}$ | [kJ/kg·s] | Power demanded from power plant |
| $\dot{W}_{pump}$ | [kJ/kg·s] | Power needed for pumps |
| $\dot{W}_{cycle}$ | [kJ/kg·s] | Power obtained by cycle |

| | | |
|---|---|---|
| $y$ | [ ] | Fraction of mass extracted from turbine stage |
| $\varepsilon$ | [ ] | Effectiveness |
| $\dot{Q}_{steam}$ | [kJ/kg·s] | Steam heat transfer |
| $\dot{Q}_{max}$ | [kJ/kg·s] | Maximum heat transfer |
| $\dot{m}_{steam}$ | [kg/s] | Steam mass flow |
| $Cp$ | [kJ/kg·K] | Specific heat |
| $NTU$ | [ ] | Number of transfer units |

# LIST OF FIGURES

# LIST OF TABLES

# LIST OF ABBREVIATIONS

| ABBREVIATION | MEANING |
|---|---|
| AC | Air Conditioning |
| CLFR | Compact Linear Fresnell Reflector |
| CPV | Concentrating Photovoltaics |
| CSP | Concentrating Solar Power |
| CST | Concentrating Solar Thermal |
| DHW | Domestic Hot Water |
| DLR | German Aerospace Center |
| DNI | Direct Normal Irradiation |
| ED | Electrodialisis |
| HCE | Heat Collector Element |
| HTF | Heat Transfer Fluid |
| IAM | Incident Angle Modifier |
| ICSS | Integral Collector Storage System |
| IST | Industrial Solar Technology |
| LFR | Linear Fresnell Reflector |
| MD | Membrane Distillation |
| ME=MED | Multiple Effect Evaporator |
| MSF | Multi-Stage Flash |
| MVC | Mechanical Vapor Compression |
| PCM | Phase Change Materials |
| PSA | Almería Solar Platform |
| PV | Photovoltaic |
| RES | Renewable Energy Sources |
| RO | Reverse Osmosis |
| SEGS | Solar Energy Generating System |
| TES | Thermal Energy Storage |
| TRNSYS | Transient Energy System Simulation |
| TVC | Thermal Vapor Compression |
| UNICEF | United Nations Children's Funds |
| VC | Vapor Compression |
| VVC | Vacuum Vapor Compression |
| WHO | World Health Organization |

# 1. INTRODUCTION

In many occasions, regions of the world that receive a noticeably high amount of daily solar irradiation are situated far away from conventional energy supplies. Therefore, in these areas it seems obvious to contemplate the possibility of establishing an autarkic solar energy based power generation plant in order to generate electricity as well as the means to accumulate solar thermal energy for other valuable uses such as hot water for housing, desalination plants, etc.

In the present document, we aim to satisfying the energy and water demands of a housing estate in the South Moroccan city of Dahkla (23°43′N 15°57′W(1)). It is a residential area intended for 5.000 families to live in all year round. They shall have both electrical needs and water supplies covered. The electrical demand levels fulfil the standard levels according to developed countries. As for the water supplies, they include basic human consumption as well as landscaping and leisure time activities (such as swimming pools, etc) and should be obtained by processing ocean water through a desalination plant.

The use of renewable energies not only pursues the goal of an autarkic system, but also offers an environmentally friendly option (zero emission systems) and permits a more sustainable global development in the world. Such layouts follow the Kyoto Protocol restrictions due to the virtually nil greenhouse effect gas generation.

In order to decide on the system we wish to implement, various technological possibilities are analyzed in order to properly choose the most pertinent model. The economical aspects have only been taken into account roughly, on a broader scale. Our project is more centred in the purely technological field.

Once we have chosen the specific disposition of our system, we proceed with the modelling of the latter, using the computer software TRNSYS. This program is a transient systems simulation program with a modular structure. It recognizes a system description language in which the user specifies the components that constitute the system and the manner in which they are connected. It is a commercial software package developed at the University of Wisconsin. As in every simulation, we contrast the results obtained with the data calculated on theoretical grounds.

Conclusively, we suggest a possible model that could be followed to achieve the meeting of the system demands previously mentioned.

# 2. ANALYSIS OF DIFFERENT AVAILABLE TECHNOLOGIES FOR VARIOUS SYSTEM POSSIBILITIES.

## 2.1 SOLAR COLLECTORS

### 2.1.1 Non-Concentrated Thermal Collector Types

This type of collector refers to the model that receives solar rays directly from the sun. The ray's trajectory is not modified and the energy per unit of surface is not intensified. Therefore, their usual working temperatures are lower as when concentrated.

#### 2.1.1.1 Flat Plate Collectors

A typical flat-plate collector is a metal box with a glass or plastic cover (glazing) on top and a dark-colored absorber plate on the bottom. The sides and bottom of the collector are usually insulated to minimize heat loss.

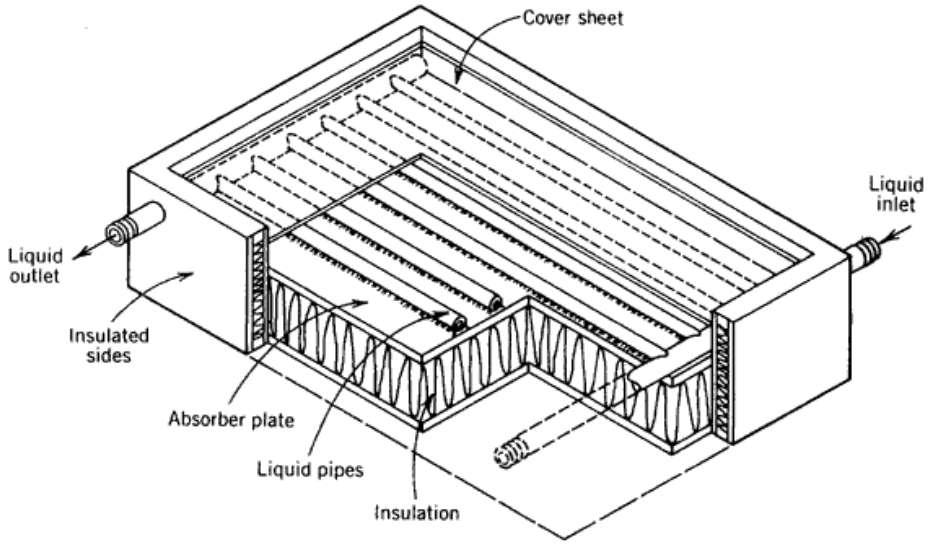


**Figure 1:** A typical flat-plate collector [1]

Sunlight passes through the glazing and strikes the absorber plate, which heats up, thus transforming solar energy into heat energy. The heat is transferred to liquid passing through pipes attached to the absorber plate. Absorber plates are commonly painted with "selective

coatings," which absorb and retain heat better than ordinary black paint. Absorber plates are usually made of metal—typically copper or aluminum—because the metal is a good heat conductor. Copper is more expensive, but is a better conductor and less prone to corrosion than aluminum. In locations with average available solar energy, flat plate collectors are sized approximately one-half- to one-square foot per gallon of one-day's hot water use.

Applications: This technology is primarily used in residential buildings, where the demand of hot water has a noticeable impact on the energy bill and where the temperatures required are not very high (~75-100ºC).

#### 2.1.1.2 Evacuated-tube Collectors

Evacuated solar collectors (tubes) operate differently than the other collectors available on the market. The basic idea is that the solar collectors consist of a heat exchanger inside a vacuum-sealed tube. The collectors are usually made of parallel rows of transparent glass tubes. Each tube contains a glass outer tube and metal absorber tube attached to a fin. The fin is covered with a coating that inhibits radiative heat loss. Air is evacuated from the space between the two glass tubes to form a vacuum, which eliminates conductive and convective heat loss. The vacuum tube envelope therefore minimizes heat loss and ensures high collector durability and steady performance.

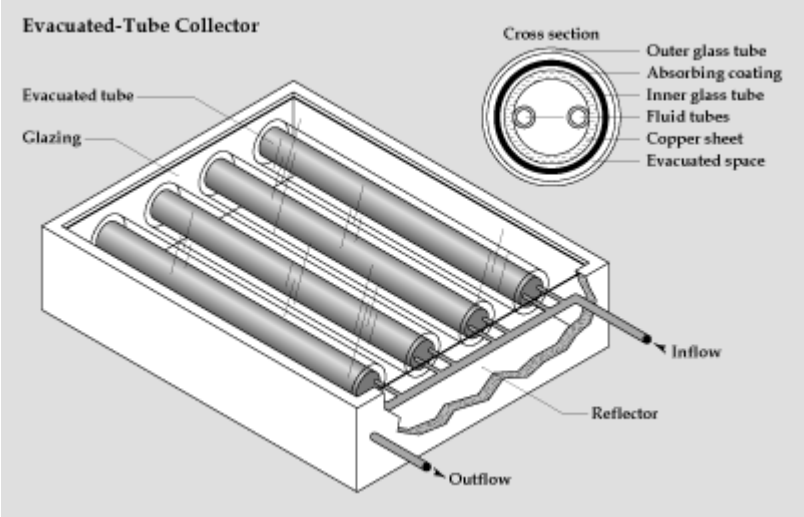


**Figure 2**: Evacuated-tube collectors are efficient at high temperatures [2]

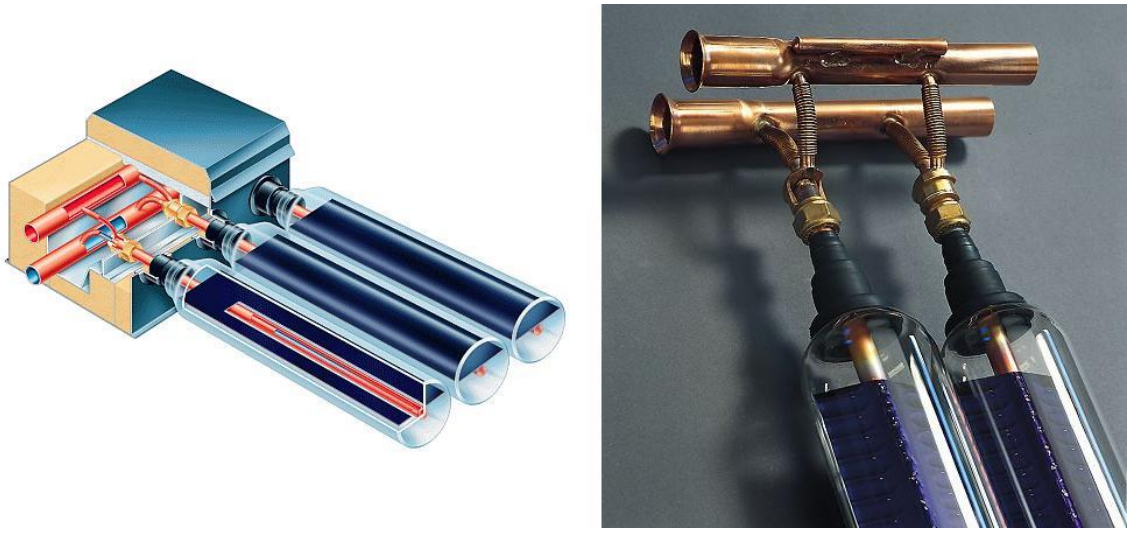

**Figure 3: H**igh efficiency vacuum tube collectors (Vitosol 200-T)[3]

The "dewar" design features a vacuum contained between two concentric glass tubes, with the absorber selective coating on the inside tube. Water is typically allowed to thermosyphon down and back out the inner cavity to transfer the heat to the storage tank. There are no glass-to-metal seals. As one could imagine, evacuated tube collectors are more expensive that flat-plate collectors, on an approximate 2:1 ratio per unit of surface although this type of evacuated tube has the potential to become cost-competitive with flat plates.

Applications: The temperatures that can achieved are much higher (~80-180ºC), making them more appropriate for industrial or cooling applications.

#### 2.1.1.3 Integral collector-storage system

Integral collector-storage systems (ICS), also known as "batch" systems, consists of one or more storage tanks placed inside an insulated box that has a glazed side facing the sun. Cold water first passes through the solar collector, which preheats the water, and then continues to the conventional backup water heater.

ICS systems are simple, reliable solar water heaters. However, they should be installed only in climates with mild freezing because the collector itself or the outdoor pipes could freeze in severely cold weather. Nonetheless, problem with freezing pipes can be overcome in some cases by using freeze-tolerant piping in conjunction with a freeze-protection method. Because the storage tank and the solar absorber act as a single unit, there is no need for other components. On an area basis, batch collector systems are less costly than glazed flat-plate collectors but also deliver less energy per year.

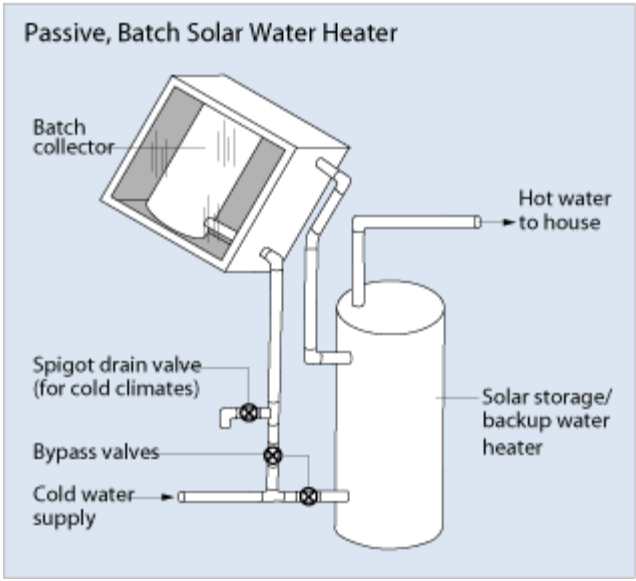


**Figure 4**: Passive batch solar water heater [4]

Cold water enters a pipe and can either enter a solar storage/backup water heater tank or the batch collector, depending on which bypass valve is opened. If the valve to the batch collector is open, a vertical pipe (which also has a spigot drain valve for cold climates) carries the water up into the batch collector. Water is heated in this tank, and another pipe takes the heated water from the batch collector into the solar storage/backup water heater, where it is then carried to the consumer, for example a house.

Applications: This system is generally used for small domestic hot water installations. The temperatures reached generally don't surpass ~100ºC.

### 2.1.2 Concentrated Collector Types

In these models, as opposed to the ones included before, the sun rays are concentrated into one designated area. This entails higher temperatures and broader uses for the heat achieved as the exergy also increases.

#### 2.1.2.1 Parabolic Trough

A parabolic trough is one of the types of solar thermal energy collectors that exist. It is constituted by a long parabolic mirror through which's focal point runs a Dewar tube. Due to their parabolic shape, this mirror reflects and concentrates the sunlight directly upon the receiver tube, focusing the sun at ~80 times its normal intensity. The trough is usually aligned on a north-south axis, and rotated to track the sun as it moves across the sky each day. Alternatively

the trough can be aligned on an east-west axis; this reduces the overall efficiency of the collector, due to cosine loss, but only requires the trough to be aligned with the change in seasons, avoiding the need for tracking motors. In any case, the latter are used to increase efficiencies.

The concentrated energy is absorbed by a heat transfer fluid (HTF), usually oil that flows through the Dewar tube. This fluid is then used to generate steam which powers a standard turbine generator.

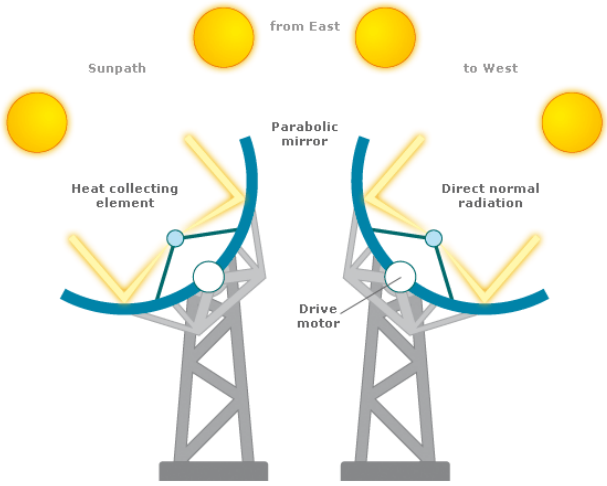


**Figure 5**: Parabolic trough following sunpath [5]

The process itself is economical and, for heating the pipe, thermal efficiency ranges from 60 to 80%. The overall efficiency from collector to grid, i.e. (Electrical Output Power)/(Total Impinging Solar Power) is about 20-25%.

The basic component of a parabolic trough solar field is the solar collector assembly or SCA. A solar field consists of hundreds or potentially thousands of solar collector assemblies. Each solar collector assembly is an independently tracking, parabolic trough solar collector composed of the following key subsystems:

- Concentrator metal support structure
- Mirrors or reflectors
- Linear receiver or heat collection element
- Tracking systems

The initial installation cost of parabolic trough solar collectors constitutes the main ingredient in the final cost of electricity produced by the power plant. And the main sources of cost (over

80%) of the collectors are the following: the metal support structure, the parabolic mirror, the receiver (heat collector element, HCE), and the tracking system

**Concentrator metal support structure (29%)**

This is the structure, usually composed of steel beams and rods, which gives and maintains the parabolic form of the mirrors. Because the mirror itself is not geometrically rigid, the rigidity of the parabolic form wholly relies on the support structure. The technical difficulty is important due to the requirements on optical precision and wind resistance. Despite the heavy structure (up to 20kg per m2 of opening), material is only a very small fraction of the total cost. This structure needs careful design, and has to be assembled, installed and aligned on the field. All these explain the high labor cost.

Improvements in the structural support system have received much attention as the collector assembly is the most expensive part of the system. SolarGenix, the contractor for two new American plants has developed a new structural support system for the collector. The design uses an aluminum frame superior in terms of structural properties, weight, manufacturing simplicity, corrosion resistance, manufactured cost and installation ease.

**Figure 6**: Parabolic concentrator metal support structure [6]

One key point of the design of the structure is that it has to have extreme tolerances and structural rigidity in order to focus the mirrors precisely on the receiver pipe. High resistance to large wind loadings on the large structure is a very important parameter.

Solargenix used computer modeling techniques that were unavailable at the time when the first designs were made. FLAGSOL Gmbh, who supplied all the collector assemblies at the California plants is supplying the trough assembly for Solar Millenium, has gone through a similar development process to develop a new steel structure. The collector assembly has been tested at the Kramer Junction SEGS plants in California.

**Mirrors or reflectors (19%)**

The parabolic mirror is pieced up from several curved glass mirrors fixed on the support structure. Again, it is the production cost that largely dominates, with the obvious technical difficulty of forming the curved glass with precision. This inevitably limits the concentration ratio and the efficiency of the collector.

**Figure 7**: Parabolic mirrors [7]

Development efforts are aimed at reducing the thickness of the mirror, improving the reliability of the glass to metal seal, surface coatings on the mirrors to improve their performance and development of a composite concentrator modules with lightweight, front-surface mirrors instead of heavy (4 mm) glass mirrors that were originally used on the original SEGS plants.

Industrial Solar Technology Company (IST) has developed a concentrator system that incorporates the reflective surface as part of the collector structure. This results in a very lightweight, low-cost concentrator module that is also very strong.

**Linear receivers or heat collection elements (HCE) (20%)**

The heat collection element (HCE) is composed of a stainless steel pipe with a glass tube surrounding it, with the space between evacuated to provide low thermal losses from the pipe. The pipe is coated with a material that improves the absorption of solar energy. The receiver collects the solar radiations reflected by the mirror, and transforms the energy into the heat conveyed out by the heat transfer fluid (HTF) that flows in the inner tube. It is the most sensitive part of the trough, with two main difficulties: the selective coating with maximal absorptivity and minimal emissivity, and the metal to glass hermetic sealing to maintain the vacuum between the two tubes. The HCE is also a huge maintenance problem, with its high rate of failures, leaks and breaks. The cost of the selective coating, as well as radiative heat loss, should be independent to the size of the trough. On the other hand, the cost of the sealing

will clearly increase if the size of the trough is decreased. Conductive heat loss will also increase with decreasing size (see the section on the receiver).

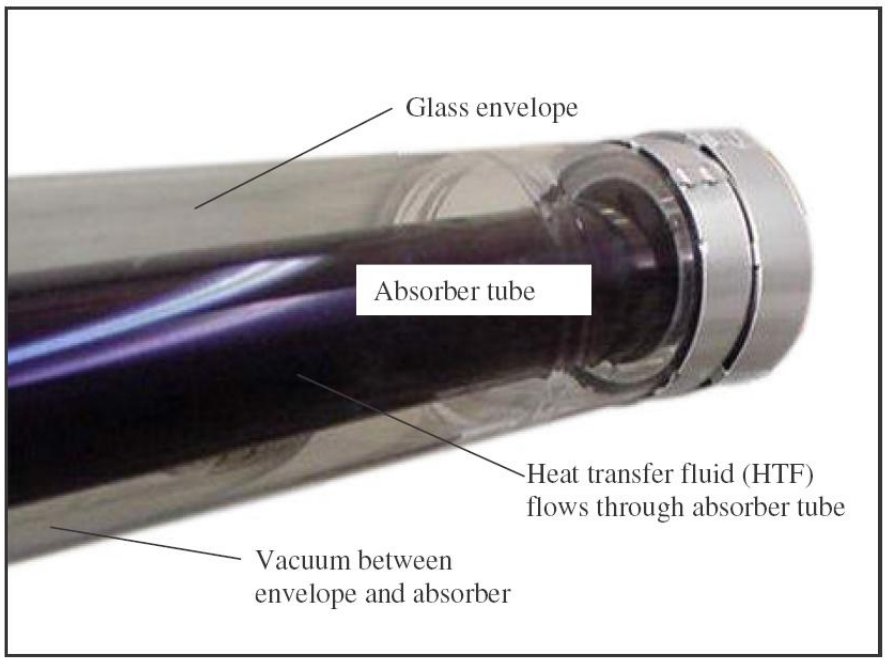


**Figure 8**: Heat Collection Element (HCE) [8]

**Tracking systems (controller and drive, 13%)**

It is the mechanism that constantly maintains the orientation of the mirrors towards the moving sun. This part clearly has a huge cost reduction potential.

The Plataforma Solar de Almería (PSA), the European Test Center for Solar Energy Applications, in southeastern Spain is Europe's test facility for concentrating solar power development. They are developing direct steam generation technology to eliminate the thermal oil system that is currently used in solar trough plants, which would greatly simplify the plants. PSA is also developing new trough collector assemblies and coatings to improve the absorption of solar energy on the receiver tubes and to decrease the reflectivity of glass.

Applications: As it has been already mentioned, the main use for the parabolic troughs is to generate power from a Rankine power plant. The temperatures reached with this procedure are around 390ºC. The power that is possible to generate goes from 20MW to almost 200MW.

#### 2.1.2.2 Solar Tower/Central Receiver

In this concentrating solar power (CSP) technology, there is a single receiver placed on top of a tower surrounded by hundreds of large, flat, mirrors (heliostats) which follow the apparent

motion of the sun in the sky and which re-direct and focus the sunlight onto the receiver. The heliostats are provided with a two-axis tracking system. A heat-transfer fluid heated in the receiver is used to generate steam, which, in turn, is used in a conventional turbine generator to produce electricity. Some power towers use water/steam as the heat-transfer fluid. Other advanced designs are experimenting with molten nitrate salt because of its superior heat-transfer and energy-storage capabilities. If a gas or even air is pressurised in the receiver, it can be used alternatively to drive a gas turbine (instead of producing steam for a steam turbine). For gas turbine operation, the air to be heated must first pass through a pressurised solar receiver with a solar window.

**Figure 9**: Power tower power plant [9]

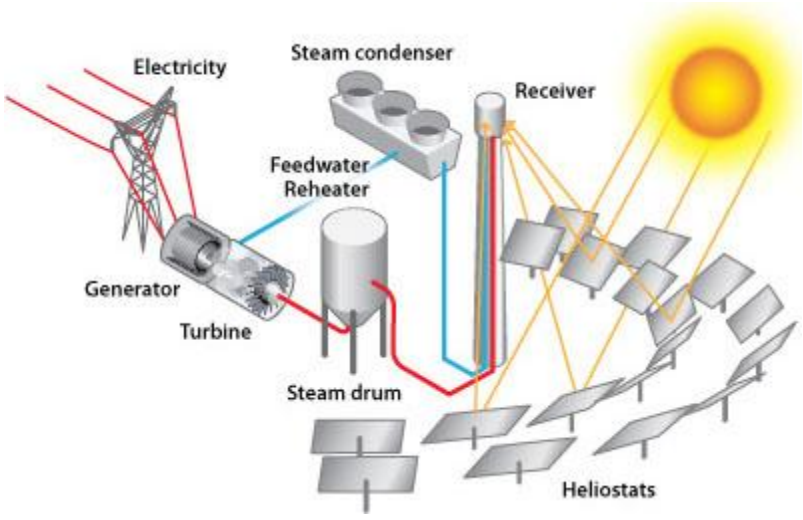


**Figure 10**: Schematics of a power tower plant **[10]**

"Solar Two" plant, a retrofit of Solar One plant built in 1982 near Barstow, California, demonstrated the advantages of molten salt for heat transfer and thermal storage. Using its highly efficient molten-salt energy storage system, Solar Two successfully demonstrated efficient collection of solar energy and dispatch of electricity. It also demonstrated the ability to

routinely produce electricity during cloudy weather and at night. In one demonstration, Solar Two delivered power to the grid for 24 hours a day for almost seven consecutive days before cloudy weather interrupted operation. Power towers also offer good longer-term prospects because of the high solar-to-electrical conversion efficiency.

Applications: It is also intended to generate electricity by means of a Rankine cycle power plant. Individual commercial plants can be sized to produce up to 200 megawatts of electricity. The main problem is the high costs and the extremely precise and complex installation requirements required to obtain maximum efficiency.

#### 2.1.2.3 Parabolic Dish/Stirling Engine

The original hot-air motor patented by Robert Stirling in 1816 did not produce propulsion energy from burning or a small explosion within the working cylinders as in a conventional combustion or diesel motor, but rather the heat used for propulsion is applied from outside. Both of the coupled cylinders of the Stirling motor are sealed gas-tight and filled with a constant amount of the working gas (helium). One cylinder is heated from the outside while the other remains cool. The pressure difference between the two cylinders drives two interconnected and phase-delayed pistons. In this fashion the cooled gas can be pushed into the hot cylinder, where it then can expand, and hence drive the piston and then the process repeats itself.
The term "Stirling engine" was later coined in order to describe all types of closed cycle regenerative gas engines.

Stirling engines are unique heat engines because their theoretical efficiency is nearly equal to their theoretical maximum efficiency, known as the Carnot Cycle efficiency. Stirling engines are powered by the expansion of a gas when heated, followed by the compression of the gas when cooled. The Stirling engine contains a fixed amount of gas which is transferred back and forth between a "cold" and and a "hot" end. The "displacer piston" moves the gas between the two ends and the "power piston" changes the internal volume as the gas expands and contracts.
The gasses used inside a Stirling engine never leave the engine. There are no exhaust valves that vent high-pressure gasses, as in a gasoline or diesel engine, and there are no explosions taking place. Because of this, Stirling engines are very quiet. The Stirling cycle uses an external heat source, which could be anything from gasoline to solar energy to the heat produced by decaying plants. No combustion takes place inside the cylinders of the engine.

A dish Stirling system consists of a parabolic-shaped point focus concentrator in the form of a dish that reflects solar radiation onto a receiver mounted at the focal point. These concentrators

are mounted on a pedestal and can pivot on two axes to follow the sun. This two-axis tracking mechanism allows the capture of the highest amount of solar energy at any time possible. The energy absorption enables fluid in the receiver to be heated to approximately 750°C. This is then used to generate electricity. Like all concentrating systems, they can be additionally powered by natural gas or biogas, providing firm capacity at any time.

**Figure 11**: Dish Stirling power plant [11]

It is a concentrating solar power (CSP) technology that produces relatively small amounts of electricity compared to other CSP technologies. Overall size typically ranges from 5 to 15 meters in diameter and 5 to 50kW of power output, with a peak efficiencies of up to 30% (net)..

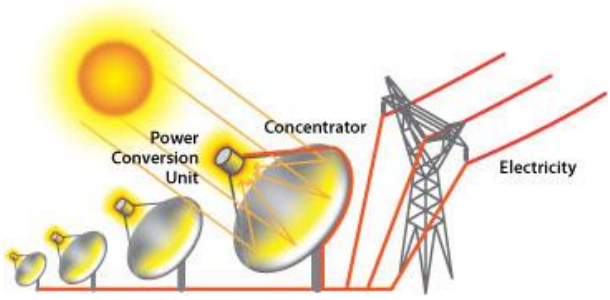


**Figure 12**: Schematics of a parabolic dish/Stirling engine system [12]

Solar dish/engine systems are still under development, but represent a new opportunity for solar-thermal electricity. If there is inadequate power or at night, the power system can operate in hybrid mode in which an alternative fuel can be burned to provide heat.

A dish system can achieve much higher temperatures due to the higher concentration of light (as in tower designs). Higher temperatures lead to better conversion to electricity and the dish system is very efficient on this point. However, there are also some disadvantages. Heat to electricity conversion requires moving parts and this results in maintenance. In general, a

centralized approach for this conversion is better than the decentralized concept in the dish design. Second, the (heavy) engine is part of the moving structure, which requires a rigid frame and strong tracking system. Furthermore, parabolic mirrors are used instead of flat mirrors and tracking must be dual-axis.

Aside from questions about the reliability of the Stirling motor, the dish Stirling is the quintessential thermal solar power plant:

- Its two-axis tracking mechanism allows it to maximize solar energy collection.
- The generation threshold is relatively low.
- The unit ramps to grid synchronization within a minute.
- It has the highest efficiency of any solar generating technology.
- It requires the least amount of land in relation to peak capacity and energy production.
- Its high engine-operating temperature allows air cooling, thus eliminating the need for cooling water.

Applications: The largest potential market for dish/engine systems is large-scale power plants connected to the utility grid. Their ability to be quickly installed, their inherent modularity, and their minimal environmental impact make them a good candidate for new peaking power installations. The output from many modules can be ganged together to form a dish/engine farm and produce a collective output of virtually any desired amount. In addition, systems can be added as needed to respond to demand increases. Hours of peak output are often coincident with peak demand. Although dish/engine systems do not currently have a cost-effective energy storage system, their ability to operate with fossil or bio-derived fuels makes them, in principal, fully dispatchable. This capability in conjunction with their modularity and relatively benign environmental impacts suggests that grid support benefits could be a major advantage of these systems.

#### 2.1.2.4 Fresnel Mirror Concentrator

A Linear Fresnel Reflector (LFR) is a single-axis tracking technology that focuses sunlight reflected by long heliostats onto a linear receiver to convert solar energy to heat. The classical linear Fresnel system uses an array of mirror strips close to the ground to direct solar radiation to a single, linear, elevated, fixed receiver. Each mirror element is tilted at an angle so that all incident solar rays falling on them are reflected to a common focus. The Fresnel reflector is

composed of parabola slices mounted on a flat surface. The flat mounting surface has advantages with regard to practical engineering and construction.

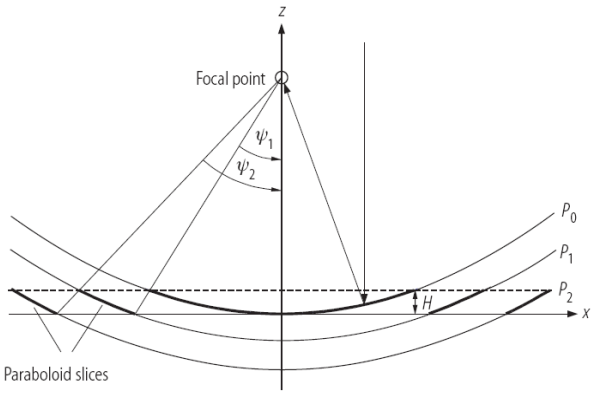


**Figure 13**: Fresnell geometry using three cofocal parabolas [13]

A set of parabolas with a common focal point are superimposed. Three parabolas $P_0$, $P_1$ and $P_2$ are shown, $P_0$ being the base parabola.

The technology is seen as a lower cost alternative to trough technology for the production of solar steam for power generation. The main advantages of the Linear Fresnel collector, compared to trough collectors, are seen to be:

- Inexpensive planar mirrors and simple tracking system.
- Fixed absorber tube with no need for flexible high pressure joints.
- No vacuum technology and no metal-to-glass sealing.
- One absorber tube with no need for thermal expansion bellows.
- Due to the planarity of the reflector strips, wind loads are substantially reduced so the reflector width for one absorber tube can easily be three times the width of parabolic trough.
- Due to direct steam generation no heat exchanger is necessary.
- Efficient use of land since the collectors can be placed close to one another.

LFR technology relies on an array of linear mirror strips which concentrate light on to a fixed receiver mounted on a linear tower. The LFR field can be imagined as a broken-up parabolic trough reflector, but unlike parabolic troughs, it does not have to be of parabolic shape, large absorbers can be constructed and the absorber does not have to move.

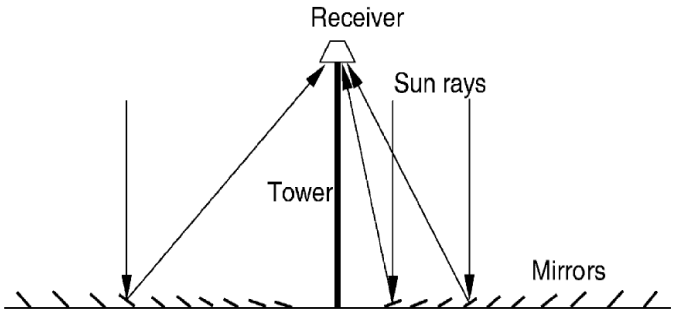


**Figure 14**: Schematic diagram of a downward facing receiver illuminated from an LFR field [14]

The greatest advantage of this type of system is that it uses flat or elastically curved reflectors which are cheaper compared to parabolic glass reflectors. Additionally, these are mounted close to the ground, thus minimizing structural requirements.

One difficulty with the LFR technology is that avoidance of shading and blocking between adjacent reflectors leads to increased spacing between reflectors. Blocking can be reduced by increasing the height of the absorber towers, but this increases cost.

Compact linear Fresnel reflector (CLFR) technology is a new configuration of the Fresnel Reflector field that overcomes the problem of reflector spacing. Traditional LFR technology design is based around one absorber tower.

**Figure 15**: Array of mirror strips of a CLFR **[15]**

The classical linear Fresnel system has only one linear receiver, and therefore there is no choice about the direction of orientation of a given reflector. However, if one assumes that the size of

the field will be large, as it must be in technology supplying electricity in the multi-Megawatt class, it is reasonable to assume that there will be many linear receivers in the system. If they are close enough then individual reflectors have the option of directing reflected solar radiation to at least two receivers. This additional variable in reflector orientation provides the means for much more densely packed arrays and lower absorber tower heights, because patterns of alternating reflector orientation can be set up such that closely packed reflectors can be positioned without shading and blocking. The interleaving of mirrors between two linear receiving towers is shown in the following figure.

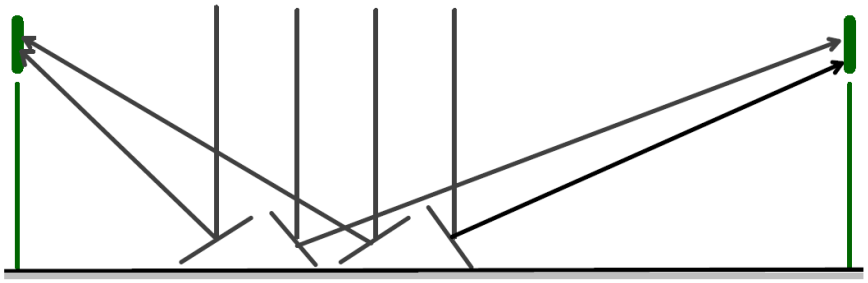

**Figure 16**: Schematic diagram showing interleaving of mirrors without shading between mirrors [16]

The avoidance of large reflector spacings and absorber tower heights is an important issue in determining the cost of ground preparation, array substructure and absorber tower structure costs, steam line thermal losses and steam line cost. The more flexible CLFR still delivers the traditional benefits of a Fresnel reflector system, namely small reflector size, low structural cost, fixed receiver position without moving joints, and the ability to use non-cylindrical receiver geometry. The CLFR power plant concept is a new optical layout that includes the following additional features which enhance the system cost/performance ratio:

- The array uses flat or elastically curved reflectors instead of costly sagged glass reflectors. The reflectors are mounted close to the ground, minimizing structural requirements.
- The heat transfer loop is separated from the reflector field and is fixed in space thus avoiding the high cost of flexible high pressure lines or high pressure rotating joints as required in the parabolic trough and Stirling dish concepts.
- The heat transfer fluid is water, and passive direct boiling heat transfer could be used to avoid parasitic pumping losses and the use of expensive flow controllers. Steam supply may either be direct to the power plant steam drum, or via a heat exchanger.
- All glass evacuated tubes very low radiative losses can be used as the core element of the linear absorber array. These tubes are inexpensive.

- Maintenance will be lower than in other types of solar concentrators because of nearly flat reflectors and ease of access for cleaning, and because the single ended evacuated tubes can be removed without breaking the heat transfer fluid circuit.

Applications: A linear Fresnel reflector (LFR) has potential for greatly reducing the initial cost of establishing solar power production. LFRs may have lower system efficiency than other concentrating geometries, but their likely reduced cost may more than compensate in some installations, providing a solution for cost-effective solar energy collection on a large scale.

### 2.1.3 Photovoltaic Collector Types

Photovoltaic (PV) systems use solar electric panels to directly convert the sun's energy into electricity. This conversion of sunlight to electricity occurs without moving parts, is silent and pollution free in its operation.

**Figure 17**: Photovoltaic collector field [17]

For the demands our system will have, the same as we have defined concentrating solar thermal (CST) energy, if the photovoltaic technology were to be selected, we would most probably have to use concentrating photovoltaic (CPV) systems analogously.

Many permutations of CPV exist. Some CPV technologies use mirrors to reflect and concentrate all the sunlight they can capture onto small high-efficiency PV cells. Other CPV technologies use lenses to concentrate the sun's light. CPV technologies also differ in how strongly they concentrate sunlight, whether they concentrate light to a line or a point, the type of solar cell that they use, and whether the cells are actively or passively cooled.

The principle of concentrating PV (CPV) is quite straightforward. In the standard, familiar 'flat-plate' PV modules, a large area of photovoltaic material (usually crystalline silicon) is exposed to the maximum naturally occurring sunlight. Normally, that maximum is achieved by installing the modules at an incline optimized for the latitude, but sometimes they are installed on moving frames that can follow, or track, the sun as it passes across the sky. The PV cells perform under direct (sunny) or diffuse (cloudy) radiation conditions, but output is at its highest when the maximum amount of light falls on the cells (assuming there are no detrimental effects from overheating). The amount of light that falls on a cloudless day (this varies according to location and season) is regarded as one 'sun', which is defined as 1000 W/m2.


**Figure 18 and Figure 19**: Photovoltaic concentrators (left [18], right [19])

The concentration ratio can vary. For example if the light that falls on 100 $cm^2$ is focused onto 1 $cm^2$ of PV material, the ratio is considered as 100 suns. If the concentrated sunlight light falls onto a well designed CPV cell, the cell will produce at least 100 times the electricity. (In fact, the conversion efficiency of cells increases under concentrated light, so the correlation is likely to be greater than one-to-one, depending on the design of the solar cell and the material used to make it). While commercial concentration ratios are around 200 to 300 suns, as much as 1000 suns is expected for future concentrating PV systems.

As most CPV systems use only direct solar radiation, these installations almost always involve trackers (rotating about either one axis or two axes and therefore called one-axis or two-axis tracking) to keep the sun focused on the solar cell.

One of the major disadvantages, besides the initial cost and the critical payback rates versus the life-span of the equipment, is the storage of the energy. There is a great variability of performance linked to the available solar radiation.

The storage possibilities would be mainly two:

- Batteries:

They increase the size, cost and complexity and maintenance of the system and reduce the efficiency.

- Germanium in amorphous silicon-germanium thin film solar cells:

It provides residual power generating capacity at night due to background infrared radiation. It is currently not sufficiently mature to withstand the total demand of our system.

## 2.2 THERMAL STORAGE

The use of thermal energy storage (TES) will be a keystone in our project since the initial intention is to develop an *autarkic* solar system. This means that it will have to supply energy even in very cloudy weather or at night-time, both scenarios with lack of sufficient sun irradiation. One of the advantages of the parabolic trough power plants is precisely their potential for storing solar thermal energy to use during non-solar periods and to dispatch when it's needed most. TES has become a critical aspect of any concentrating solar power (CSP) system deployed nowadays. Besides allowing electric energy to be dispatched at the times when it is needed most, thermal storage allows parabolic trough projects to achieve favorable capacity factors in excess of 50 percent. During the past recent years, a significant effort has been undertaken to identify thermal storage technologies for parabolic trough plants

Several TES technologies have been tested and implemented since 1985.
Parabolic trough thermal energy storage technology includes the following sections:

- Storage systems:
  Two-tank direct system
  Two-tank indirect system
  Single-tank thermocline

- Storage media:
  Concrete
  Phase-change material

- Molten Salt
  Molten salt heat transfer fluid

### 2.2.1 Thermal Energy Storage Systems

#### 2.2.1.1 Two-Tank direct system

Solar thermal energy in this system is stored in the same fluid used to collect it. The fluid is stored in two tanks—one at high temperature and the other at low temperature. Fluid from the low-temperature tank flows through the solar collector or receiver, where solar energy heats it to the high temperature and it then flows back to the high-temperature tank for storage. Fluid from the high-temperature tank flows through a heat exchanger, where it generates steam for

electricity production. The fluid exits the heat exchanger at the low temperature and returns to the low-temperature tank.

**Figure 20**: Two-tank direct molten-salt thermal energy storage system at the Solar Two power plant [20]

Two-tank direct storage was used in early parabolic trough power plants. The first Luz trough plant, SEGS I, included a direct two-tank thermal energy storage system with 3 hours of full-load storage capacity. This system simply used the mineral oil (Caloria) heat transfer fluid (HTF) to store energy for later use. It operated between 1985 and 1999 and was used to dispatch solar power to meet the Southern California Edison winter evening peak demand period (weekdays between 5-10 p.m.).

#### 2.2.1.2 Two-Tank Indirect System

This system functions in the same way as the two-tank direct system, except different fluids are used as the heat-transfer and storage fluids. This system is used in plants where the heat-transfer fluid is too expensive or not suited for use as the storage fluid.

The thermal energy storage system is charged by taking hot, heat transfer fluid (HTF) from the solar field and running it through the heat exchangers. Cold molten-salt is taken from the cold storage tank and run counter currently through the heat exchangers (oil-to-salt heat exchanger). It's heated and stored in the hot storage tank for later use. Later, when the energy in storage is needed, the system simply operates in reverse to reheat the solar heat transfer fluid, which generates steam to run the power plant. It's referred to as an indirect system because it uses a fluid for the storage medium that's different from what's circulated in the solar field.

The storage fluid from the low-temperature tank (cold storage tank, operating a nominal temperature of approximately 290 °C) flows through an extra heat exchanger, where it is heated by the high-temperature heat-transfer fluid. The high-temperature storage fluid then flows back to the high-temperature storage tank (hot storage tank, operating at a nominal temperature of 385 °C). The fluid exits this heat exchanger at a low temperature and returns to the solar

collector or receiver, where it is heated back to the high temperature. Storage fluid from the high-temperature tank is used to generate steam in the same manner as the two-tank direct system.

During storage discharging, the fluid flows are reversed, and heat is transferred from the nitrate salt to the oil through the same heat exchanger.

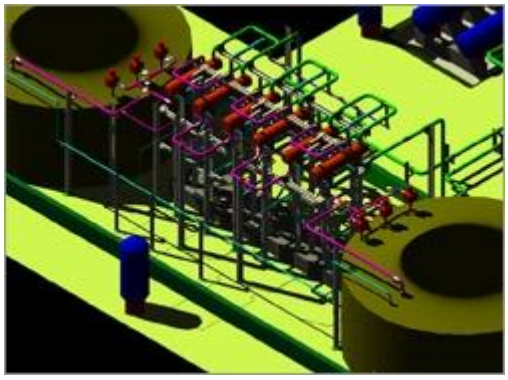

**Figure 21**: Two-tank indirect thermal energy storage system for Andasol 1 and 2 [21]

The system is relatively expensive—its primary disadvantage. The expense is due to the extra heat exchanger and the relatively small temperature difference between the cold and hot fluid in the storage system. Several parabolic trough power plants under development in Spain plan to use this thermal energy storage concept and have also been proposed for several U.S. parabolic plants. The plants use organic oil as the heat-transfer fluid and molten salt as the storage fluid.

#### 2.2.1.3 Single-Tank Thermocline

A thermocline tank is one that uses a single tank to store thermal energy. It stores thermal energy in a solid medium, most commonly silica sand. This model provides one possibility for further reducing the cost of a direct two-tank storage system. A thermal gradient separates the lower density hot (top) from the higher density cold fluid (bottom). A low-cost filler material is used to displace the higher-cost liquid. The filler material as well as buoyant forces helps to maintain the thermal gradient. The zone between the hot and cold fluids is called the thermocline.

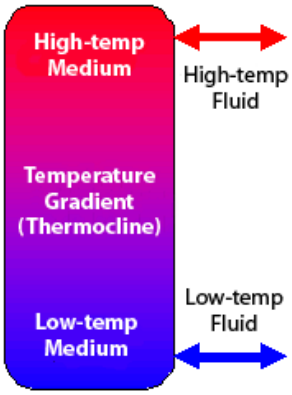


**Figure 22**: Single-tank thermocline thermal energy storage system [22]

When the system is charged, cold fluid is drawn from the bottom, heated as it passes through a heat exchanger (heated with the receiver heat transfer fluid) and is returned to the top of the tank. When the tank is discharged, hot fluid is drawn from the top, cooled as it passes through a heat exchanger (to transfer heat for steam generation), and is returned to the bottom of the tank.

Depending on the cost of the storage fluid, the thermocline can result in a substantially lower cost storage system in relation to the two-tank systems. However, the thermocline storage system must maintain the thermocline zone in the tank, so that it does not expand to occupy the entire tank. This system was demonstrated at the Solar One power tower, where steam was used as the heat-transfer fluid and mineral oil was used as the storage fluid.

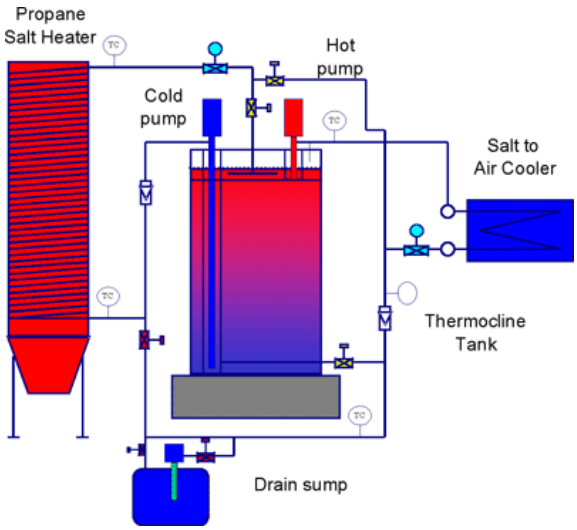


**Figure 23**: Thermocline test at Sandia National Laboratories [23]

### 2.2.2 Thermal energy Storage Media

#### 2.2.2.1 Concrete

The German Aerospace Center (DLR) is examining the performance, durability and cost of using solid, thermal energy storage media (high-temperature concrete or castable ceramic materials) in parabolic trough power plants. They constructed a facility at the University of Stuttgart for testing a concrete, thermal energy storage system.

This system uses the standard heat transfer fluid (HTF) in the solar field. The heat transfer fluid passes through an array of pipes imbedded in the solid medium to transfer the thermal energy to and from the media during plant operation.

**Figure 24**: Concrete energy storage system [24]

The primary advantage of this approach is the low cost of the solid media. Primary issues include maintaining good contact between the concrete and piping, and the heat transfer rates into and out of the solid medium.

At the Plataforma Solar de Almeria in Southern Spain, Ciemat and DLR performed initial testing that found both the castable ceramic and high-temperature concrete suitable for solid media, sensible heat storage systems. However, the high-temperature concrete is favored because of lower costs, higher material strength, and easier handling. There is no sign of degradation between the heat exchanger pipes and storage material.

DLR has also developed a design tool that helps optimize the storage layout, including the geometric dimensions and piping and module arrangement to minimize pressure losses and optimize manufacturing aspects and costs.

Because of the modular nature of concrete storage, DLR has identified approaches that allow the storage system to better integrate with the solar field and power cycle. This allows for improved overall utilization of the concrete storage system.

#### 2.2.2.2 Phase-change Material

Phase-change materials (PCMs) allow large amounts of energy to be stored in relatively small volumes, resulting in some of the lowest costs for storage media of any storage concept.

Initially, PCMs were considered for use with parabolic trough plants that used a synthetic heat-transfer fluid (Therminol VP-1) designed to withstand high temperatures in the solar field. In this approach, thermal energy is transferred to a series of cascading heat exchangers containing PCMs that melt at slightly different temperatures. To discharge the storage, the flow of heat-transfer fluid is reversed, thus reheating the fluid. Testing proved this system to be technically feasible. However, further development of this concept is hindered by the following:

- Complexity of the system
- Thermodynamic penalty of going from sensible heat to latent heat and back to sensible heat
- Uncertainty over the lifetime of phase-change materials.

Phase-change thermal storage is now being considered (by DLR) for application with direct steam generation in the parabolic trough solar field. This approach allows a better thermodynamic match between the phase-change material and the phase change of steam used in the solar field. Here, a single PCM can be used to preheat, boil, and superheat steam. The cost of such a system is driven by the cost of phase-change storage material, but also by the rate at which energy is charged or discharged from the material.

### 2.2.3 Molten-Salt Thermal Storage

Molten nitrate salt is an excellent thermal storage medium. It is a mixture of 60 percent sodium nitrate and 40 percent potassium nitrate, commonly called saltpetre. It is non-flammable and nontoxic, and has already been used in the chemical and metals industries as a heat-transport fluid, so experience with such systems exists in non-solar applications.

Using it in both the solar field and thermal energy storage system eliminates the need for expensive heat exchangers. It allows the solar field to be operated at higher temperatures than

current heat transfer fluids allow. This combination also allows for a substantial reduction in the cost of the thermal energy storage (TES) system.

Unfortunately, it can be a troublesome fluid to deal with because of its relatively high freezing point (220°C/428°F). To keep the salt molten, a fairly complex heat trace system must be employed. (Heat tracing is composed of electric wires attached to the outside surface of pipes. Pipes are kept warm by way of resistance heating.) Problems were experienced during the startup of Solar Two due to the improper installation of the heat trace.

Also, valves can be troublesome in molten-salt service. Special packings must be used, oftentimes with extended bonnets, and leaks are not uncommon. Furthermore, freezing in the valve or packing can prevent it from operating correctly. While today's valve technology is adequate for molten-salt power towers, design improvements and standardization would reduce risk and ultimately reduce O&M costs.

The Italian research laboratory, ENEA, has proven the technical feasibility of using molten-salt in a parabolic trough solar field with a salt mixture that freezes at 220°C (430°F). And Sandia National Laboratories are developing new salt mixtures with the potential for freeze points below 100°C (212°F). At 100°C the freeze problem is expected to be much more manageable.

Several parabolic trough power plants under development in Spain and solar power tower developer SolarReserve plan to use this thermal energy storage concept.

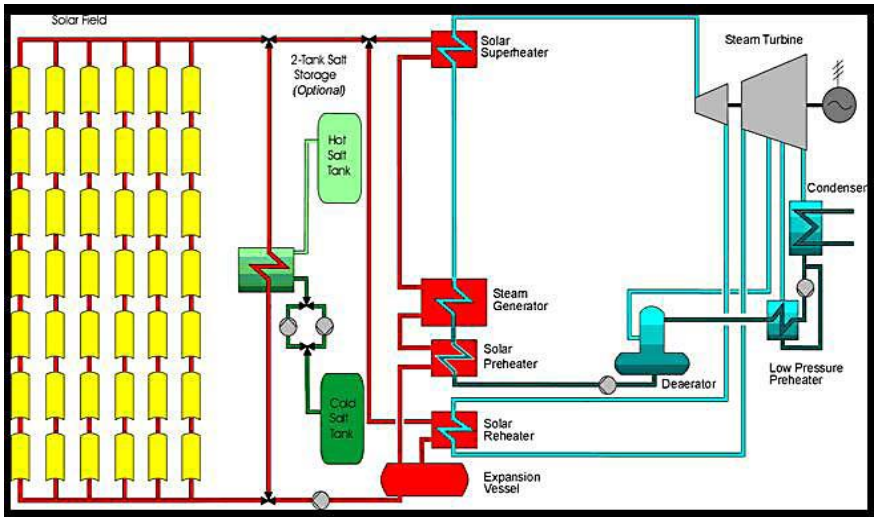


**Figure 25**: Molten salt storage in solar power plant [25]

The fluid going through the receiver pipe is routed through a thermal storage system which permits the plant to keep operating for several hours after sunset while the electrical demand is still relatively high. The thermal storage system (to be used in Spain) is a two tank system in

which the HTF flows through the solar field and then through a heat exchanger where it gives up a portion of its heat to heat a nitrate salt solution that is stored in a hot salt tank. The slightly cooled HTF continues on to the power generation system. At night the hot salt solution flows through the same heat exchanger heating up the HTF for generating power. The cooler oil flows from the heat exchanger to the cold storage tank where it stays until daytime when it is reheated and returned to the hot storage tank.

## 2.3 WATER DESALINATION

Production of fresh water using desalination technologies driven by Renewable Energy Sources (RES) is thought to be viable solution to the water scarcity at remote areas characterized by lack of potable water and lack of electricity grid. Desalination units driven by RES, such as those driven by solar and wind energy, guarantee friendly to the environment, cost effective and energy efficient production of desalinated water in regions with severe water problems, which nevertheless are fortunate to have renewable energy resources. Renewable energy driven desalination technologies fall into two categories. The first category includes distillation desalination technologies driven by heat produced by RES, while the second includes membrane and distillation desalination technologies driven by electricity or mechanical energy produced by RES.

Due to the conditions and characteristics of our project and its location, we will center our system possibilities to those powered by solar energy as a renewable energy source.

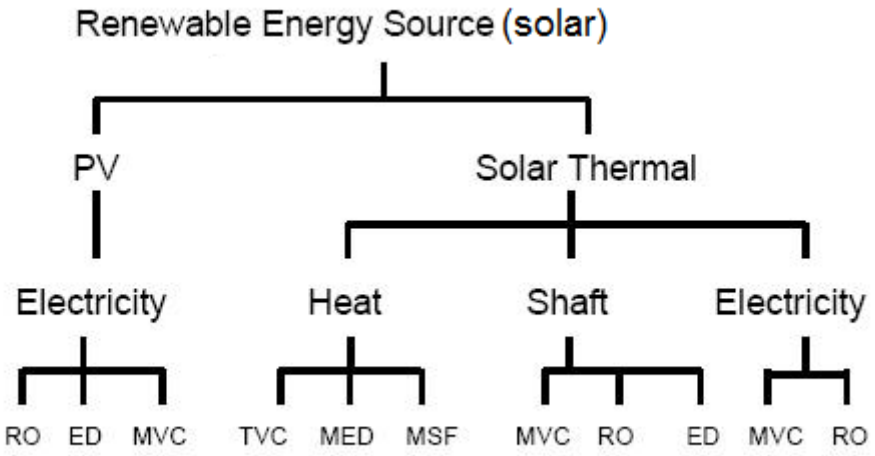


**Figure 26**: Solar energy desalination combinations [26]

From the above diagram, we further select the following branches:

- Thermal Desalination (Distillation)
    - Multi-Stage Flash (MSF)
    - Multiple-Effect Evaporator (MED)
    - Thermal Vapor Compression (TVC)

- Electric Desalination (Membrane and Distillation Processes)
    - Reverse Osmosis (RO)

- Mechanical Vapor Compression (MVC)
- Membrane Distillation (MD)
- Electrodialisis (ED)

Photovoltaic electric desalination systems have been directly discarded due to high costs, efficiency reasons, but mainly due to the limited cogenerative interaction possibilities the desalination plant would then offer between the main power plant and itself as well as with the rest of sub-systems (DHW, AC).

### 2.3.1 Thermal Desalination (Distillation)

#### 2.3.1.1 Multi-Stage Flash (MSF)

Multiple stage flash (MSF) distillation is the most widely used desalination process, in terms of capacity. In this process, as well as in all distillation processes, the seawater is heated, producing water vapor that is in turn condensed to form fresh water. The water is heated to the boiling point to produce the maximum amount of water vapor.

There are two configurations concerning MSF process. The first one, the "once through" consists of two sections:

- heat rejection section
- brine heater

The second MSF configuration, the "brine recirculation" consists of the three following sections:

- heat rejection section
- heat recovery section
- brine heater

The recovery and rejection sections of the latter process are made up of a series of stages. Each stage consists of a flash chamber and a heat exchanger / condenser. The flash chamber is separated from the condenser by a demister to remove entrained droplets from the flashing vapor and a distillate channel to catch the condensate from the condenser above.
In both processes, the seawater is heated in the brine heater. In the brine recirculation process the seawater is taken into the plant and fed through the heat rejection stage. The function of this

section is to reject thermal energy from the plant and to allow to the product water and brine to exit the plant at the lowest possible temperature. The feed water is mixed with the large mass of water which is recirculated round the plant, known as the "brine recirculation" flow. Then the feed water passes through a number of heat exchangers (stages), raising its temperature.

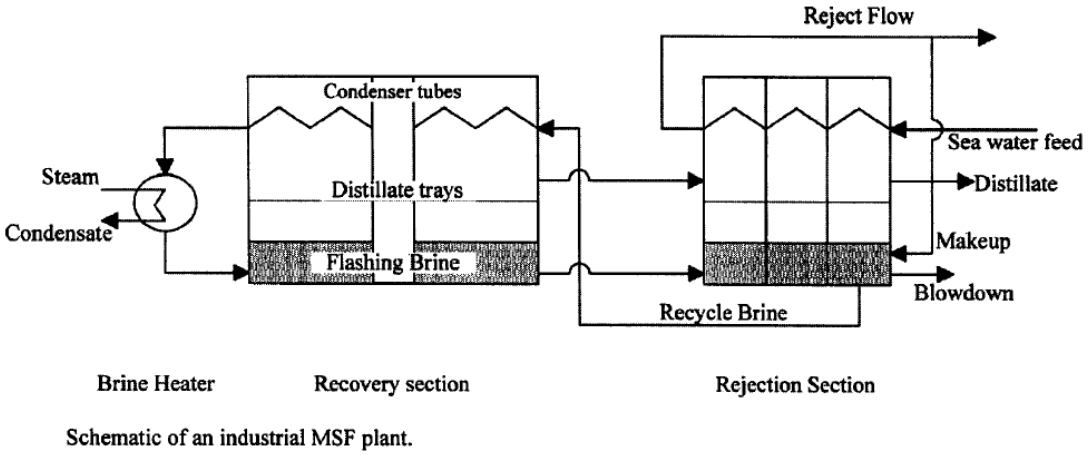


**Figure 27**: Basic schematics of an industrial MSF plant [27]

After passing through the last stage of the recovery section the water is heated up to its terminal temperature in the brine heater. The brine then enters the first heat recovery stage through an orifice, thus reducing the pressure. As the brine was already at its saturation temperature, it will become superheated for a lower pressure and flashes to give off water vapor. It is then passes up through a demister into the condenser where the vapor is condensed and the distillate produced is dripped into a collector. This process continues right down to the bottom stage of the plant in the rejection section, where part is rejected as "blowdown" and the rest is mixed with the incoming make up (feed water) and then recycled once again via the brine recirculation pump. The distillate condensed in each of the condensers is collected in a distillate train.

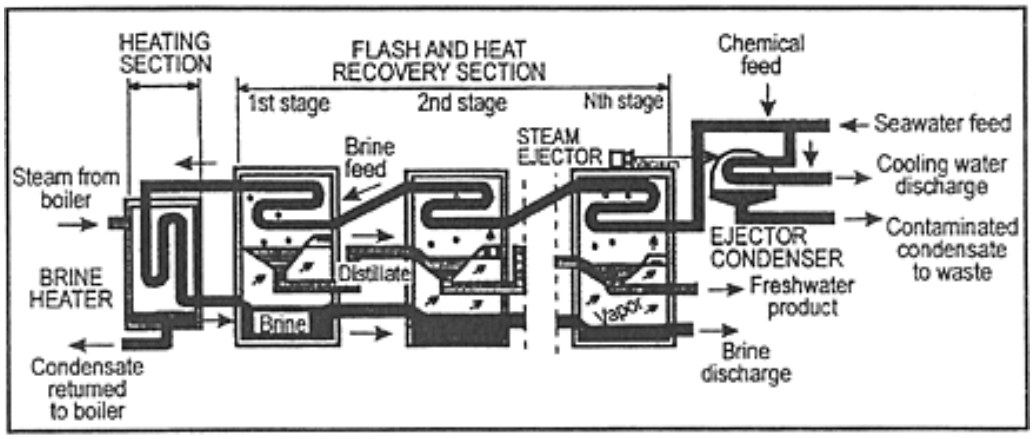


**Figure 28**: Schematics of an industrial MSF plant [28]

In practice, MSF plants are designed for various performance ratios (mass of distillate produced per unit mass of steam consumed). The performance ratio is an important parameter used for gauging the performance of a plant. A performance ratio of 12 is the practical upper limit for this type of plant.

An MSF plant can contain from 4 up to 40 stages. Increasing the number of stages reduces the heat transfer surface that is required, reducing the capital cost. This has to be offset against the cost of providing extra stages. Complicated optimization calculations have to be undertaken where the main parameters are capital cost versus operating cost. MSF plants usually operate at top brine temperatures of between 90-120º C, depending on the feed water treatment. Operation at higher temperatures than 120º C is not workable because of problems of scale deposition in the brine heater.

The capital cost as well as the energy cost of an MSF plant is significant. The main energy requirement is thermal energy. Electricity demand is low and is used for auxiliary services such as pumps, dosifiers, vacuum ejectors, etc. Nonetheless, the success and popularity of the process is due to its simplicity, inherent robustness and vast amount of acquired experience which resulted in reducing material and operating costs and increasing life expectancy. With the appropriate maintenance, modern plants can operate with long intervals between shutdowns. Life spans of up to 40 years are now being predicted for large plants in the Arabian Gulf area.
The installed capacity of the process has grown considerably over the last twenty-five years. MSF has been developed and adapted to large-scale applications, usually greater than 5000 m3/d. At present, the largest MSF plant, contracted or in operation is of 60 000 m3/d product water capacity.

#### 2.3.1.2 Multiple-Effect Evaporator (MED)

Multiple effect distillation (MED or ME) was the first process used for seawater desalination. The MED process is similar to the MSF process; the majority of the distillate is produced by boiling. MED, like MSF, takes place in a series of vessels (effects) and uses the principle of reducing the ambient pressure in the various effects. This permits the feed water to undergo multiple boiling phases without supplying additional heat after the first effect.

A MED consists of several consecutive cells (or effects) maintained at decreasing levels of pressure (and temperature) from the first (hot) cell to the last one (cold). Each cell mainly consists of a bundle of horizontal tubes.

The incoming feed water is pumped into the plant through a number of preheaters located in each effect (evaporators) in order to raise its temperature. This feed water is sprayed onto the surface of the evaporator tubes to form a thin film to promote rapid boiling and evaporation. This reaction takes place as the feed water flows down from tube to tube due to gravity. Inside these tubes runs heating steam that is obtained from a boiler or another source. The vapor produced outside the tubes due to evaporation then goes, in part, to heat the incoming feed and in part to provide the heat supply for the second effect which is at lower pressure and receives its feed from the brine of the first effect. From the second effect the vapor itself is condensed (product water) while at the same time giving up heat to evaporate a portion of the remaining feed water in the next effect. This process is repeated all the way down the plant. The effects are gradually operated at lower temperatures. This is accomplished by maintaining the effects at successively lower pressure (or higher vacuum by means of an air ejector).

Due to evaporation, sea water slightly concentrates when flowing down the bundle and gives brine at the bottom of the cell. The decreasing pressure from one cell to the next one allows brine and distillate to be drawn to the next cell where they will flash and release additional amounts of vapor at the lower pressure. This additional vapor will condense into distillate inside the next cell.

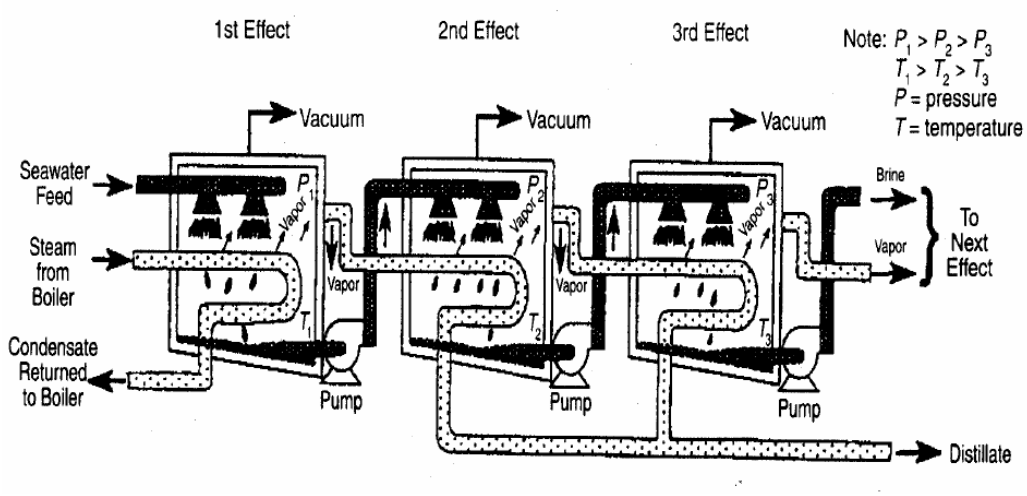


**Figure 29**: Schematics of the MEd process [29]

This process is repeated in a series of effect (Multiple Effect Distillation) (see sketch above with 3 effects). In the last cell, the produced steam condenses on a conventional shell and tubes heat exchanger. This exchanger, called "distillate condenser" is cooled by sea water. At the outlet of this condenser, part of the warmed sea water is used as make-up of the unit and the other part is

rejected to the sea. Brine and distillate are collected from cell to cell till the last one from where they are extracted by centrifugal pumps.

The thermal efficiency of such evaporator can be quantified as the number of kilos of distillate produced per one kilo of steam introduced in the system. Such number is called the Gain Output Ratio (GOR).

Most of the new MED plants have been built around the concept of operating at lower temperatures. Some of the more recent plants have been built to operate with top temperatures (in the first effect) around 70 ºC reducing the potential for scaling within the plant.
MED plants tend to have smaller number of effects than MSF stages. Usually 8-16 effects are used in typical large plants, due to the relation of the number of effects with the performance ratio (which cannot exceed the number of effects of the plant).
As in an MSF plant, special attention is required concerning the operating temperature to avoid scaling and corrosion of materials. Also, extra care is required concerning the control of the brine level in each effect.

Some of the early water distillation plants used the MED process, but this process was displaced by the MSF units because of cost factors, fewer operating problems, and their apparent higher efficiency. However, interest in the MED process has increased and a number of new designs have been developed, such as MED units of up to 5000 $m^3$/d in capacity.

The cost of an MED plant heavily depends on the performance ratio. Capital and energy costs are significant factors. The main energy requirement is thermal energy.

The following diagram shows a possibility for a solar MED installation.

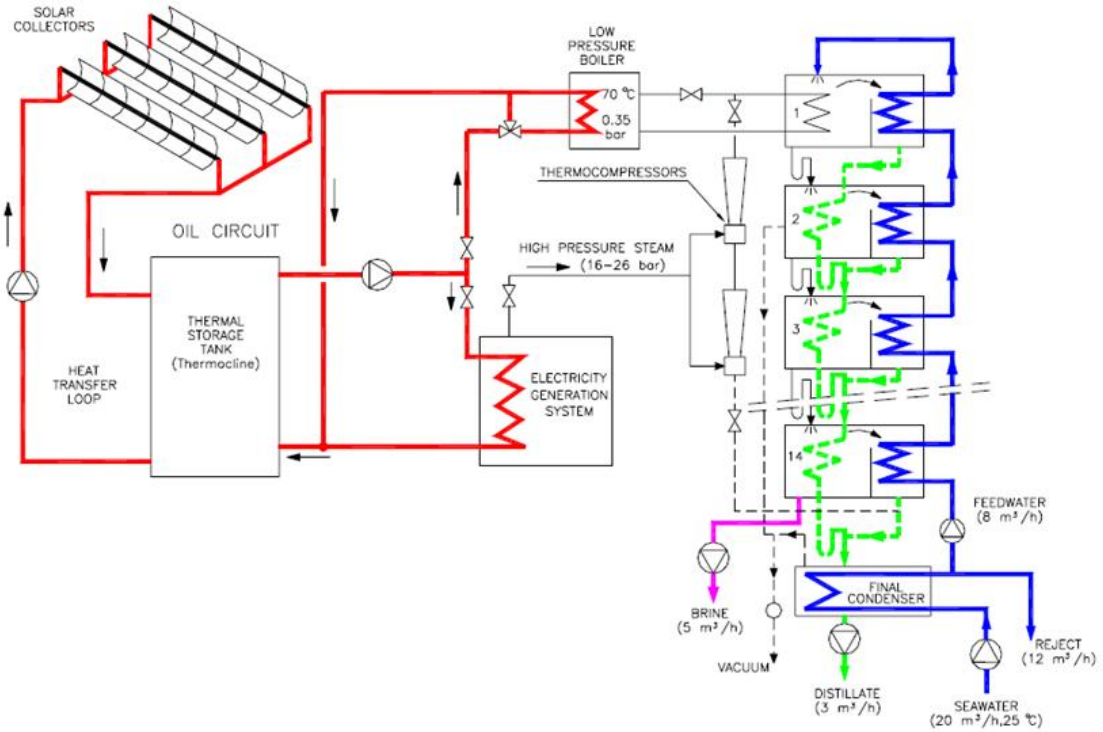


**Figure 30**: Schematics of the solar MED system installed in PSA during Phase I of the project [30]

#### 2.3.1.3 Thermal Vapor Compression (TVC)

Vapor compression desalination refers to a distillation process where the evaporation of sea or saline water is obtained by the application of heat delivered by compressed vapor. Since compression of the vapor increases both the pressure and temperature of the vapor, it is possible to use the latent heat rejected during condensation to generate additional vapor. The effect of compressing water vapor can be done by two methods.

The first method utilizes an ejector system motivated by steam at manometric pressure from an external source in order to recycle vapor from the desalination process. The form is designated Ejecto or Thermo Compression. In the second method, water vapor is compressed by means of a mechanical device, electrically driven in most cases. This form is designated mechanical vapor compression (MVC). This method will be discussed in point 2.3.2.2.

In the process, the feed water is preheated in a heat exchanger or a series of heat exchangers by the hot discharge of the brine blowdown and the distillate. The hot feed water enters the evaporator (any type of evaporator can be used), where it is heated up to its boiling point and some of it is evaporated. The vapor formed in the evaporator goes to the compressor where its pressure and consequently its saturation temperature are raised. The power consumption of the

compressor, and therefore the efficiency of the process, is dependent on this pressure difference. Thus the compressor represents the main energy consumer in the system.

The compressed vapor is then fed back into the evaporator to be condensed, providing the thermal energy to evaporate the applied seawater on the other side of the tubes. The process has the potential of delivering high performance ratios due to the effective recirculation of the latent heat around the plant. By increasing the surface area and lowering the compression ratio (temperature difference) it is possible to decrease the energy consumption of the process. The distilled water produced by this condensation leaves the plant through the preheaters as the product water. Extra care is required with the control of the brine level in the evaporator and the proper maintenance of the compressor. Some manufacturers use compressors that rotate at very high speeds. Operation at low temperatures minimizes the formation of scaling and corrosion of materials.

The vapor compression process is usually used for small and medium scale water desalination units in a range of 20-2500 $m^3$/d. Capital and energy costs are significant factors in the determination of the total water production cost. The energy demand mainly required is the necessary to drive the vapor compressor motor. Its operation and maintenance sometimes covers half of the total operating and maintenance cost. However, the energy requirements of VC plants have been reduced (from 20 kWh/$m^3$) and currently range between 8 to 12 kWh/$m^3$ - with the potential for further reduction.

The following figure shows a large modern 4-effect thermo-compression plant. The thermo-compressor can be seen running along the top of the plant from the last to the first effect.

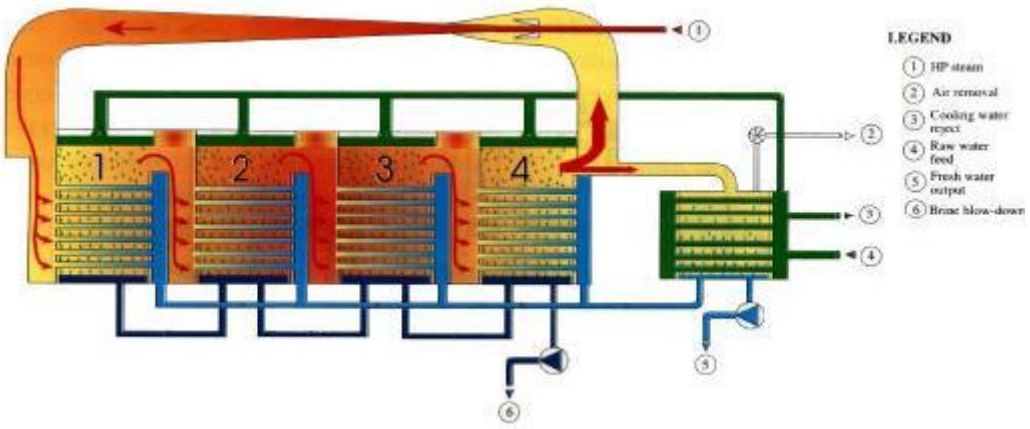


**Figure 31**: Schematic of 4-effect thermocompression [31]

### 2.3.2 Electric Desalination (Membrane and Distillation Processes)

#### 2.3.2.1 Mechanical Vapor Compression (MVC)

The basic principle has been already described in 2.3.1.3. In this case, water vapor is compressed by means of a mechanical device, electrically driven in most cases. The MVC process comprises two different versions:

- Vapor Compression (VC)
- Vacuum Vapor Compression (VVC).

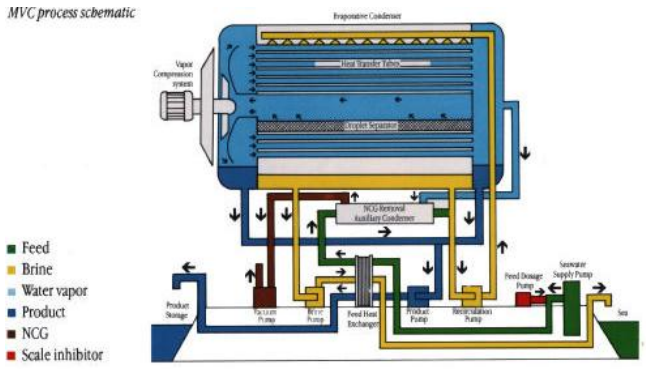


**Figure 32**: Schematics of a mechanical vapor compressor [32]

VC designates those systems in which the evaporation effect takes place at manometric pressure, and VVC the systems in which evaporation takes place at sub-atmospheric pressures (under vacuum). In the VVC system, the mechanical compressor creates a vacuum in the vessel and then compressed the vapor taken from the vessel and condenses it inside a tube bundle.
The compression is mechanically powered by something such as a compression turbine. As vapor is generated, it is passed over to a heat exchanging condenser which returns the vapor to water. The resulting fresh water is moved to storage while the heat removed during condensation is transmitted to the remaining feedstock.

#### 2.3.2.2 Reverse Osmosis (RO)

There are two types of membrane process used for desalination: reverse osmosis (RO), described in this section, and electrodialysis (ED), described in the next section, (2.3.2.3).

The principle of osmosis involves the transfer of a solvent through a semi-permeable membrane under the influence of a concentration gradient.

In reverse osmosis, an increase in the pressure applied to the saline solution beyond the osmotic pressure will drive a flow of water in the opposite direction to the normal osmotic flow. More precisely, water from a pressurized saline solution (sea water in this instance) is separated from the dissolved salts by flowing through a water-permeable membrane. The permeate (the liquid flowing through the membrane) is encouraged to flow through the membrane by the pressure differential created between the pressurized feedwater and the product water, which is at near-atmospheric pressure. The remaining feedwater continues through the pressurized side of the reactor as brine. As the water passes through the membrane, the remaining feed water increases in salt concentration. This water is discharged from the vessel in a controlled manner in order to ensure problems such as precipitation of supersaturated salts and increased osmotic pressure across the membranes does not occur. No heating or phase change takes place. The major energy requirement is for the initial pressurization of the feedwater.

In practice, the feedwater is pumped into a closed container, against the membrane, to pressurize it. As the product water passes through the membrane, the remaining feedwater and brine solution becomes more and more concentrated. To reduce the concentration of dissolved salts remaining, a portion of this concentrated feedwater-brine solution is withdrawn from the container. Without this discharge, the concentration of dissolved salts in the feedwater would continue to increase, requiring ever-increasing energy inputs to overcome the naturally increased osmotic pressure.

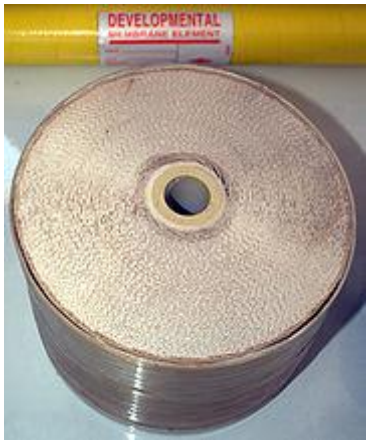


**Figure 33**: Semi-permeable membrane coil used in desalinization [33]

A reverse osmosis system consists of four major components/processes: (1) pretreatment, (2) pressurization, (3) membrane separation, and (4) post-treatment stabilization. Figure 16 illustrates the basic components of a reverse osmosis system.

**Pretreatment:** The incoming feedwater is pretreated to be compatible with the membranes by removing suspended solids, adjusting the pH, and adding a threshold inhibitor to control scaling caused by constituents such as calcium sulphate.

**Pressurization:** The pump raises the pressure of the pretreated feedwater to an operating pressure appropriate for the membrane and the salinity of the feedwater.

**Separation:** The permeable membranes inhibit the passage of dissolved salts while permitting the desalinated product water to pass through. Applying feedwater to the membrane assembly results in a freshwater product stream and a concentrated brine reject stream. Because no membrane is perfect in its rejection of dissolved salts, a small percentage of salt passes through the membrane and remains in the product water. Reverse osmosis membranes come in a variety of configurations. They are generally made of cellulose acetate, aromatic polyamides, or, nowadays, thin film polymer composites. Both types are used for brackish water and seawater desalination, although the specific membrane and the construction of the pressure vessel vary according to the different operating pressures used for the two types of feedwater.

**Stabilization:** The product water from the membrane assembly usually requires pH adjustment and degasification before being transferred to the distribution system for use as drinking water. The product passes through an aeration column in which the pH is elevated from a value of approximately 5 to a value close to 7. In many cases, this water is discharged to a storage cistern for later use.

Although the membranes are used to separate salts and water in each RO and ED processes, the membranes are used differently in each of these two processes. *Reverse Osmosis* is a pressure driven process, with the pressure applied used to separate water and dissolved salt by allowing some of the feedwater to move through membrane, which blocks the passage of the dissolved salts, thereby producing desalted water (permeate) while leaving concentrated salt solution (concentrate) behind.

*Electrodialysis* is an electrochemical separation process, in which ions are transferred through ion selective membranes by means of a DC voltage, leaving the product water behind. Diagram 8.3 shows simplified schematics of typical RO process configurations.

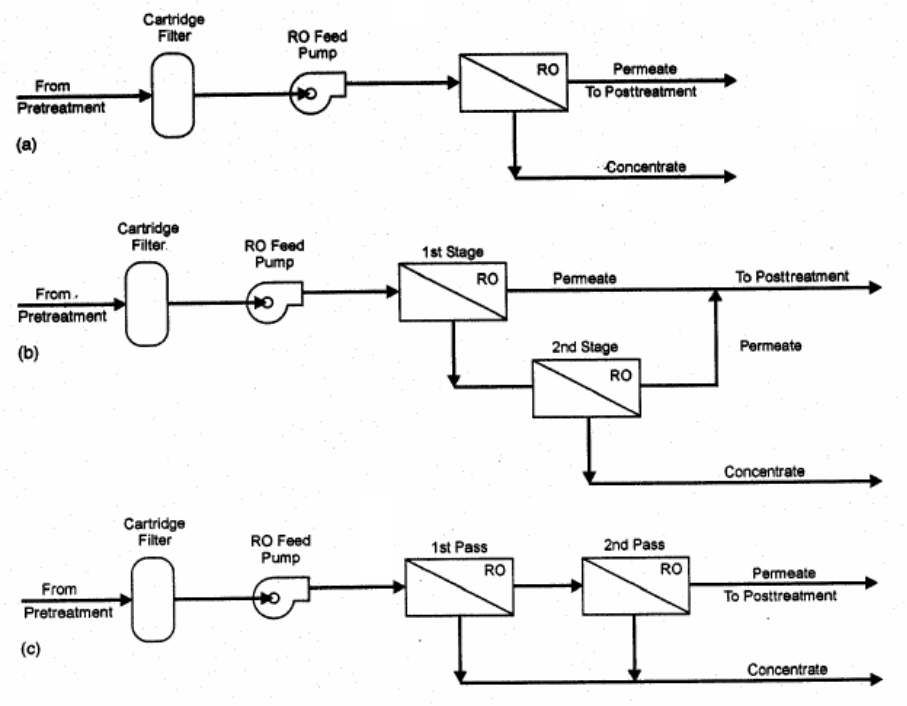


**Figure 34**: Typical RO Processes Schematics; (a) Single-stage, single-pass, (b) Twostage, single-pass, (c) Two-pass [34]

#### 2.3.2.3 Electrodialisis (ED)

Electrodialysis (ED) involves the movement of water through a filtering membrane. Instead of using pressure to overcome the membrane's resistance as in the RO system, pretreated water is pumped between electrodialysis cells by means of a low voltage direct current (DC) electrical field. An electrodialysis cell consists of a large number of feed (diluate) compartments and concentrate (brine) compartments through which the feedwater for desalination is pumped. These compartments are separated by membranes that are permeable to either positive ions (cations) or negative ions (anions). The cations and anions migrate through the appropriate membranes by the influence of the DC electrical field, forming compartments of electrolyte-enriched wastewater and electrolyte depleted product water.

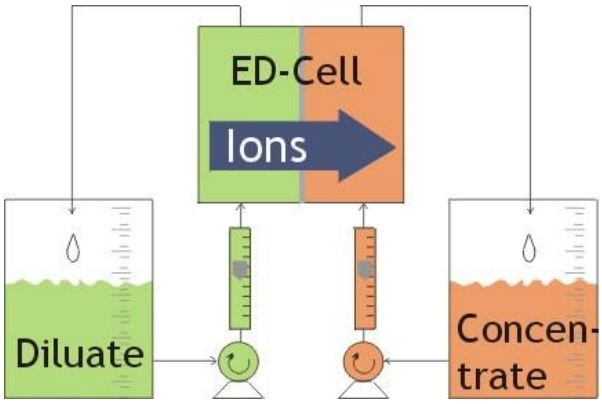


**Figure 35**: A basic schematics of the Ed process [35]

The partially deionised water is removed from the ED cell with the electrolyte concentrations reduced by a factor of at least two. If further desalination is required then treatment via one or more additional stages of cells may be necessary. Non-ionic particulates, bacteria and residual turbidity may also pass through the cells with the product water, and therefore this may require further treatment to achieve the desired product water standards.

The basic electrodialysis unit consists of several hundred cell-pairs bound together with electrodes on the outside and is referred to as a membrane stack. Feedwater passes simultaneously in parallel paths through all of the cells to provide a continuous flow of desalinated water and brine to emerge from the stack. Depending on the design of the system, chemicals may be added to the streams in the stack to reduce the potential for scaling.

The raw feedwater must be pre-treated to prevent materials that could harm the membranes or clog the narrow channels in the cells from entering the stack. The feedwater is circulated through the stack with a low pressure pump with enough power to overcome the resistance of the water as it passes through the narrow passages.

A table with general advantages and disadvantages between membrane process and distillation process is included below[1] although, from a global perspective, primarily the volume of processed water our system demands together with the difference in costs and maintenance, and the higher pre and post-treatment of the feedwater in the membrane layout are key factors that tilt the balance towards choosing a distillation process over the membrane one.

[1] http://www.livingstone.qld.gov.au/commser/watersupply/8.pdf

**Comparison of Membrane and Distillation Processes**

| Parameter | Membrane Processes | Distillation Processes |
|---|---|---|
| Advantages | • Membrane plants normally have lower energy requirements.<br>• The capital cost for membrane plants is lower than distillation plants.<br>• Membrane plants have a high space/production capacity ratio.<br>• Membrane plants generally have higher recovery ratios than distillation plants.<br>• Membrane plants operate at ambient temperature. This minimises the scaling and corrosion potential, which increases with higher temperatures. | • Distillation plants produce higher quality product water than membrane plants.<br>• Distillation plants do not need to be cleaned as often as membrane plants.<br>• Distillation plants do not need to be monitored as strictly as membrane plants.<br>• Distillation plants only require a minimal amount of operating staff. |

| Parameter | Membrane Processes | Distillation Processes |
|---|---|---|
| Disadvantages | • Membrane processes do not destroy biological substances, unlike distillation processes. Therefore they must be removed in either pre-treatment or post-treatment if the water is to be used for potable water or process water.<br>• Membranes that are of the polyamide type can not be used if there is chlorine in the water. The chlorine must be chemically removed.<br>• Membrane plants need to be cleaned more regularly than distillation plants.<br>• Membrane plants need more rigid monitoring than distillation plants. | • Distillation plants are more vulnerable to corrosion than membrane plants. This is controlled by the selection of materials.<br>• Distillation plants require more room for a given capacity than membrane plants.<br>• Distillation plants have a higher capital cost than membrane plants.<br>• Distillation plants consume more energy than membrane plants.<br>• The temperature of the product water is higher for distillation plants, than for membrane plants. This means that the product water needs to be cooled to be used as potable water. |

### 2.3.3 Fresh Water Storage

Given the nature of our project with solar energy as the energy type used, it would be technically more feasible and logical to desalinate an amount of water that exceeds our demands during the sun hours in order to store it so during the hours we have no direct sunlight we can still fulfill the water demands of the population. It is certainly more viable to store water than energy.

In any case, sizing the storage facility is a challenging task. Additionally, when selecting a storage tank, the associated costs, potential environmental and health impacts have to be taken into account. The cost of water storage tanks depends on many factors, mainly on the size, the material and the specific on-site conditions. The environmental and social impacts of the water storage tank/s that will be selected have to be considered for all stages including the selection of the site and of the materials that will be used, the availability in the specific region of the latter, the construction phase, the operation phase and the final disposal of the tank. The cost of a tank is about 1 to 5% of the total capital expenditure for an autonomous desalination system and has almost no contribution to the running cost of the unit. In order to minimize such costs, the optimum solution must be selected. Avoiding extreme over dimensioning is one of the first options to reduce costs. And of course, special attention has to be paid though in order not to mix the produced water with lower quality water.

## 2.4 CONCLUSIONS

Our system can be divided into four different blocs according to the different needs that should be fulfilled:

- Solar electric generation system
- Seawater desalination plant
- Domestic hot water
- Air conditioning system

### 2.4.1 Solar Electric Generation System

For the large amount of electric energy we need to generate, the ideal system would be to implement a power plant based on turbine + generator electric production. Therefore, we need to achieve high temperatures in order to assure a reasonable efficiency factor. This leads us to choose a "concentrated collector type". We then have the following already mentioned options:

- Parabolic trough
- Solar tower/central receiver
- Parabolic dish/Stirling engine
- Fresnell mirror concentrator

Since the temperatures reachable are in any case not extremely high, a Rankine power plant would best fit, as opposed to other models like a Bryton or combined cycle plant.

As we have mentioned, the high temperatures the heat transfer fluid needs to achieve in order to generate steam in are absolutely necessary, so therefore we are able to directly discard the Fresnell mirror concentrators, which would otherwise entail a lower efficiency factor of the whole system.

An important factor to consider in reference to the power plant a storage system will be needed in order to have electricity availability 24 hours/day.

Consequently, the most feasible options for our goal given these characteristics would be to install a sort of thermal storage rather than an electric storage operated by batteries or an even less viable option (like Germanium in amorphous silicon-germanium thin film solar cells). And so then, due to the technical complexity that would appear with this combination, we can discard the option of the parabolic dish/Stirling engine.

From the remaining two concentrated collector types available, we discard the solar tower/central receiver because, in spite of its valid functionality, it comparatively requires a more complicated design and layout due to the extreme precision needed to place and orient the heliostats, key to assure the optimal degree of efficiency possible.

Thus, as a final selection for the solar concentrated collector type for electric generation, we choose to implement a **solar trough field**.

As for the storage linked to the power generation system, a rather intensive study should be carried out in order to choose appropriately from the different models. But specifically in our project, we are somewhat less flexible in this section due to the fact that we are linked to the TRNSYS simulator to carry out our work. In the "type" libraries currently available in this program, we are directed to choosing a **concrete storage media**, together with **thermal oil** as a **HTF** due to the limited range of possibilities offered.

### 2.4.2 Seawater Desalination Plant

As for the seawater desalination plant, we opt for the distillation processes over the membrane process, specifically a **multi-stage flash desalination plant** since it is the one that best is combined with thermal solar energy. In the membrane processes, more electric energy is required, and a more complicated maintenance is needed. Intuitively, it will always seem more logical to use the solar energy as heat, directly from the sun rather than use that heat to then generate electricity to run the system.

### 2.4.3 Domestic Hot Water

In the present project, the following sections are not developed. In any case, we will mention that the optimal choice would be in the non-concentrated collector types. The flat plate collectors are widely used for this purpose, although the evacuated tube collectors might be more efficient. A further viability study should be undertaken, taking into account economical aspects as well as space use.

### 2.4.4 Air Conditioning System

For this option, an absorption machine should be contemplated, since the traditional mechanical compressor systems require great amounts of electricity to operate. In this case, either the evacuated plate collectors which offer a higher operating temperature, or a cogeneration system with the power plant would be the most feasible options to be considered.

# 3. WATER DEMAND ESTIMATION

In the following section, the total water quantity required by the housing estate and its population is estimated. The calculations are divided into different sections:

- Human consumption
- Swimming pools and ornamental water landscaping
- Maintenance
- Golf course and gardens

## 3.1 HUMAN CONSUMPTION

This estimation refers to basic needs of the population in the housing estate (guests and staff). It contemplates primarily water for hygiene, for drinking and for cooking.

- *Population:* 5000 families.
- *Members per family:* It is considered that each family has an average of 4 people.
- *Daily needs per person:* The needs for each person according to WHO (World Health Organization) and UNICEF (United Nations Children's Funds) is approximately **80 liters/person*day** (2). Increasing the amount of water intended primarily for personal hygiene (showers, baths, etc.) and for cooking, it is estimated that each person in the housing estate would consume 150 liters/person*day.

  This totals up to:

$$\boxed{\boldsymbol{Q_{HC}} = 5000 family \cdot 4 \frac{person}{family} \cdot 150 \frac{liter}{person \cdot day} = \mathbf{3.000.000} \ \frac{\boldsymbol{liters}}{\boldsymbol{day}}} \qquad (3.1)$$

## 3.2 MAINTENANCE

In this section we include the water assigned for maintenance, such as cleaning (floors, bathrooms, dishes, etc.) and laundry service (rooms, restaurants, guests). We estimate that it is 10% of the total water used for human consumption. This is:

$$\boxed{\boldsymbol{Q_{Maint}} = 10\% \ of \ 3.000.000 l = \mathbf{300.000} \ \frac{\boldsymbol{liters}}{\boldsymbol{day}}} \qquad (3.2)$$

## 3.3 SWIMMING POOLS AND LANDSCAPING

For this purpose, the amount of water to fill 3 Olympic swimming pools has been considered necessary.

The surface of an Olympic swimming pool is (50x22) m2.

The depth goes from 1,3m to 2,1m.

The total volume of each Olympic pool is of 2.500$m^3$, or 2.500.000 liters.

Therefore,

$$\mathbf{Q_{SP}} = 3 \cdot 2.500.000 \text{ liters} = \mathbf{7.500.000 \text{ liters.}} \quad (3.3)$$

This is the initial amount of water needed, but since the pools are constantly operable (all year around), the actual daily need of water for them, initial filling up excluded, would be the one due to compensate evaporation and filtration losses.

In a relatively dry, sunny environment, using *silex* filters, we esteem the evaporation rate is of 8mm/$m^2$·day (3).

Therefore:

$$\boxed{\mathbf{Q_{ev+filt}} = 0{,}008 \frac{m}{day} \cdot 3 \cdot (50x22) m^2 = 26{,}4 \frac{m^3}{day} = \mathbf{26.400} \frac{\boldsymbol{liters}}{\boldsymbol{day}}} \quad (3.4)$$

## 3.4 GOLF COURSE AND GARDENS

In a southern country, a golf course has specific vegetation that is not a part of the natural environment. In order to maintain the land green with grass, high quantities of water are needed. It is esteemed that approximately 10.000$m^3$ (4) of water are needed yearly per hectare (10.000$m^2$) of golf course. In a sunny, dry environment where rainfall is low, a golf course is not the most sustainable idea. But, if it were to be built, the estimation would be for a surface of 25 hectares (9 holes). Together with this, it is estimated that the amount of water necessary for watering all of the gardens in the area is also included.

Therefore, we should need:

$$\boxed{\boldsymbol{Q_{Golf}} = 25\ ha \cdot 10.000 \frac{m^3}{ha \cdot year} \cdot 1000 \frac{liters}{m^3} \cdot \frac{1 year}{365\, days} = \mathbf{684.931} \frac{\boldsymbol{liters}}{\boldsymbol{day}}} \quad (3.5)$$

## 3.5 TOTAL QUANTITY

Consequently, as a sum of all separate estimations, we obtain the following grand total:

| | **WATER DEMAND** (LITERS/DAY) |
|---|---|
| HUMAN CONSUMPTION | 3.000.000 |
| SWIMING POOLS/ LANDSCAPING | 26.400 |
| MAINTENANCE | 300.000 |
| GOLF COURSE/GARDENS | 684.931 |
| **TOTAL** | **4.011.331** |

Table 1 Total water demands

# 4. ELECTRIC DEMAND ESTIMATION

The following points are the requirements that our housing estate demands, independent of the system we decide to implement.

- ELECTRICITY:
  - Power for lighting, appliances, laundry, etc.

- DESALINATION PLANT:
  - Primary energy needed: heat (desalination process)
  - Secondary energy: electricity (pumps, valves)

- AIR CONDITIONING (AC):
  - Cold air
  - Hot air

- DOMESTIC HOT WATER (DHW):
  - Mainly hygiene purposes (kitchen, bathroom, etc)

In this project, we are only going to work directly with the power generation plant (electricity) and the desalination plant (treated water). Nonetheless, we estimate the energy demand for the remaining parts of the system, such as AC and DHW in order to know how much power we will need to generate to achieve to run a complete system.

For the AC and the DHW, we can either design a standard, conventional, electricity-run system (mechanical compressors and electrical water heaters) or we can use alternative methods, such as absorption machines and flat plate or vacuum tube collectors.

## 4.1 ELECTRICAL DIMENSIONING FOR STANDARD SYSTEM

The following is an estimation of the amount of electricity needed to run the whole system considering that the AC and the DHW are withdrawing the energy needed from standard electrical installations such as mechanical compressors or electric hot water heaters.

### 4.1.1 Desalination Plant

It should provide **4012 $m^3$/day** of desalinated water to satisfy demands. The system we choose to implement is the multi-stage flash (MSF). The average electrical demand to run a plant of this nature is [3500-7000] kWh/AF (5)[2].

Our atmospheric conditions are not too critical, especially considering the geographical position of our desalination plant, situated in a southern country where the water temperature is approximately 20ºC year round and the water quality levels of more than half of the amount of water to de processed are not intended for direct human ingestion. Therefore, from the energy interval previously mentioned, we choose an average **5500 kWh/AF**.

Our water necessity is of 4012 $m^3$/day.

Therefore, the electrical demand for our desalination plant is:

$$\boldsymbol{ED_{desalination}} = 5500\,\frac{kWh}{AF} \cdot 0{,}00082\,\frac{AF}{m^3} \cdot 4012\,\frac{m^3}{day} = \mathbf{18094{,}12}\,\frac{\boldsymbol{kWh}}{\boldsymbol{day}} \qquad (4.1)$$

### 4.1.2 Standard Air Conditioning Installation

We choose standard, split fix air conditioning systems, which have one exterior unit and one or various interior units. Optionally, they have heat pumps as well. In our case, we would choose units that are capable of both heating and cooling the environment. In order to proceed with the estimation, we need to define a standard room which we want to condition.

Average room dimensioned:

- Room surface: aprox.25 $m^2$
- Exterior wall oriented towards the East, 4$m^2$ surface, with (1,5x1,5)$m^2$window.
- Exterior wall oriented towards the South, 5$m^2$ surface, with (1,5x1,5)$m^2$window.
- Height of ceiling: 2,5m
- Adjacent rooms not acclimatized.

For this average room dimensioned, we would need approximately 2,4 kW/h (6).

[2]For future reference, the average heat quantity needed is 22.000 kWh/AF. 1 AF (acre-foot) =1233,5 $m^3$. Therefore, 1$m^3$=0,00082 AF.

The current more environmentally friendly AC models available in the market have a cooling power superior to 4kW, sufficient to fulfill our demands. Taking an average between standard models, we need **1,3kW/hour** (7). Given a 10h/day use and that there are 5000 rooms plus 2500 extra systems for common spaces, we can obtain the following electrical demand for air conditioning:

$$1{,}3\frac{kW}{system}\cdot 10\frac{h}{day}=13\frac{kWh}{day\cdot system}$$

$$\boxed{\boldsymbol{ED_{AC}}=13\frac{kWh}{day\cdot system}\cdot 7500\ systems=\mathbf{97.500}\frac{\boldsymbol{kWh}}{\boldsymbol{day}}} \qquad (4.2)$$

Since the AC systems can also generate hot air, no further installations or calculations are needed.

### 4.1.3 Domestic Hot Water Electric Heaters

We are dealing with 3.000.000 l/day of water for direct human consumption. As already established, we have 150 liters/person·day. We consider that 50% of this amount would be heated. This would leave us with 1.500.000 liters of water to heat.

Since there is initially no gas available in the premises, we will assume the standard water heating method will be with electric heaters. According to main manufacturers[3], an average of (2200-2400) W is needed to heat 150 liters, and a 4 hour time span, from 10ºC to 60ºC. We consider 300.000 liters of hot water for maintenance. Therefore, our total water heated is **1.800.000 liters**.

We have 2400w · 4 hours = 9,6kWh/day per every 150 liters. With a simple proportion, we can calculate the electric demand for hot water for housing:

$$\boxed{\boldsymbol{ED_{Hot\_Water}}=\mathbf{115.200}\frac{\boldsymbol{kWh}}{\boldsymbol{day}}} \qquad (4.3)$$

### 4.1.4 Electricity Demand

In this section, we estimate the amount of electricity needed to supply the whole estate.

[3] Product manuals from Junkers, Saunvier Duval, etc.

This estimation is based on references of other existing housing estates and hotels of similar characteristics. We are taking into account the characteristics of the following type of hotel (8), which adjusts to our model. We will consider this model a "hotel unit":

- Superior category (4 or 5 stars)
- 300 rooms each, including suites
- 10/15 common area event halls, with capacity for 1000 persons
- 1 Restaurant and 1 snack bar
- Laundry and room service 24 hours
- Fitness center
- Climate: warm

Carrying out a comparison between our housing estate and other existing ones similar in size and in features, we reach the conclusion that **12 hotel units** (9) of the previously defined are needed to constitute our estate.

This electricity is intended for:

- Rooms (lighting, TV, …) (15%)
- Kitchen (14%)
- Public areas (8%)
- Halls/Function rooms (11%)
- Laundry (8%)
- Elevators (3%)
- Exterior Illumination (2%)
- Others (11%)

In the following table we include the distribution of energy consumed daily on average each month by one hotel unit. The energy units are kWh.

| (Energy in kWh) | | | | | | | | | | | | |
|---|---|---|---|---|---|---|---|---|---|---|---|---|
| | JAN | FEB | MAR | APR | MAY | JUN | JUL | AUG | SEP | OCT | NOV | DEC |
| HOUR | | | | | | | | | | | | |
| 00 to 01 | 5577 | 5696 | 5843 | 5556 | 6450 | 6816 | 7044 | 6452 | 6695 | 6054 | 5460 | 5991 |
| 01 to 02 | 3334 | 3343 | 3371 | 3135 | 3870 | 4305 | 4719 | 4075 | 4017 | 3416 | 3150 | 3400 |
| 02 to 03 | 3076 | 3085 | 3110 | 2893 | 3612 | 4054 | 4486 | 3838 | 3749 | 3152 | 2906 | 3137 |
| 03 to 04 | 3007 | 3016 | 3041 | 2828 | 3543 | 3987 | 4424 | 3774 | 3677 | 3081 | 2841 | 3067 |
| 04 to 05 | 3299 | 3309 | 3336 | 3103 | 3836 | 4272 | 4688 | 4044 | 3981 | 3381 | 3117 | 3365 |
| 05 to 06 | 3162 | 3171 | 3197 | 2973 | 3698 | 4138 | 4564 | 3917 | 3838 | 3240 | 2987 | 3224 |
| 06 to 07 | 3007 | 3016 | 3041 | 2828 | 3543 | 3987 | 4424 | 3774 | 3677 | 3081 | 2841 | 3067 |
| 07 to 08 | 6162 | 6179 | 6230 | 5794 | 6774 | 7204 | 7501 | 6819 | 7031 | 6313 | 5821 | 6283 |
| 08 to 09 | 6497 | 6566 | 6671 | 6265 | 7290 | 7720 | 7998 | 7307 | 7567 | 6826 | 6233 | 6710 |
| 09 to 10 | 6187 | 6308 | 6460 | 6129 | 7146 | 7580 | 7869 | 7175 | 7417 | 6679 | 6036 | 6479 |
| 10 to 11 | 6823 | 6997 | 7205 | 6883 | 7970 | 8403 | 8661 | 7954 | 8273 | 7500 | 6732 | 7212 |
| 11 to 12 | 6411 | 6688 | 6993 | 6807 | 7889 | 8324 | 8588 | 7880 | 8189 | 7417 | 6533 | 6961 |
| 12 to 13 | 6411 | 6687 | 6992 | 6806 | 7889 | 8324 | 8587 | 7879 | 8188 | 7416 | 6533 | 6961 |
| 13 to 14 | 6256 | 6584 | 6938 | 6817 | 7935 | 8405 | 8711 | 7956 | 8236 | 7428 | 6482 | 6888 |
| 14 to 15 | 6617 | 7152 | 7710 | 7778 | 9031 | 9543 | 9863 | 9033 | 9373 | 8476 | 7204 | 7594 |
| 15 to 16 | 5981 | 6721 | 7475 | 7803 | 9128 | 9710 | 10115 | 9191 | 9474 | 8503 | 6985 | 7284 |
| 16 to 17 | 6600 | 7445 | 8305 | 8696 | 10221 | 10917 | 11429 | 10334 | 10608 | 9476 | 7759 | 8084 |
| 17 to 18 | 6393 | 7342 | 8300 | 8814 | 10487 | 11321 | 11998 | 10716 | 10885 | 9603 | 7755 | 8043 |
| 18 to 19 | 6256 | 7411 | 8569 | 9307 | 11154 | 12114 | 12928 | 11467 | 11577 | 10141 | 8007 | 8242 |
| 19 to 20 | 6239 | 7083 | 7940 | 8357 | 10000 | 10847 | 11559 | 10268 | 10380 | 9106 | 7419 | 7716 |
| 20 to 21 | 5680 | 6317 | 6968 | 7209 | 8565 | 9234 | 9772 | 8741 | 8890 | 7855 | 6510 | 6809 |
| 21 to 22 | 6076 | 6506 | 6959 | 6958 | 8157 | 8693 | 9075 | 8228 | 8466 | 7582 | 6502 | 6873 |
| 22 to 23 | 5835 | 6162 | 6512 | 6421 | 7513 | 7994 | 8331 | 7567 | 7798 | 6996 | 6084 | 6458 |
| 23 to 24 | 5457 | 5679 | 5926 | 5754 | 6732 | 7162 | 7462 | 6780 | 6987 | 6270 | 5537 | 5904 |
| SUM | 130343 | 138463 | 147092 | 145914 | 172433 | 185054 | 194796 | 175169 | 178973 | 158992 | 137434 | 145752 |
| TOTAL SUM | 2811718 | | | | | | | | | | | |

**Table 2: Distribution of energy consumed daily on average each month by one hotel unit**

The following table presents the total energy consumed every hour in each month (on average) and for our 12 hotel units. In other words, we will have the total amount of energy that our entire system demands in one year.

| (Energy in kWh) | | | | | | | | | | | | |
|---|---|---|---|---|---|---|---|---|---|---|---|---|
| | JAN | FEB | MAR | APR | MAY | JUN | JUL | AUG | SEP | OCT | NOV | DEC |
| HOUR | | | | | | | | | | | | |
| 00 to 01 | 2074644 | 1913856 | 2173596 | 2000160 | 2399400 | 2453760 | 2620368 | 2400144 | 2410200 | 2252088 | 1965600 | 2228652 |
| 01 to 02 | 1240248 | 1123248 | 1254012 | 1128600 | 1439640 | 1549800 | 1755468 | 1515900 | 1446120 | 1270752 | 1134000 | 1264800 |
| 02 to 03 | 1144272 | 1036560 | 1156920 | 1041480 | 1343664 | 1459440 | 1668792 | 1427736 | 1349640 | 1172544 | 1046160 | 1166964 |
| 03 to 04 | 1118604 | 1013376 | 1131252 | 1018080 | 1317996 | 1435320 | 1645728 | 1403928 | 1323720 | 1146132 | 1022760 | 1140924 |
| 04 to 05 | 1227228 | 1111824 | 1240992 | 1117080 | 1426992 | 1537920 | 1743936 | 1504368 | 1433160 | 1257732 | 1122120 | 1251780 |
| 05 to 06 | 1176264 | 1065456 | 1189284 | 1070280 | 1375656 | 1489680 | 1697808 | 1457124 | 1381680 | 1205280 | 1075320 | 1199328 |
| 06 to 07 | 1118604 | 1013376 | 1131252 | 1018080 | 1317996 | 1435320 | 1645728 | 1403928 | 1323720 | 1146132 | 1022760 | 1140924 |
| 07 to 08 | 2292264 | 2076144 | 2317560 | 2085840 | 2519928 | 2593440 | 2790372 | 2536668 | 2531160 | 2348436 | 2095560 | 2337276 |
| 08 to 09 | 2416884 | 2206176 | 2481612 | 2255400 | 2711880 | 2779200 | 2975256 | 2718204 | 2724120 | 2539272 | 2243880 | 2496120 |
| 09 to 10 | 2301564 | 2119488 | 2403120 | 2206440 | 2658312 | 2728800 | 2927268 | 2669100 | 2670120 | 2484588 | 2172960 | 2410188 |
| 10 to 11 | 2538156 | 2350992 | 2680260 | 2477880 | 2964840 | 3025080 | 3221892 | 2958888 | 2978280 | 2790000 | 2423520 | 2682864 |
| 11 to 12 | 2384892 | 2247168 | 2601396 | 2450520 | 2934708 | 2996640 | 3194736 | 2931360 | 2948040 | 2759124 | 2351880 | 2589492 |
| 12 to 13 | 2384892 | 2246832 | 2601024 | 2450160 | 2934708 | 2996640 | 3194364 | 2930988 | 2947680 | 2758752 | 2351880 | 2589492 |
| 13 to 14 | 2327232 | 2212224 | 2580936 | 2454120 | 2951820 | 3025800 | 3240492 | 2959632 | 2964960 | 2763216 | 2333520 | 2562336 |
| 14 to 15 | 2461524 | 2403072 | 2868120 | 2800080 | 3359532 | 3435480 | 3669036 | 3360276 | 3374280 | 3153072 | 2593440 | 2824968 |
| 15 to 16 | 2224932 | 2258256 | 2780700 | 2809080 | 3395616 | 3495600 | 3762780 | 3419052 | 3410640 | 3163116 | 2514600 | 2709648 |
| 16 to 17 | 2455200 | 2501520 | 3089460 | 3130560 | 3802212 | 3930120 | 4251588 | 3844248 | 3818880 | 3525072 | 2793240 | 3007248 |
| 17 to 18 | 2378196 | 2466912 | 3087600 | 3173040 | 3901164 | 4075560 | 4463256 | 3986352 | 3918600 | 3572316 | 2791800 | 2991996 |
| 18 to 19 | 2327232 | 2490096 | 3187668 | 3350520 | 4149288 | 4361040 | 4809216 | 4265724 | 4167720 | 3772452 | 2882520 | 3066024 |
| 19 to 20 | 2320908 | 2379888 | 2953680 | 3008520 | 3720000 | 3904920 | 4299948 | 3819696 | 3736800 | 3387432 | 2670840 | 2870352 |
| 20 to 21 | 2112960 | 2122512 | 2592096 | 2595240 | 3186180 | 3324240 | 3635184 | 3251652 | 3200400 | 2922060 | 2343600 | 2532948 |
| 21 to 22 | 2260272 | 2186016 | 2588748 | 2504880 | 3034404 | 3129480 | 3375900 | 3060816 | 3047760 | 2820504 | 2340720 | 2556756 |
| 22 to 23 | 2170620 | 2070432 | 2422464 | 2311560 | 2794836 | 2877840 | 3099132 | 2814924 | 2807280 | 2602512 | 2190240 | 2402376 |
| 23 to 24 | 2030004 | 1908144 | 2204472 | 2071440 | 2504304 | 2578320 | 2775864 | 2522160 | 2515320 | 2332440 | 1993320 | 2196288 |
| SUM | 48487596.00 | 46523568.00 | 54718224.00 | 52529040.00 | 64145076.00 | 66619440.00 | 72464112.00 | 65162868.00 | 64430280.00 | 59145024.00 | 49476240.00 | 54219744.00 |
| TOTAL SUM (kWh) FOR 12 HOTEL UNITS | 697921212.00 | | | | | | | | | | | |

**Table 3: distribution of energy consumed daily on average each month by 12 hotel units**

The total sum of energy for the entire year is **697.921 MWh**.

This amount divided into the hours in a year (8760h) gives us the average power our system will demand. This amount is **79,67 MW.**

If we consider that the daytime goes from 8:00 to 19:00 and that it is nighttime the rest of the day, we will have average values of power of:

98,3MW during daytime

65,6MW during nighttime

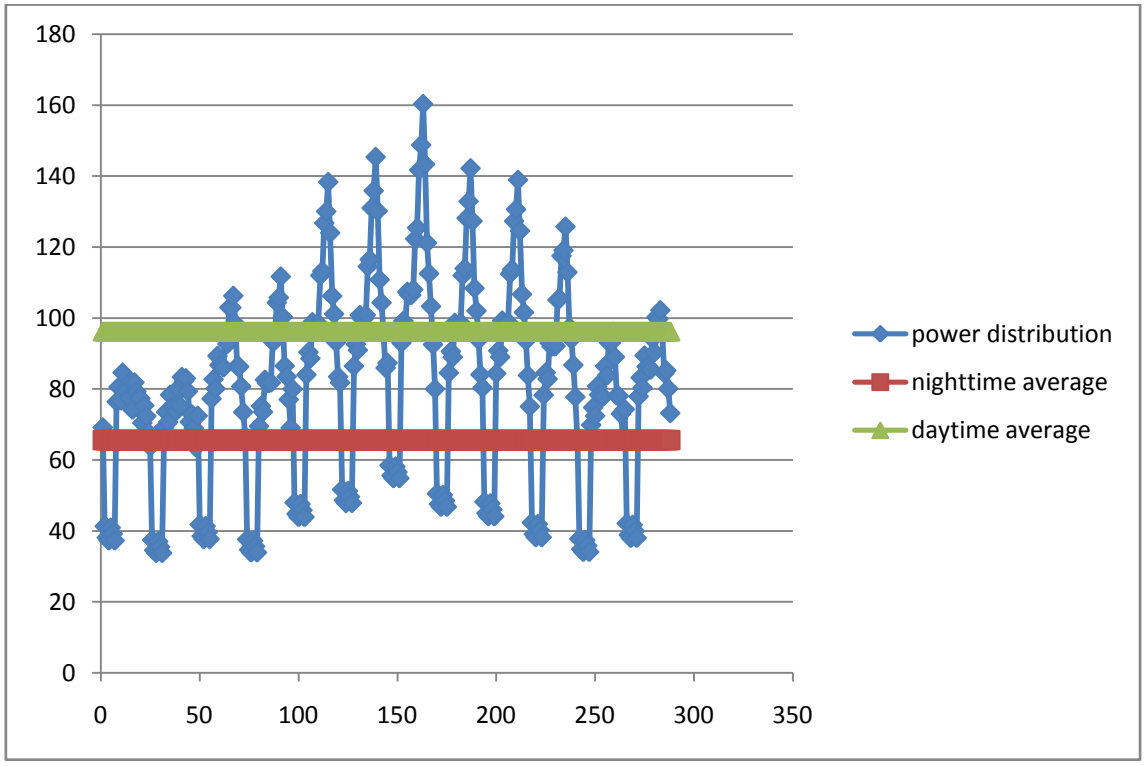


**Figure 36:** Power average distribution for each month of the year

We notice that the maximum energy required on average throughout the whole year corresponds to July, from 18:00 to 19:00 ($\frac{4.809.216\ kWh}{30 days} = 160.307{,}2 kWh$) and the minimum amount is from 03:00 to 04:00 in the month of April ($\frac{1.018.080\ \text{kWh}}{30 days} = 33.936 kWh$).

Therefore, for dimensioning purposes, to get an idea of the magnitude of our system, if we were to imagine that all hours in the year required only the minimum amount of power, 33.936 kWh per hour, we would need a power plant that would have to constantly generate

$$\boxed{Min. Power\ Generation \approx 34MW}$$

At the same time, if we were to calculate the power needed considering that every hour of the year demanded the maximum power of 160.307,2 kWh, we would obtain:

$$\boxed{Maximum\ Power\ Generation \approx 160MW}$$

The problem we encounter now is to decide how much of the demand we should cover. In other words, the doubt comes up whether it is better to be able to cover maximum demand with our solar system or is it more convenient to achieve coverage of an average demand consumption level and supply the remaining needs at peak points with electricity directly from the grid.

The following graph shows the power demand (kWh) over the year and the day percentage each of these values appear.

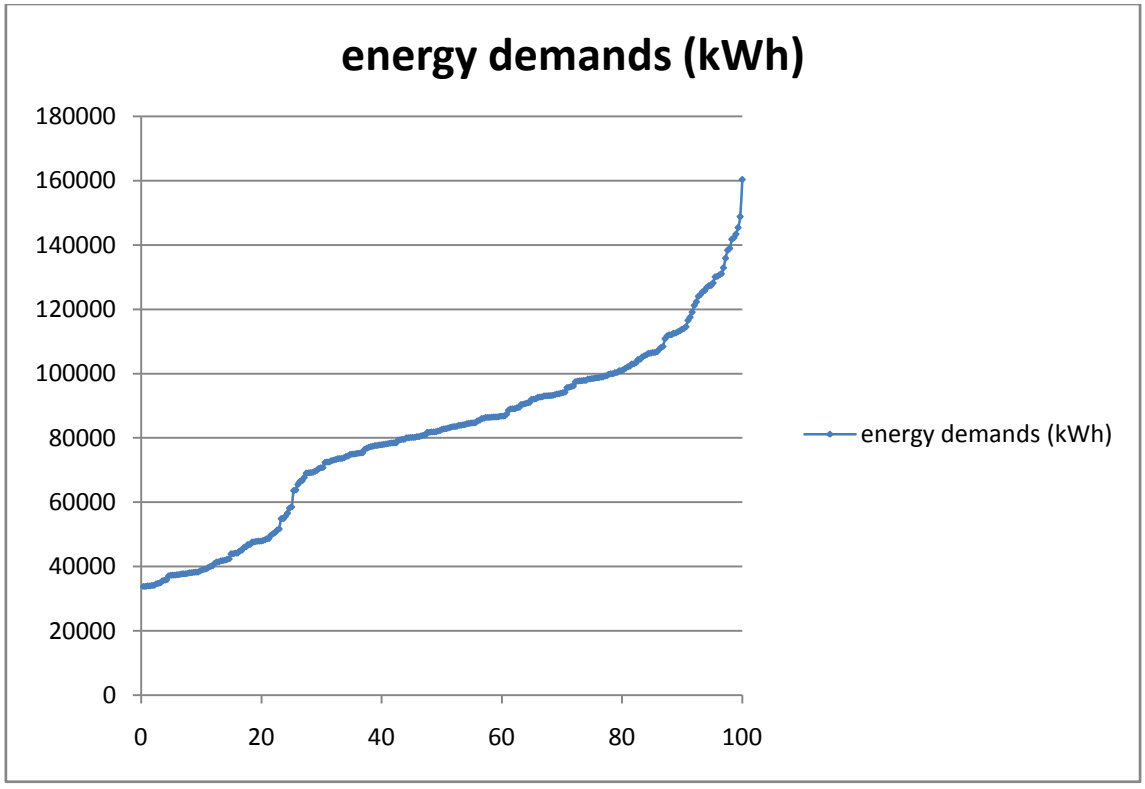


**Figure 37: Power demand (kWh) over the year and the percentage each of these values appear in days**

One can observe that approximately 50% of the demand values are between 75 and 100 MW. Another graph that can be included is the following one, which reflects the frequency in which certain power demands appear:

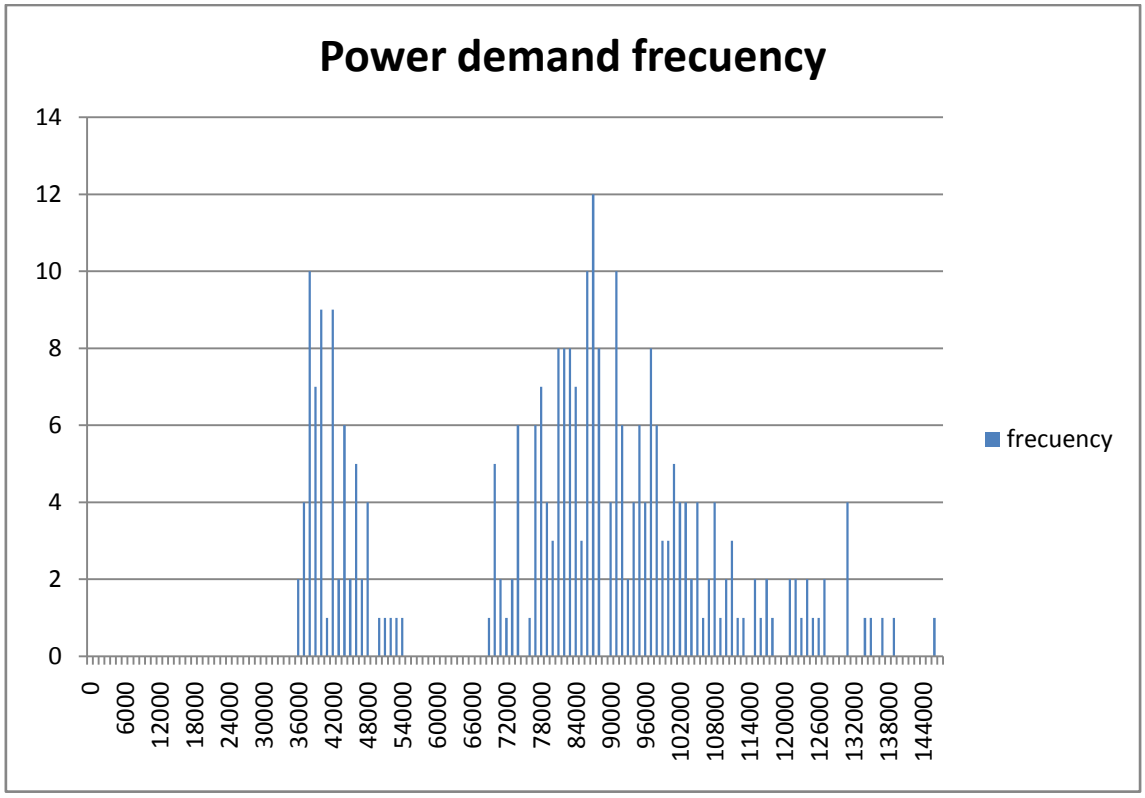


**Figure 38:** Power demand frequency

The initial approach we will follow to estimate the electric demand needed by our system will be to contemplate the total system needs for an entire year. Then, we will adjust our power generation plant generation to this yearly demand. After we have coordinated this initial global balance, we will try to adjust the variable demand and power generation throughout the day.

| | **ENERGY DEMAND** (MWh/year) | **PERCENTAGE** (%) |
|---|---|---|
| DESALINATION PLANT (ELECTRIC) | 6605 | 0.84 |
| STANDARD AC SYSTEMS | 35588 | 4.54 |
| DOMESTIC HOT WATER (ELECTRIC) | 42048 | 5.37 |
| ELECTRICITY | 697921 | 89.22 |
| **TOTAL** | 782162 | 100 |

**Table 4: Percentage of energy demand**

If we observe the results obtained, we realize that the demand of electricity is about a 10% for the AC and the DHW systems. This can be optimized and therefore other options should be contemplated for these two sections of our global system. Intuitively, it doesn't seem too efficient to transform the sun's energy into electricity in order to heat up water with resistances

or to electrically activate a mechanical compressor to enjoy AC. Therefore, we present the following layout of electrical demand for our system.

## 4.2 ELECTRICAL DEMAND FOR ALTERNATIVE SYSTEM

The desalination plant and the electricity generation power plant remain the same. The changes occur in the AC and DHW systems.

### 4.2.1 Alternative Air Conditioning Installation

As an alternative method, we will use an **absorption machine** for the air conditioning system. It will run primarily with heat, obtained either from solar vacuum collectors or from solar troughs. Still, it requires a minimum amount of electricity to run. We estimate that this amount is 10% of the requirements of the standard system.

### 4.2.2 Alternative Hot Water For Housing

We will use solar collectors for this matter, either flat plate collectors or **solar vacuum collectors** that will be installed in the vicinity of the housing (roofs, for example). We also contemplate that a 10% of the energy needed to run the standard systems will be what is required for this layout, in order to run the pumps, valves, regulators, etc.

This way, we reach the following new electrical demand table for our system:

| | **ENERGY DEMAND** (MWh/year) | **PERCENTAGE** (%) |
|---|---|---|
| DESALINATION PLANT (ELECTRIC) | 6605 | 0.92 |
| STANDARD AC SYSTEMS | 3558 | 0.49 |
| DOMESTIC HOT WATER (ELECTRIC) | 4204 | 0.59 |
| ELECTRICITY | 697921 | 97.98 |
| **TOTAL** | 712288 | 100 |

Table 5: Percentage of new electric demand

As we can see, we have reached a more reasonable electrical demand for the AC and the DHW. Our total annual electric demand is:

$$\boxed{\boldsymbol{Annual\ electrical\ demand = 712.288 MWh}}$$

$$\boxed{\boldsymbol{Average\ Power\ (MW) = \frac{712288 Mwh}{8760 h} = 81,31 MW}}$$

With the total energy demand, the daytime and nighttime values increase slightly to:

| |
|---|
| 99,05MW during daytime |
| 66,48MW during nighttime |

The following table includes a resume of the important values calculated, such as the average power of the entire system, the average energy demand during day and night, the maximum and minimum power generation values and, again, the annual total electric demand of our system:

| | |
|---|---|
| Annual demand | 712.288 MWh |
| Average hourly power demanded | 81,31 MW |
| Average daytime (11 hours/day) | 99,05 MW |
| Average nighttime (13 hours/day) | 66,48 MW |
| Minimum power demand in year | ≈36 MW |
| Maximum power demand in year | ≈162 MW |

Table 6: Electric demand values

## 4.3 DAILY DEMAND CURVES

In the following section, we include daily electrical demand curves. They are electrical demand in real time from the energy consumption in Spain, courtesy of "Red Electrica Española" [36]. They give us a good idea of what the standard shape of an electric demand curve looks like. The days contemplated are all weekdays. There is one example for each trimester of the year, having data from January, April, July and October. In all of the examples one can see the maximum and minimum demand values in reference to the time of day. This behavior will help us further along when we deal with our own demand curves.

- January 15th, 2008:

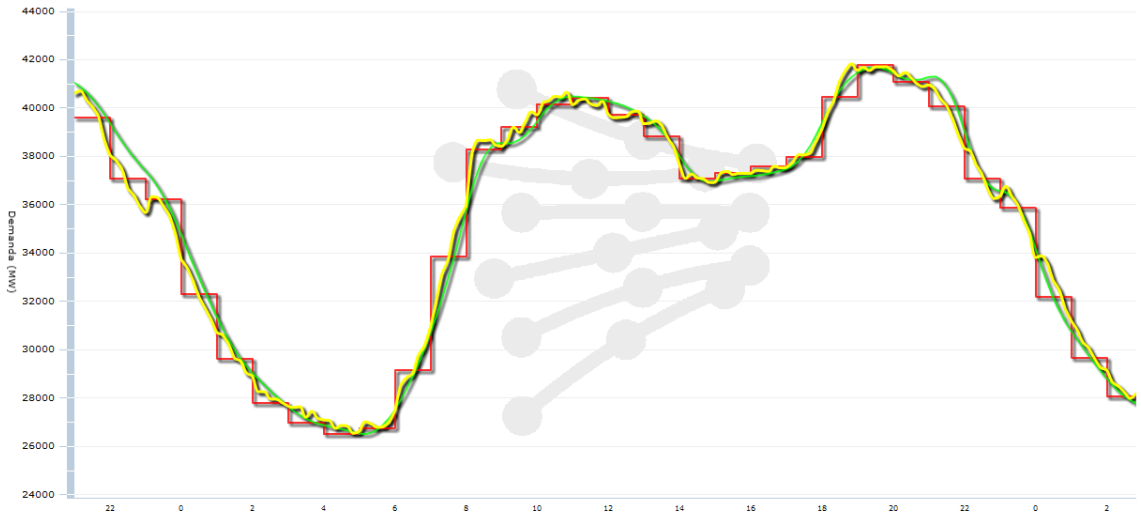


**Figure 39:** Daily demand curve for Jan. 15th [36]

- April 15th, 2008:

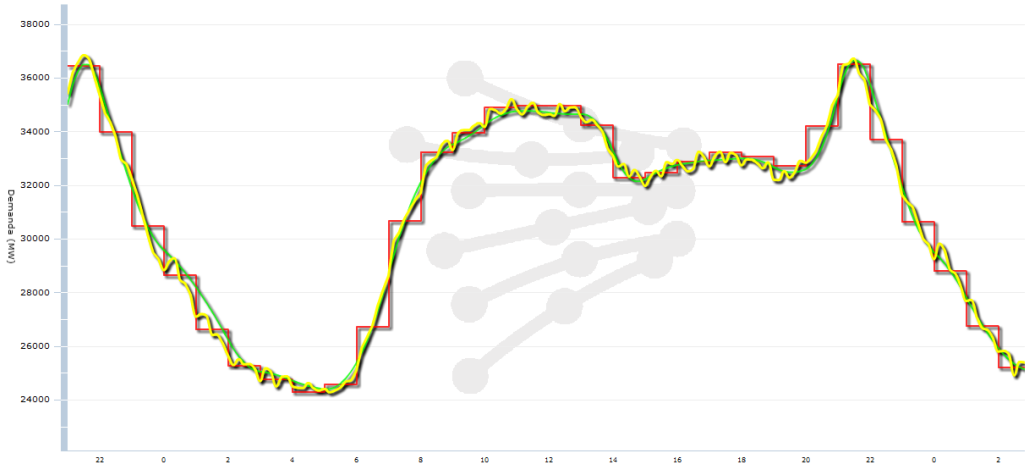


**Figure 40:** Daily demand curve for Apr. 15th [36]

- July 15th, 2008:

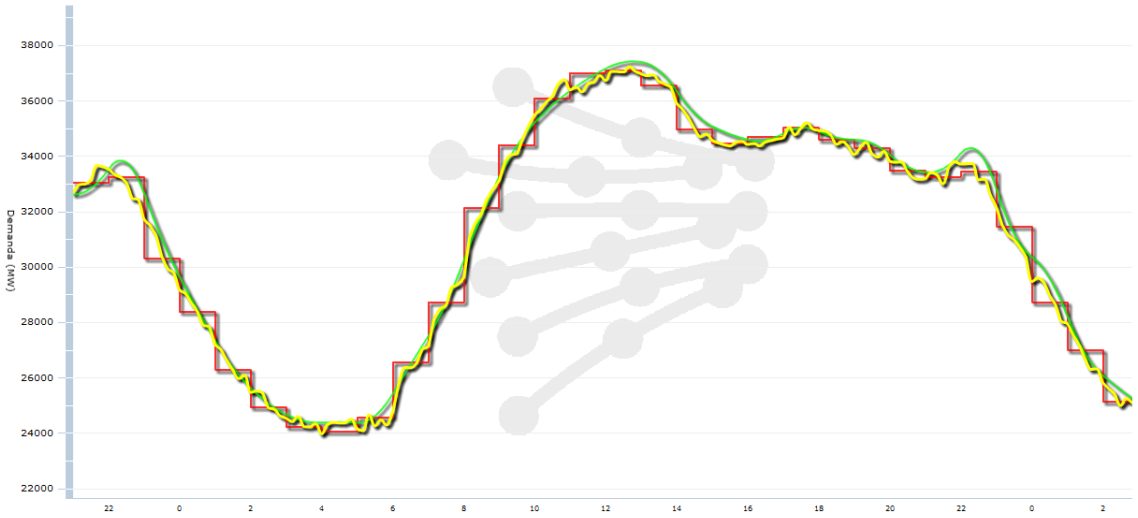


**Figure 41:** Daily demand curve for Jul. 15th [36]

- October 15th, 2008:

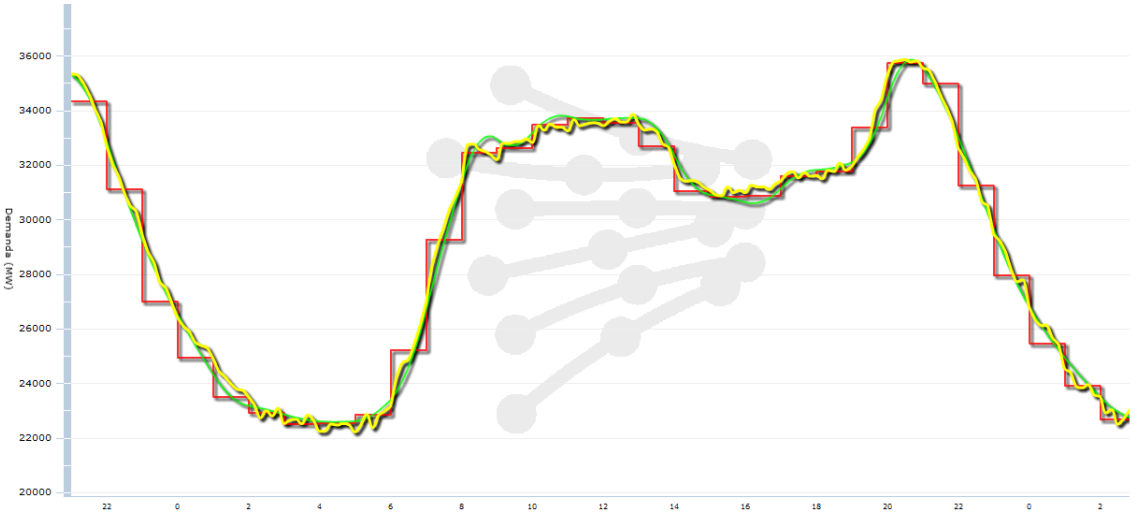


**Figure 42:** Daily demand curve for Oct. 15th [36]

# 5. SOLAR FIELD

## 5.1 INTRODUCTION

In this section, the information about the solar field needed to supply the power cycle with energy is laid out. As a reference, we will use in various occasions mentions of existing SEGS solar field dispositions, such as the ones located in the Mojave Desert, in Kramer Junction, California (mainly SEGS VI, from which there is available a lot of detailed, empirical, reliable data).

A solar field is shown from an aerial perspective in the following picture.

**Figure 43**: Solar field at Kramer Junction [37]

In general, the heat transfer fluid (HTF) is pumped from the steam heat exchangers in the power cycle to the solar fields through supply headers. The supply headers distribute the HTF through the different parallel loops of solar collectors. The HTF travels away from the supply (cold) header through one row of the collector loop and back toward the return (hot) header through the other row. The hot HTF from the collector loops then merges in the return headers and is pumped back to the central power plant.

The gross HTF temperature rise across the solar field during peak summer periods is on the order of 100°C, from a cold inlet temperature of 293°C to a hot outlet temperature around

390°C. During cloudy days and off-summer periods, the temperature rise will be lower for a constant flow rate. The actual temperature achieved at the solar field outlet depends on a number of variables including:

- HTF flow rate
- Solar field inlet temperature
- Incident solar radiation
- Thermal losses
- Cleanliness of the collectors
- Tracking precision
- Surface properties of the collector field materials.

The solar collector field is modeled as one single component within TRNSYS. Before we go into the details of our specific model, a general information flow diagram for a solar field model is shown in the next Figure.

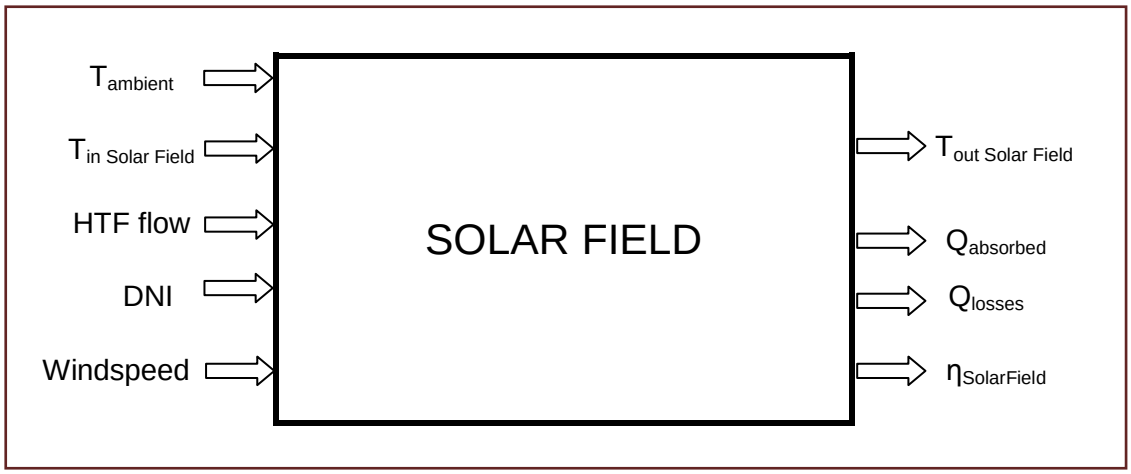


**Figure 44**: General Flow diagram for solar field component

In the specific model we will be using (Type536), the necessary inputs to the solar field are:

- The heat transfer fluid temperature at the field inlet [°C]
- The volumetric inlet flow rate of the HTF [$m^3/s$]
- The ambient air temperature [°C]
- Beam radiation over the field [W/m2]
- The incidence angle
- The maximum outlet HTF temperature [ºC]

The *incidence angle*[2] refers to the angle between the beam radiation on a surface and the plane normal to that surface. The angle of incidence will vary over the course of the day (as well as throughout the year) and will heavily influence the performance of the collectors. The angle of incidence results from the relationship between the sun's position in the sky and the orientation of the collectors for a given location.

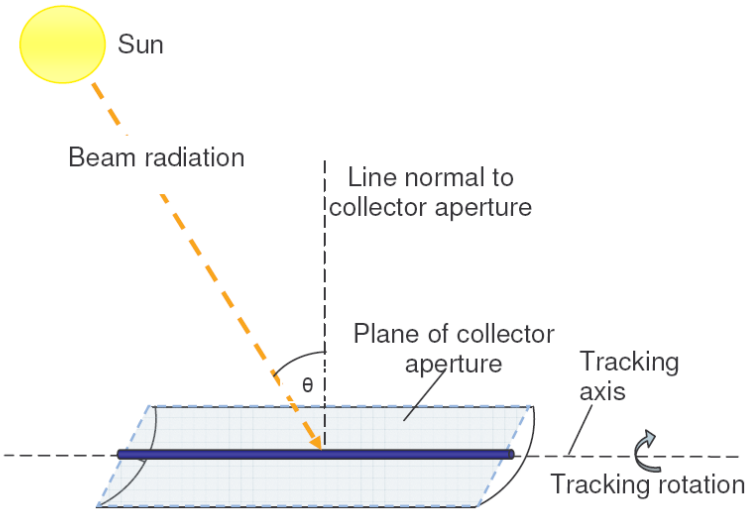


**Figure 45**: Angle of incidence on a parabolic trough collector [38]

The parameters defined in such model (Type536) are the following:

- Number of collectors in series
- Number of collectors in parallel
- Aperture area [$m^2$]
- Concentration ratio
- Intercept efficiency (FrTran)
- Efficiency slope (FrUI) [$kJ/h \cdot m^2 \cdot K$]
- Fluid specific heat [$kJ/kg \cdot K$]
- Logical unit
- Number of IAM points
- Tested flow rate [$kJ/m^2 \cdot s$]

## 5.2 TRNSYS TYPE 536: LINEAR PARABOLIC CONCENTRATING SOLAR COLLECTOR

Type536 is the specific TRNSYS element we will be using for our solar field simulation model. It models a type of solar collector called a linear parabolic concentrator that is commonly used in high temperature applications. In the simplest form of a linear parabolic concentrator, fluid passes through a long evacuated tube located in the focal line of each parabolic trough that runs along an east-west axis and is horizontal to the plane of the ground or which runs on a north-south axis and is in a plane tilted with respect to the ground. In doing so, it absorbs concentrated solar radiation. It is chosen for its simplicity because this way it offers less compatibility problems when it must interact with the other components. It offers as well less convergence problems. The Type536 parabolic concentrator is modeled based on theoretical equations developed in Solar Engineering of Thermal Processes (10).

### 5.2.1 Detailed description

The evacuated tube in a parabolic concentrating solar collector is located at the focus of a parabola made of some highly reflective material. As such, parabolic concentrating collectors do not receive a significant amount of diffuse radiation; their useful energy output is dictated by beam radiation as all the beam radiation incident on the aperture area (the area formed by the "mouth" of the parabola) is reflected onto the absorber contained in the evacuated tube. Thermal losses from parabolic concentrating collectors occur only from the absorbing surfaces which, while high in temperature, have comparatively small area. Because beam radiation is of such importance to the performance of a linear parabolic concentrating solar collector, the reflector is often tracked so that beam radiation remains within its acceptance angle. Figure 46 shows some schematic views of a linear parabolic concentrating collector.

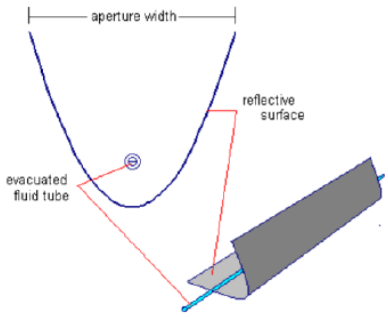


**Figure 46**: Linear Parabolic Concentrating Solar Collector Schematic [39]

#### 5.2.1.1 Concentration ratio

The *concentration ratio* (10) is the area of the aperture to the area of the receiver.

#### 5.2.1.2 Intercept efficiency

The *intercept efficiency* (11) is defined as the fraction of the rays incident on the collector aperture that reach the absorber. In most concentrating collectors the intercept efficiency ranges from 0,9 to 1,0 and its calculations can be complicated.

#### 5.2.1.3 Efficiency slope

The *efficiency slope* (12) is the slope of the collector efficiency curve. This parameter is FrUl in the following equation:

$$Q_u = I_{beam}*A_{ap}*X_{kat}*(FrTan - FrUl*A_{ap}/Conc*(T_{in}-T_{amb}) \quad (5.1)$$

#### 5.2.1.4 Incident angle modifiers

In addition to losses due to the angle of incidence, there are other losses from the collectors that can be correlated to the angle of incidence. These losses occur due to additional reflection and absorption by the glass envelope when the angle of incidence increases. The *incidence angle modifier (IAM)* (13) corrects for these additional reflection and absorption losses. The incidence angle modifier is given as an empirical fit to experimental data for a given collector type.

Type536 relies upon an external data file to provide information on how the transmittance absorptance product of the evacuated tube changes with incidence angle. Because linear parabolic concentrators have an axis of symmetry and are often installed such that they track beam radiation throughout the day, only a one dimensional incidence angle modifier is necessary. For any given solar incidence angle, Type536 calls the TRNSYS Data Reading utility routine, which returns the corresponding value of the incidence angle modifier. Because Type536 uses the TRNSYS Data Reading utility, care must be taken in setting up the syntax of the external data file. That is to say that the first line of the data file must contain at least one value of the solar incidence angle. The subsequent lines of the data file must each contain a single value of the incidence angle modifier that corresponds to a given incidence angle. One side effect of using the built in Data Reading utility is that while this subroutine is able to interpolate between provided values, it is unable to extrapolate beyond the data range given. If

an incidence angle higher than the maximum value or lower than the minimum value present in the data file is sent to the Data Reading utility, the incidence angle modifier corresponding to the maximum or minimum value will be returned. For example, if the highest incidence angle present in the data file is 80 degrees and a solar incidence angle of 90 degrees is sent, the incidence angle modifier corresponding to an angle of 80 degrees will be returned and a warning will be printed in the simulation list and log files.

The following four sub-sections are taken from TRNSYS user manual and Type description.

#### 5.2.1.5 Logical unit

The *logical unit* is the value through which the collector incidence angle modifiers (IAM) data file will be read. This logical unit number must be unique to the simulation. This data file must contain N points relating the incidence angle modifier to the Incidence angle. The format of the data file is

0 30 60 90 {Incidence angles, total=N)

| | | | |
|---|---|---|---|
| 1.00 | (IAM at 0} | 0.43 | {IAM at 60} |
| 0.86 | {IAM at 30} | 0.00 | {IAM at 90} |

#### 5.2.1.6 Number of IAM points

It refers to the number of incidence angles and incidence angle modifiers contained in the external data file.

#### 5.2.1.7 Collector performance

The thermal performance of the Type536 linear parabolic concentrating collector is based upon theoretical equations described in “Solar Engineering of Thermal Processes” (10). It develops a modified loss coefficient called F’UL. F’UL is based upon the standard collector loss coefficient FRUL provided by collector manufacturers and corrects the manufacturer specified loss coefficient for flow rates other than the rated flow rate.

$$F'U_L = \begin{cases} F_R U_L & if \quad \dfrac{F_R U_L}{g_{test}\ Cp_{fluid}\ ConcRat} \geq 1 \\ g_{test}\ Cp_{fluid}\ \left(1 - e^{\left(F_R U_L / \left(g_{test}\ Cp_{fluid}\ ConcRat\right)\right)}\right) & if \quad \dfrac{F_R U_L}{g_{test}\ Cp_{fluid}\ ConcRat} < 1 \end{cases} \tag{5.2}$$

The concentration ratio (ConcRat) in equation 1 above is defined as the ratio of the aperture area to the receiver area.

The standard collector performance equation is shown in equation 5.3.

$$\dot{Q}u = A_c\left[F_R\left(\tau\alpha\right)_n\ I_t - F_R U_L\ \Delta T\right] \tag{5.3}$$

Numerous temperature differences (ΔT in the equation above) can be used as the basis of the useful energy gain calculation. Some common standards are the collector inlet temperature minus the ambient temperature or the mean collector fluid temperature minus the ambient temperature. Type536 bases its calculation on the collector inlet temperature minus the ambient temperature. For parabolic concentrators, two modifiers (R1 and R2) are applied to equation 5.3 in order to correct for other flow rates than under test conditions and to account for more than one collector in a series string. R1 includes a term called Rtest as shown in equation 5.4.

$$R_{test} = g_{test}\ Cp_{fluid}\ \left(1 - e^{\left(-F'U_L / \left(g_{test}\ Cp_{fluid}\right)\right)}\right) \tag{5.4}$$

R1 is given by equation 5.5.

$$R_1 = \frac{N_{series}\ \dot{m}_{fluid}\ Cp_{fluid}}{A_{aperture}}\left(\frac{1 - e^{\left(\left(-F'U_L\ A_{aperture}\right)/\left(N_{series}\ \dot{m}\ Cp_{fluid}\right)\right)}}{R_{test}}\right) \tag{5.5}$$

R2 is given by equation 5.6.

$$R_2 = \frac{1 - \left(1 - \dfrac{R_1\ A_{aperture}\ F_R U_L}{\dot{m}\ Cp_{fluid}\ N_{series}\ ConcRat}\right)^{N_{series}}}{N_{series}\left(\dfrac{R_1\ A_{aperture}\ F_R U_L}{\dot{m}\ Cp_{fluid}\ N_{series}\ ConcRat}\right)} \tag{5.6}$$

The modified overall useful energy gain from the collector is based upon equation 5.3 as modified by the inclusion of incidence angle modifier effects, R1, and R2.

$$Qu = R_1\ R_2\ A_{aperture}\ N_{parallel}\left[ F_R(\tau\alpha)_n\ IAM\ I_{beam} - \frac{F_R U_L}{ConcRat}(T_{in} - T_{amb}) \right] \tag{5.7}$$

Provided that there is flow, the temperature of fluid at the collector outlet is given by equation 5.8.

$$T_{out} = T_{in} + \frac{\dot{Q}u}{\dot{m}_{fluid}\ Cp_{fluid}} \tag{5.8}$$

The flow rate in equation 5.8 is the mass flow rate of fluid in a single parallel branch of the collector array. Under no flow conditions, the fluid outlet temperature is

$$T_{out} = T_{amb} + F_R(\tau\alpha)_n\ IAM\ I_{beam}\ \frac{ConcRat}{F_R U_L} \tag{5.9}$$

Type536 is able to limit the outlet fluid temperature to a user specified maximum value. The theoretical outlet temperature calculated in either 5.8 or 5.9 is limited to the maximum allowable value specified by the user as an input to the model. The remaining energy is assumed to be dumped and is reported as an output to the model. The dumped energy for a single parallel branch of the collector array is given by equation 5.9.

$$\dot{Q}_{dump} = \dot{m}_{fluid}\ Cp_{fluid}\ (T_{out} - T_{\max}) \tag{5.10}$$

Again, the mass flow rate in the above equation is the mass flow rate for one parallel branch of the collector.

#### 5.2.1.8 Tested flow rate

The flow rate per unit area at which the collector efficiency was obtained. The collector performance will be modified for flow rates other than the tested flow rate.

# 6. POWER CYCLE MODEL

## 6.1 INTRODUCTION

In this chapter, the power cycle that generates electricity will be described. The energy that is collected by the solar field will be converted in this power cycle. Due to the characteristics of the solar field, and the temperature range the HTF works in, the ideal power cycle to be used is the traditional Rankine cycle. It is in fact the power cycle used typically for SEGS plants.

The Rankine cycle that is specifically used in our system has the following layout:

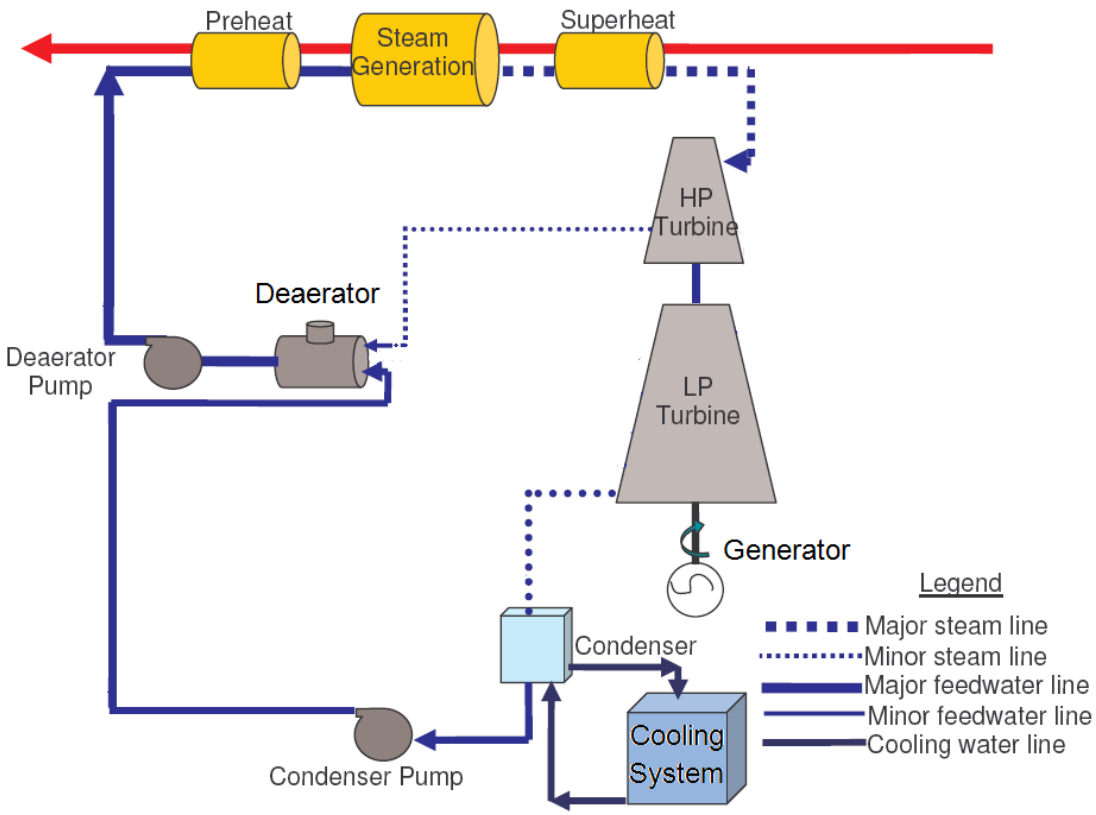


**Figure 47**: General schematics of Rankine Power Cycle

The heated HTF heats the feedwater in the preheater, generates dry steam in the steam generator and superheats this steam in the superheater up to 390ºC and 100 bar pressure. All is done by direct heat exchange. After the superheated steam leaves the superheater, it flows into the high pressure turbine stage, where it is expanded and the turbine blades are propelled, generating rotation of the axis that will be transmitted to the generator. There is an extraction steam line that flows into the deaerator (or open feedwater heater). The other branch that leaves the high

pressure turbine drives the exhaust steam into a low pressure turbine where again, the steam expands and propels the turbine blades. The steam leaving the low pressure turbine is condensed in a surface condenser by heat exchange with circulating water. The condenser water is cooled using the oceans water. Also, cogeneration connections can be implemented. The condenser steam (feedwater) is pumped into the deaerator (pressure increases from 0,08 bar to approximately 15 bar). The deareator (14) is a type of feed water that condenses steam extracted from the turbine to heat feed water before it enters the preheater, thereby increasing the Rankine cycle efficiency. Also, it purges oxygen from the feed water, controlling corrosion. Conservation of energy and mass are used to calculate the required steam flow rate from a turbine extraction to achieve this process. The feedwater is pumped again at the outlet of the deaerator and flows back into the preheater, where it completes the cycle.

This Rankine cycle disposition is only a basic power cycle model. It can be further elaborated with added characteristics, such as a regeneration branch, or more turbine stages and the corresponding steam bleeds, achieving higher cycle efficiencies. But this system model will suffice our needs and simplify the simulation arrangements. Any further expansion can be easily achieved if desired.

## 6.2 CALCULATIONS

### 6.2.1 Temperature-Entropy diagram

In the following sections, the needed calculations have been done in order to obtain the different parameters and key points from the Rankine cycle. Included in the next figure is also the T-S diagram together with schematics of the system.

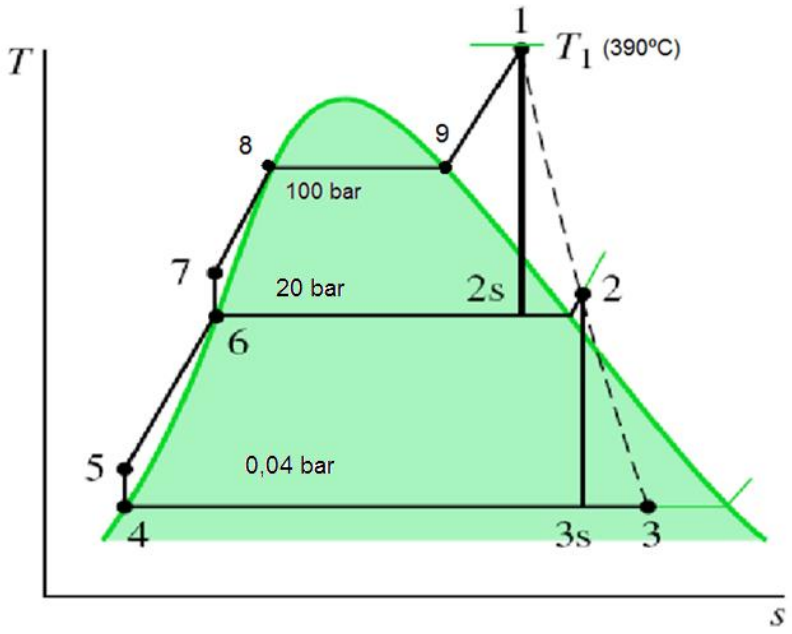


**Figure 48**: Temperature-Entropy diagram of power cycle at reference state [40]

### 6.2.2 Parameters of cycle key points

*State 1:*

The specific enthalpy at state 1 can be read directly from water steam tables. With the help of linear interpolation, at $T_1$=390ºC, $P_1$=100bar, we obtain:

$$h_1=3065{,}86 \text{ kJ/kg}$$
$$s_1=6{,}1668 \text{ kJ/kg·K}$$

*State 2s (isentropic):*

The specific entropy at state 2 can be obtained from the steam tables using the known values of enthalpy and pressure at this state. With $P_2$=20bar and $s_2=s_1$=6,1668 kJ/kg·K:

$$x_{2s}=\frac{s_{2s}-s_f}{s_g-s_f}=\frac{6{,}1605-2{,}4474}{6{,}3409-2{,}4474}=0{,}95 \qquad (6.1)$$

$$h_{2s} = h_f + x_{2s} \cdot h_{fg} = 908{,}79 + 0{,}95 \cdot 1890{,}7 = 2704{,}29\ kJ/kg \qquad (6.2)$$

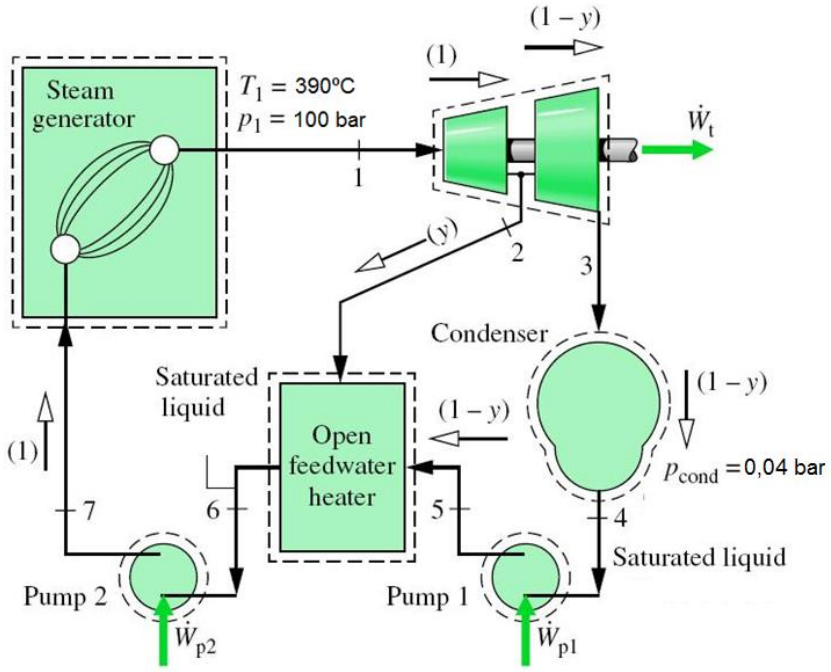


**Figure 49**: Schematics of Rankine cycle calculated [40]

*State 2 (real):*

The specific enthalpy at state 2 can be determined by solving the expression for the turbine

$$h_2 = h_1 - \eta_t \cdot (h_1 - h_{2s}) = 3065{,}86 - 0{,}85(3065{,}86 - 2704{,}29) = 2758{,}28 kJ/kg \quad (6.3)$$

$$s_2 \approx 6{,}19 kJ/kgK$$

Note that the turbine efficiency has been contemplated to be 85%.

*State 3s (isentropic):*

With $s_{3s}$=$s_2$=6,19 kJ/kg·K, and $P_3$=$P_{3s}$=0,04 bar, the quality at state 3 is:

$$x_{3s} = \frac{s_{3s} - s_f}{s_g - s_f} = \frac{6{,}19 - 0{,}4226}{8{,}47 - 0{,}4226} = 0{,}72 \qquad (6.4)$$

Using this, we get

$$h_{3s} = h_f + x_{3s} \cdot h_{fg} = 121{,}46 + 0{,}72 \cdot 2432{,}9 = 1873{,}15\ kJ/kg \qquad (6.5)$$

*State 3 (real):*

The specific enthalpy at state 3 can be determined using the efficiency of the second-stage turbine:

$$h_3 = h_2 - \eta_t \cdot (h_2 - h_{3s}) = 2758{,}28 - 0{,}85(2758{,}28 - 1873{,}15) = 2005{,}9 kJ/kg \qquad (6.6)$$

*State 4:*

The specific enthalpy at state 4 can be read directly from water steam tables. We have saturated liquid at $P_4$=0,04 bar:

$$h_4=121,40 \text{ kJ/kg} \quad (6.7)$$

Note: The condensator uses the ocean for cooling the steam. The ocean is considered a constant temperature mass of water at T=20ºC

*State 5:*

The pumps are assumed to operate with no irreversibilities, therefore the specific enthalpy value at this state can be calculated with the following expression:

$$h_5 = h_4 + v_4(p_5 - p_4) = 121,4 + 1,004(20 - 0,04) = 141,44kJ/kg \quad (6.8)$$

*State 6:*

State 6 is saturated liquid at 20 bar. Thus, $h_6$=908,62kJ/kg

*State 7:*

With $P_7$=100 bar, we apply the same expression as in stage 5:

$$h_7 = h_6 + v_6(p_7 - p_6) = 908,62 + 1,1767(100 - 20) = 1002,76kJ/kg \quad (6.9)$$

Applying mass and energy rate balances to a control volume enclosing the open heater, we find the fraction *y* of the flow extracted at state 2 from:

$$y = \frac{h_6 - h_5}{h_2 - h_5} = \frac{908,4 - 141,44}{2758,28 - 141,44} = 0,29 = 29\% \quad (6.10)$$

*Stage 8:*

$P_8$=100 bar

$T_8$=310,99ºC

$h_8$=1407,87 kJ/kg

The following table includes the specific enthalpies of each stage:

| | |
|---|---|
| $h_1$=3065,86 kJ/kg | $h_5$=141445$kJ/kg$ |
| $h_2$=2758,28$kJ/kg$ | $h_6$=908,62kJ/kg |
| $h_3$=2005,9$kJ/kg$ | $h_7$=1002,76$kJ/kg$ |
| $h_4$=121,40 kJ/kg | $h_8$=1407,87 kJ/kg |

Table 7: Enthalpy values of key points in Rankine cycle

### 6.2.3 Work extraction and addition and heat addition

On the basis of a unit of mass passing through the turbine, the total turbine work output is:

*Turbine Stages*
$$\frac{\dot{W}_t}{\dot{m}_1} = (h_1 - h_2) + (1 - y)(h_2 - h_3) = 834{,}25\ kJ/kg \quad (6.11)$$

The total pump work per unit of mass passing through the first-stage turbine is

*Pumps*
$$\frac{\dot{W}_p}{\dot{m}_1} = (h_7 - h_6) + (1 - y)(h_5 - h_4) = 108{,}34\ kJ/kg \quad (6.12)$$

The heat added in the steam generator per unit of mass passing through the first-stage turbine is

*Evaporator*
$$\frac{\dot{Q}_{in}}{\dot{m}_1} = (h_1 - h_7) = 2063{,}1\ kJ/kg \quad (6.13)$$

### 6.2.4 Cycle efficiency

The thermal efficiency of the cycle is

*Efficiency*
$$\eta = \frac{\dot{W}_t/\dot{m}_1 - \dot{W}_p/\dot{m}_1}{\dot{Q}_{in}/\dot{m}_1} = 0{,}35 = 35\% \quad (6.14)$$

### 6.2.5 Mass flow rate

The mass flow rate of the steam entering the turbine can be determined using the given value for the net power output, 162 MW[4]. Since

$$\dot{W}_{cycle} = \dot{W}_t/\dot{m}_1 - \dot{W}_p/\dot{m}_1 = 725{,}91 kJ/kg \quad (6.15)$$

We can calculate the total mass flow rate of the Rankine cycle with the following formula:

$$\dot{m}_1 = \frac{\dot{W}_{demand}}{\dot{W}_{cycle}} = \frac{162\,MW}{725{,}91 kJ/kg} = 223\,\frac{kg}{s} = 802800\,\frac{kg}{h} \quad (6.16)$$

[4] This value is the one calculated in our electric demand, in section 4.1.3. As a reference, SEGS 8 and 9 from the Kramer Junction work with values of approximately 160M. (http://ludb.clui.org/ex/i/CA9679/)

### 6.2.6 Assumptions

The following assumptions have been made to carry out the calculations in the Rankine cycle:

- Each component in the cycle is analyzed as a steady-state control volume.
- All processes of the working fluid are internally reversible, except for the expansions through the two turbine stages and mixing in the open feedwater heater.
- The turbines, pumps, and feedwater heater operate adiabatically.
- Kinetic and potential energy effects are negligible.
- Saturated liquid exits the open feedwater heater, and saturated liquid exits the condenser.
- From the preheater, the open feedwater heater and the condenser, the steam exits as saturated liquid (x=0)
- From the steam generator the steam exits as saturated vapor (x=1)

## 6.3 HEAT EXCHANGER OVERALL HEAT TRANSFER FACTOR, UA. ε-NTU (15)

### 6.3.1 Superheater/Preheater

The superheater is a counter-flow shell-and-tube heat exchanger that increases the temperature of the inlet steam (which enters as saturated vapor) beyond the saturation temperature corresponding to the prevailing operating pressure.

The preheater is also a counter-flow shell-and-tube heat exchanger that increases the temperature of the inlet steam before it enters the steam generator at liquid saturation point.

Steam enthalpy at the inlet of the preheater is calculated from the given inlet temperature and pressure. The enthalpy of steam at the superheater inlet is calculated from the inlet enthalpy and pressure; temperature equals saturation temperature at the given inlet pressure. Outlet enthalpies are calculated from the outlet pressure and quality or outlet pressure and temperature, depending on which two values are given. The heat transfer between streams may be calculated either from the change in enthalpy of the feedwater/steam or from the change in enthalpy of the heat transfer fluid. These calculations will therefore be based on the feedwater/steam change of enthalpy since the properties of water/steam are better known to us than those of the thermal oil.

The thermal performance of the superheater is expressed in terms of the effectiveness of the component. Heat exchanger effectiveness is defined as the actual heat transfer realized between streams over the maximum heat transfer possible for the given streams[14]

$$\varepsilon = \frac{\dot{Q}_{steam}}{\dot{Q}_{max}} \tag{6.17}$$

The expression for the maximum heat flow rate can be represented by:

$$\dot{Q}_{steam} = \dot{m}_{steam} \cdot (h_{in,steam} - h_{out,steam}) \tag{6.18}$$

The specific heat of the heat transfer fluid is evaluated at the average temperature of the HTF in the heat exchanger.

$$C_{HTF} = C_{HTF}\left(\frac{T_{HTF,in}+T_{HTF,out}}{2}\right) \tag{6.19}$$

The capacitance rate of each stream is the product of its mass flow rate and specific heat

$$C_C = \dot{m}_{steam} \frac{h_{steam\ ,out} - h_{steam\ ,in}}{T_{steam\ ,out} - T_{steam\ ,in}} \quad (6.20)$$

$$C_H = \dot{m}_{HTF} \cdot C_{HTF} \quad (6.21)$$

Where:

$\dot{m}$ refers to the mass flow from the steam or the HTF [kg/s]. The mass of heat transfer fluid is approximately 7 or 8 times more than the feedwater/steam flow. This is due to the fact that its Cp is lower than that of water, and that water goes through phase changes from liquid to vapor (with its corresponding latent heat requirements)

Cp are the average specific heats between the inlet and outlet of the steam and of the HTF [kJ/kg·K]

The minimum and maximum heat capacitance rates of the two streams are identified, and the capacitance rate ratio is calculated:

$$C_{min} = MIN(C_C, C_H) \quad (6.22)$$

$$C_{max} = MAX(C_C, C_H) \quad (6.23)$$

The capacitance rate ratio of the fluid streams is the ratio of the smaller total heat capacitance of the two streams to the larger heat capacitance of the streams.

$$C_r = \frac{C_{min}}{C_{max}} \quad (6.24)$$

The maximum heat transfer possible between streams will equal the smaller total heat capacitance of the two fluid streams, multiplied by the difference in inlet temperatures between the streams.

$$\dot{Q}_{max} = C_{min}\,(T_{HTF,in} - T_{steam\ ,in}) \quad (6.25)$$

For counter-flow sensible heat exchangers, the following relationship determines heat exchanger effectiveness as a function of capacitance ratio and NTU (Incropera and DeWitt, 2004):

$$\varepsilon = \frac{1 - \exp\left[-NTU \cdot (1 - C_r)\right]}{1 - C_r \cdot \exp\left[-NTU \cdot (1 - C_r)\right]} \quad (6.26)$$

The ratio of the NTU to the heat capacitance of the feed water equals the reference UA of the heat exchanger:

$$NTU_{steam} = \frac{UA_{steam}}{C_{min}} \tag{6.27}$$

The following figure represents effectiveness graph for counter-flow heat exchangers:

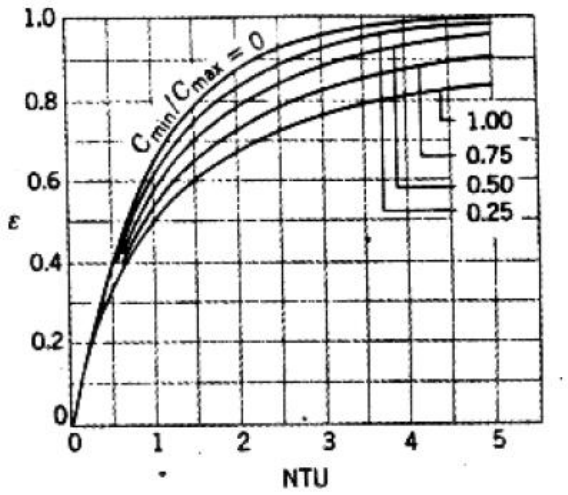


**Figure 50**: Effectiveness for cross-flow heat exchangers [41]

From the graph, through ε and $C_{min}/C_{max}$, we obtain the value of NTU from which we can work out the value of $UA_{steam}$.

### 6.3.2 Steam generator

Enthalpies at the inlet and outlet of the steam generator are calculated assuming the inlet and outlet quality to the steam generator are 0 and 1, respectively. The temperature at the steam generator inlet and outlet is the saturation temperature at the specified steam generator pressure.

The calculations for the steam generator are analogous to those for the steam preheater and superheater with only a couple of modifications or adjustments:

To calculate Cc, the specific heat of the boiling steam is assumed to be infinite.
Furthermore, for heat exchangers in which one fluid undergoes a phase change, the effectiveness is related to the number of transfer units (NTU). Therefore, effectiveness for the steam generator is calculated according the equation:

$$\varepsilon_{steam} = 1 - \exp(-NTU_{steam}) \qquad (6.28)$$

After proceeding with the calculations (included in Appendix A), we obtain the values included in the following table:

| ELEMENT | UA [kW/K] |
|---|---|
| Preheater | 5464 |
| Steam Generator | 11230 |
| Superheater | 5170 |

## 6.4 TEMPERATURE VERSUS HEAT FLUX IN HEAT EXCHANGES

In this section, the temperature of the working fluid (feedwater/steam) (blue) is contrasted with the temperature of the HTF (red) in reference to the heat flux (x-axis).

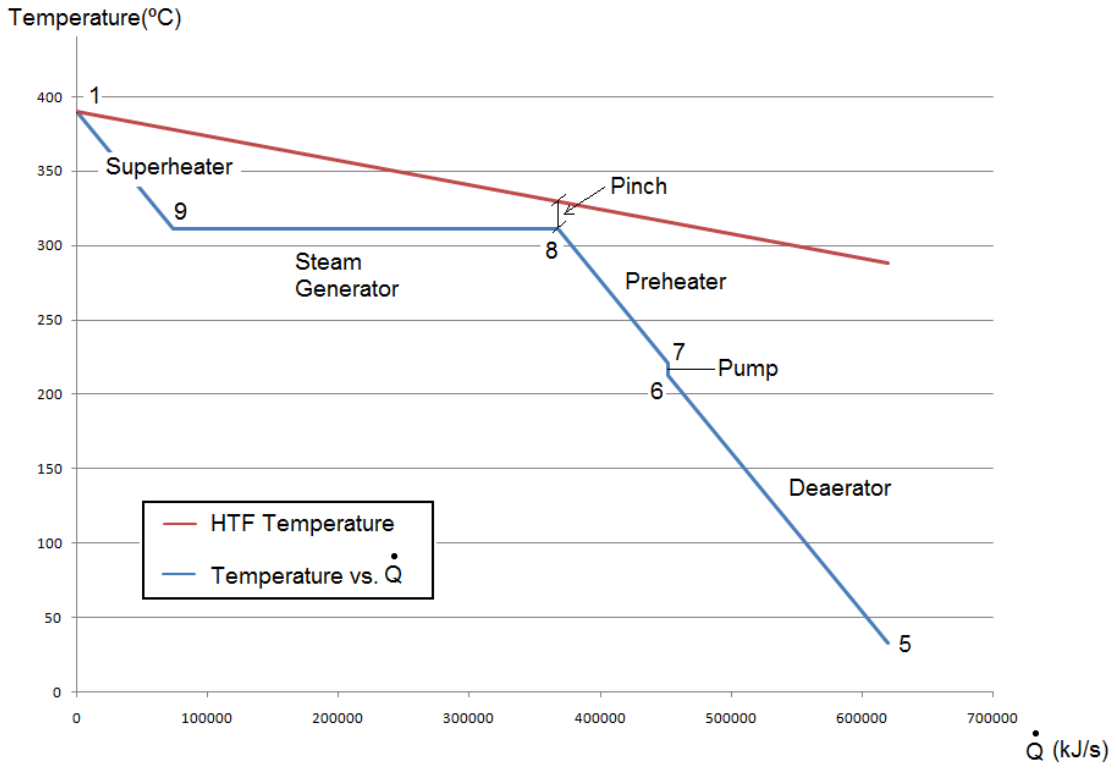


**Figure 51: Temperature (ºC) vs. Heat Flux (kJ/s)**

The parameters needed to develop this graph are gathered in the tables bellow. The temperature of all stretches except for the one corresponding to the steam generator is calculated with the following formula:

$$\dot{Q} = \dot{m}_{water} \cdot C_p (T_{out} - T_{in})$$

The one referring to the steam generator stretch in which the temperature is constant uses this other formula:

$$\dot{Q} = \dot{m}_{water} \cdot (h_{out} - h_{in})$$

| TEMPERATURE (ºC) |
|---|
| T5=33 |
| T6=212,38 |
| T7=221 |
| T8=310,99 |
| T9=310,99 |
| T1=390 |

| ENTHALPY(kJ/kg) |
|---|
| h8=1407,81 |
| h9=2725 |

The results obtained are reasonable. In the graph we can see that the pinch point is reasonably small. The blue line can of course never be above the red one, so the closer it is, the better. Point 8 is considered to be a bottle-neck. The area between the two lines is proportional to the exergy loss. In other words, the bigger the area is, the less efficient the use of energy is going to be. So it is obviously in our interest to keep it as small as possible.

Since the feedwater is evaporating in the stretch from 8 to 9, the temperature is constant and all the energy is used to change phases. Therefore, a way developed to lower the area corresponding to this stretch is to use a Rankine organic cycle. In it, the working fluid is not water, but an organic medium which has a gradual evaporation process, creating in this matter a sort of gradual step increase instead of the horizontal stretch.

It also gives us a good idea of where is the highest heat flux given as well as the lowest and where do we obtain bigger temperature increments. One can see, for example, that both parameters are almost insignificant in the pump stretch, especially when compared to the behavior in the deaerator or in the steam generator.

## 6.5 MODEL IN TRNSYS

In this chapter, the complete Rankine power plant model designed for the housing estate is described gradually in three steps. First it appears as only a Rankine cycle, then it incorporates the solar field that will generate the steam that run the turbines and finally it also includes the concrete heat storage system that allows the system to work during hours where the solar irradiation is low or non-existent (during cloudy weather or at night).

### 6.5.1 TRNSYS (TRransient eNergy SYstem Simulation)

TRNSYS is a transient systems simulation program with a modular structure. It recognizes a system description language in which the user specifies the components that constitute the system and the manner in which they are connected. The TRNSYS library includes many of the components commonly found in thermal and electrical energy systems, as well as component routines to handle input of weather data or other time-dependent forcing functions and output of simulation results. The modular nature of TRNSYS gives the program tremendous flexibility, and facilitates the addition to the program of mathematical models not included in the standard TRNSYS library. TRNSYS is well suited to detailed analyses of any system whose behavior is dependent on the passage of time. TRNSYS has become reference software for researchers and engineers around the world. Main applications include: solar systems (solar thermal and photovoltaic systems), low energy buildings and HVAC systems, renewable energy systems, cogeneration, fuel cells.

### 6.5.2 Rankine cycle

An independent Rankine model is displayed in this section. This means that it is not connected to anything else, and that it has a constant behavior due to the fact that all the values are inscribed as parameters and do not fluctuate with time. Therefore, if we describe the system with all the data we have calculated/esteemed, we obtain a behavior from the simulation that coincides with the theoretical expectancies.

#### 6.5.2.1 Schematics

The schematics respond directly to the figures in previous section 2.2.2.

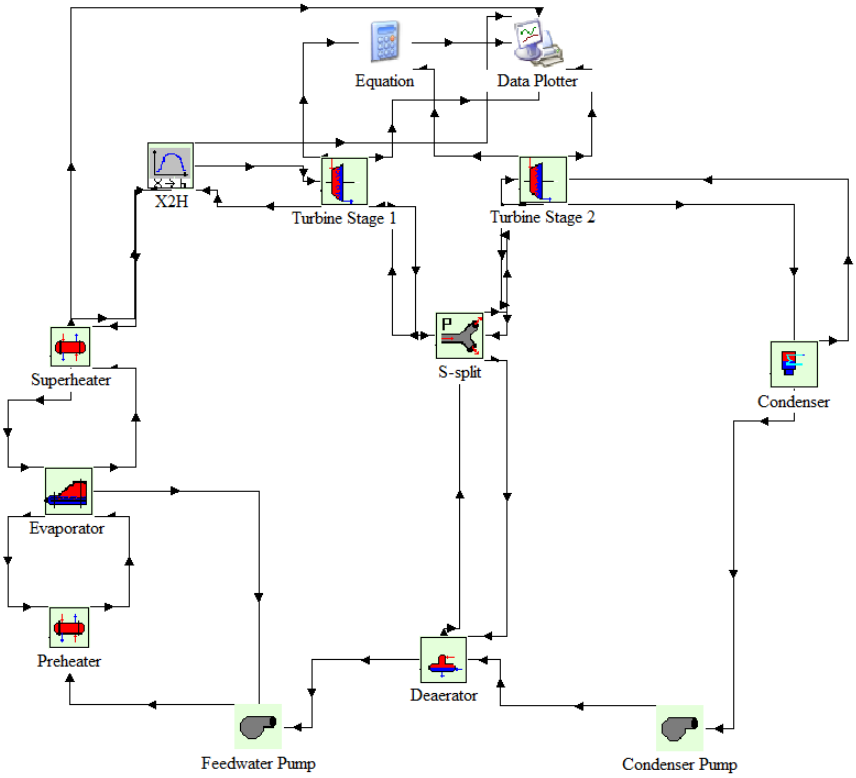


**Figure 52**: Schematics of the Rankine power plant in TRNSYS

We describe two elements that needed to be included that are not mentioned before:
"X2H": This type deploys a conversion routine to convert steam property given in temperature, pressure and quality magnitudes used in the superheater to enthalpy and pressure used in component turbine stage 1.

"Equation": It has the turbine power obtained from both turbine stages as an input and adds them to give the total power obtained as an output value.

"Data Plotter": This is an online graphics component used to display selected system variables while the simulation is progressing. The selected variables will be displayed in a separate plot window on the screen. In this instance of the Type65 online plotter, data sent to the online plotter is automatically printed, once per time step to a user defined external file.

The TRNSYS (STEC library) details of each type are included in Appendix B.

#### 6.5.2.2 Results and validation

The simulation we have run had the length of one whole year, 8760 hours, and the time step is of 5 minutes. The following graph is the most important result we obtain from the model, the power obtained throughout the whole year.

On the x-axis (h) time is represented and on y-axis the power in kJ/h. Our estimated energy (section 4.2.2) is 162 MW, which is equal to $5{,}83 \cdot 10^3$ kJ/h.

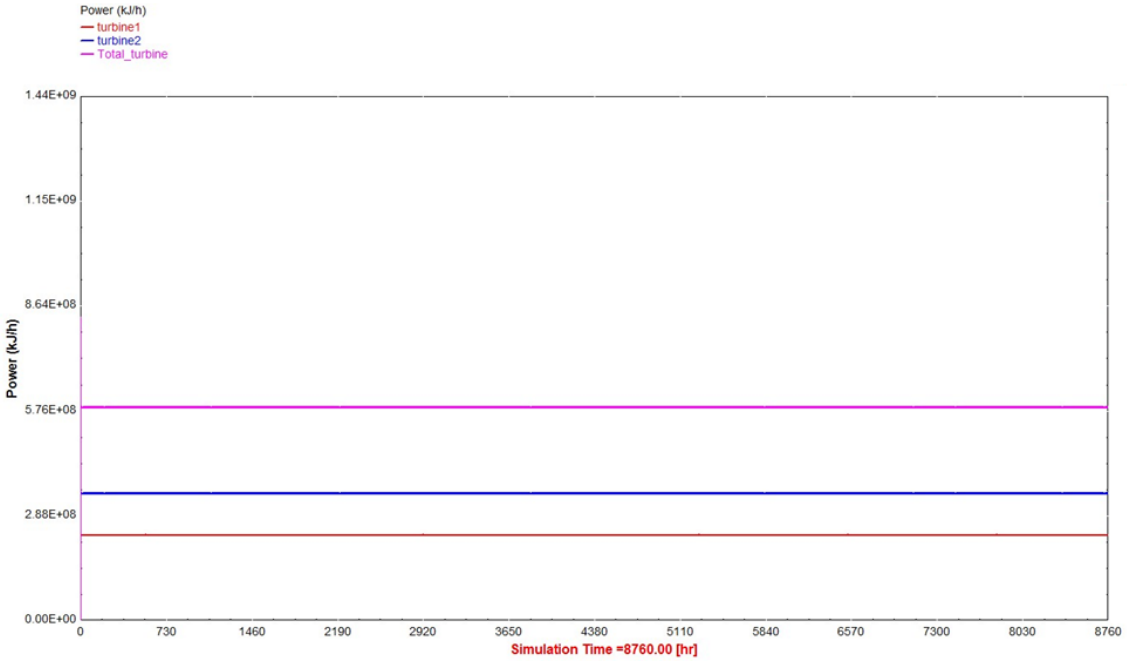


**Figure 53**: Time (h) on x-axis vs. Power (kJ/h) (y-axis)

One can perceive that the values are constant throughout the whole year due to the constant input values. The blue line indicates the power obtained in the first turbine stage and the red line the power generated in the second. Together, they add up to the pink line, which has a practically constant value of $5{,}8598 \cdot 10^8$ kJ/h. As we mentioned, our demand was $5{,}83 \cdot 10^8$ kJ/h so the maximum requirements are covered. Also some representative values of temperatures and enthalpies were plotted out giving the following results:

| PARAMETER | TRNSYS VALUE | THEORETICAL VALUE |
|---|---|---|
| h1 (turbine 1 inlet) | 3077 kJ/kg | 3065 kJ/kg |
| h2 (turb1 outlet/turb2 inlet) | 2716 kJ/kg | 2758 kJ/kg |
| h3 (turbine 2 outlet) | 1872 kJ/kg | 2005,9 kJ/kg |
| Preheater water Temp (outlet) | 309,5 ºC | 310,99ºC |
| Superheater Steam Temp (outlet) | 388,5 ºC | 390 ºC |
| Condenser pressure | 0,046 bar | 0,04 bar |
| Total Turbine Power | $5{,}87 \cdot 10^8$ kJ/h | $5{,}83 \cdot 10^8$ kJ/h |
| Pressure at 1 | 96,10 bar | 100 bar |

| PARAMETER | TRNSYS VALUE | THEORETICAL VALUE |
|---|---|---|
| Pressure at 2 | 18,80 bar | 20 bar |
| Pressure at 4 | 0,0426 bar | 0,04 bar |
| Pressure at 7 | 99,12 bar | 100 bar |
| Pressure at 8 | 98,12 bar | 100 bar |
| Pressure at 9 | 97.16bar | 100 bar |
| Temperature at 1 | 389,7ºC | 390ºC |
| Temperature at 4 | 30ºC | 28,96ºC |
| Temperature at 7 | 208,9ºC | 231,9ºC |
| Temperature at 9 | 308,4ºC | 310,11ºC |

Table 8: Comparison of TRNSYS values with theoretical independent Rankine cycle values

The results obtained are quite similar to the ones expected from the theoretical calculations. The error is in general less than 5%, except for the temperature at 7, which has an error of 10%, still acceptable value.

Attached to this text are the TRNSYS files in electronic format. The following is simply an example of the numerical data that is given by the online plotter:

| TIME | nthalpy inletTurbine1 | enthalpy outletTurbine1 | enthalpy outlet Turbine2 | Superheat_out_SteamTemp | CondPressure |
|---|---|---|---|---|---|
| 2.25E+01 | 3.01E+03 | 2.71E+03 | 1.98E+03 | 3.88E+02 | 4.26E-02 |
| 2.30E+01 | 3.01E+03 | 2.71E+03 | 1.98E+03 | 3.88E+02 | 4.26E-02 |
| 2.35E+01 | 3.01E+03 | 2.71E+03 | 1.98E+03 | 3.88E+02 | 4.26E-02 |
| 2.40E+01 | 3.01E+03 | 2.71E+03 | 1.98E+03 | 3.88E+02 | 4.26E-02 |
| 2.45E+01 | 3.01E+03 | 2.71E+03 | 1.98E+03 | 3.88E+02 | 4.26E-02 |
| 2.50E+01 | 3.01E+03 | 2.71E+03 | 1.98E+03 | 3.88E+02 | 4.26E-02 |
| 2.55E+01 | 3.01E+03 | 2.71E+03 | 1.98E+03 | 3.88E+02 | 4.26E-02 |

Table 9: TRNSYS data given by online plotter

### 6.5.3 Rankine cycle plus solar field

Having successfully designed and modeled the Rankine power plant, we now incorporate a solar field to it. Now the power plant will no longer have constant values since it is directly related to the weather (solar irradiation), transient phenomenon by definition.

A representation of a general connection between a solar field and a Rankine cycle energy producing plant is shown in the following figure. It gives us a clear idea of the general disposition of components.

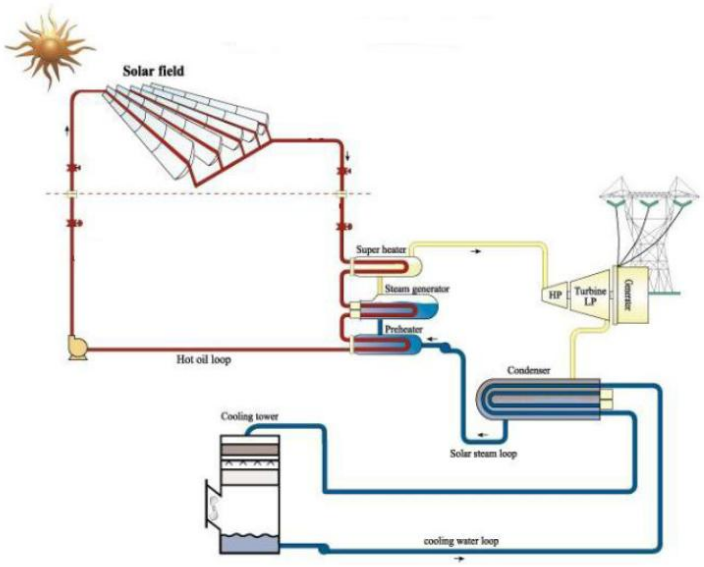


**Figure 54**: General model of Rankine power plant connected to solar field [42]

#### 6.5.3.1 Estimation of the solar field area

According to the calculations in section 4.2.2, the annual energy demand that will need to be covered is 712.288 MWh. On average, this means we will need to obtain

$$Average\ power\ demand: \frac{712288MWh}{8760h} = 81311{,}4\frac{kJ}{s}$$

Calculations proceed of the energy the solar field receives from the sun. From the basic following TRNSYS layout we can obtain as a system output the beam radiation (kJ/h·m$^2$) that reaches the surface of the area we wish to work in. The integrator will integrate this variable throughout time and feed back the total power obtained per square meter (kJ/m$^2$).This value is represented in the graph, where x-axis is for time (h) and y-axis for the beam radiation integrated through time (kJ/m$^2$).

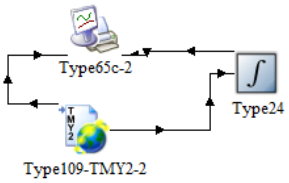


TRNSYS Weather file layout

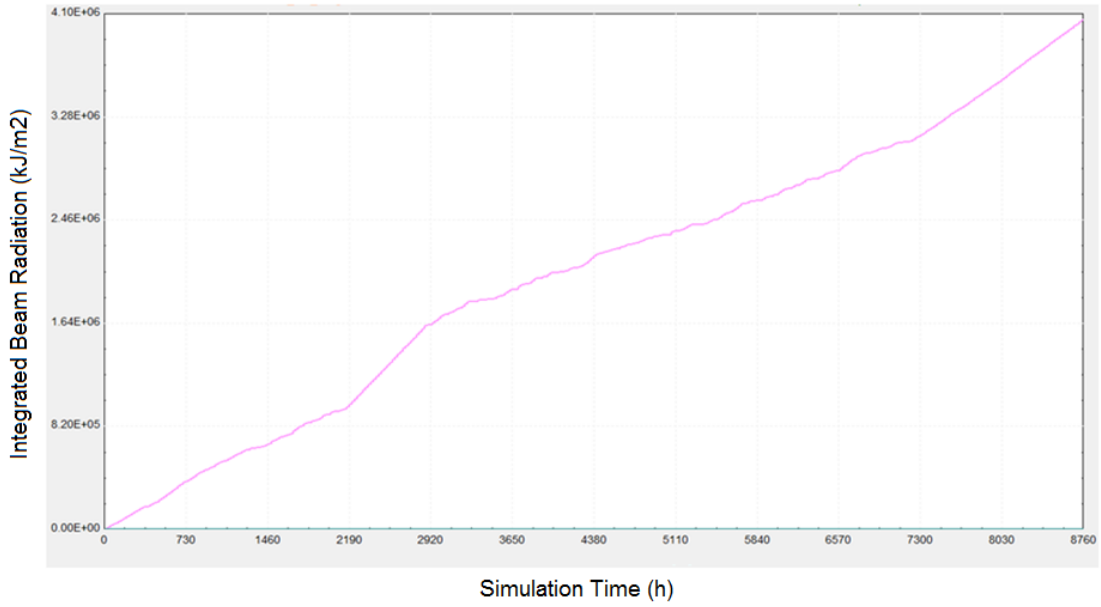


**Figure 55**: Integrated beam radiation (kJ/m2) vs. time (h)

The total energy received per unit of surface is $4{,}0542 \cdot 10^6$ kJ/m$^2$. If we further calculate the average power we would need to receive this energy, we obtain:

$$Average\ Solar\ Power = \frac{4{,}0542 \cdot 10^6 \frac{\text{kJ}}{\text{m}^2}}{8760\cancel{\text{h}} \cdot 3600 \frac{\text{s}}{\cancel{\text{h}}}} = 0{,}13 \frac{kJ}{\text{m}^2 \cdot \text{s}}$$

By now dividing the average power demand into the average solar energy received per unit of surface we obtain the surface that would be required to receive this amount of energy:

$$\boxed{Area\ solar\ field = \frac{81311{,}4 \frac{\cancel{kJ}}{\cancel{s}}}{0{,}13 \frac{\cancel{kJ}}{\text{m}^2 \cdot \cancel{s}}} = 625.473\text{m}^2} \qquad (6.29)$$

Therefore, since our solar troughs have an aperture area of 6m$^2$ (which coincides with standard sizing as was already mentioned in the section about the solar field), we dimension a field that has 323 panels displayed in series as well as in parallel. (323x323x6m$^2$=625.974m$^2$).

#### 6.5.3.2 Schematics

The following figure represents our system layout in TRNSYS.

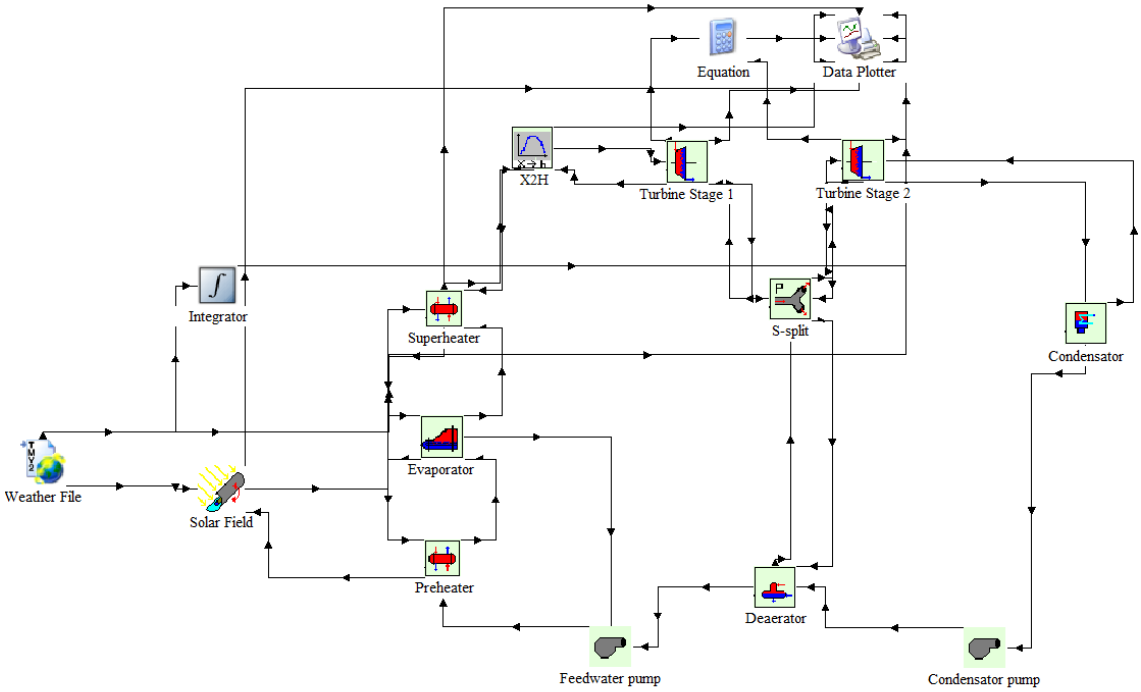


**Figure 56**: Schematics of the Rankine power plant plus solar field attached, in TRNSYS

To the existing Rankine cycle, the "*solar field"* was incorporated in such a way that the outlet HTF from the troughs goes into the superheater, the evaporator (steam generator) and through the preheater, in this order, exchanging heat to the lesser temperature feedwater and steam. After it exits the preheater heat exchanger, it returns as a HTF inlet into the solar field again in order to again get reheated.

The *"weather file"* holds the meteorological data of specific areas throughout the globe. In our case, the project is to be implemented in Dahkla, Morocco. This specific location is not included in the TRNSYS weather files, but we can alternatively choose Nouadhibou, Mauritania, which is only approximately 300 kilometers south-east along the coast, and has accurate weather and geographic similarities to the site of our project.

The *"integrator"* is only serving to integrate the beam radiation received.

#### 6.5.3.3 Results and validation

Since the behavior of our system is now extremely transient, it is very complicated to achieve a convergent solution for a simulation throughout the whole year. In order to do so, there should be precise and continuous adjusting and controlling of the HTF and steam flows. Therefore, a series of sunny days have been selected to observe the system's behaviour. From the following

graph of beam radiation for every day of the year, we can more easily select a time range that is highly irradiated.

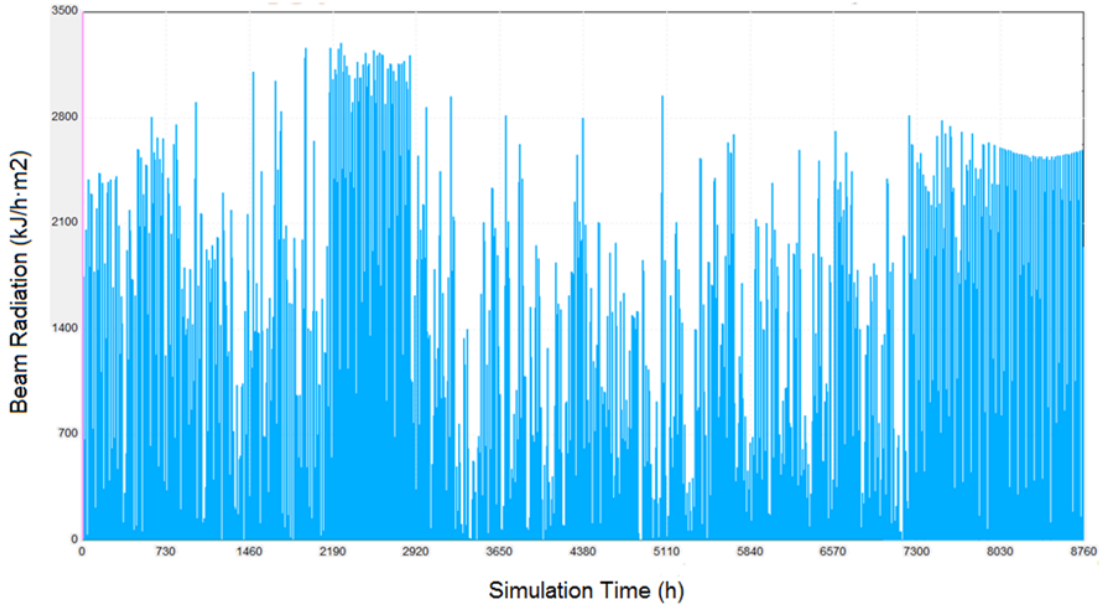


**Figure 57**: Beam radiation [kJ/h·m$^2$](y-axis) vs. Time [h] (x-axis)

The following graph includes the outlet power given by the turbines in reference to the action of the sun.

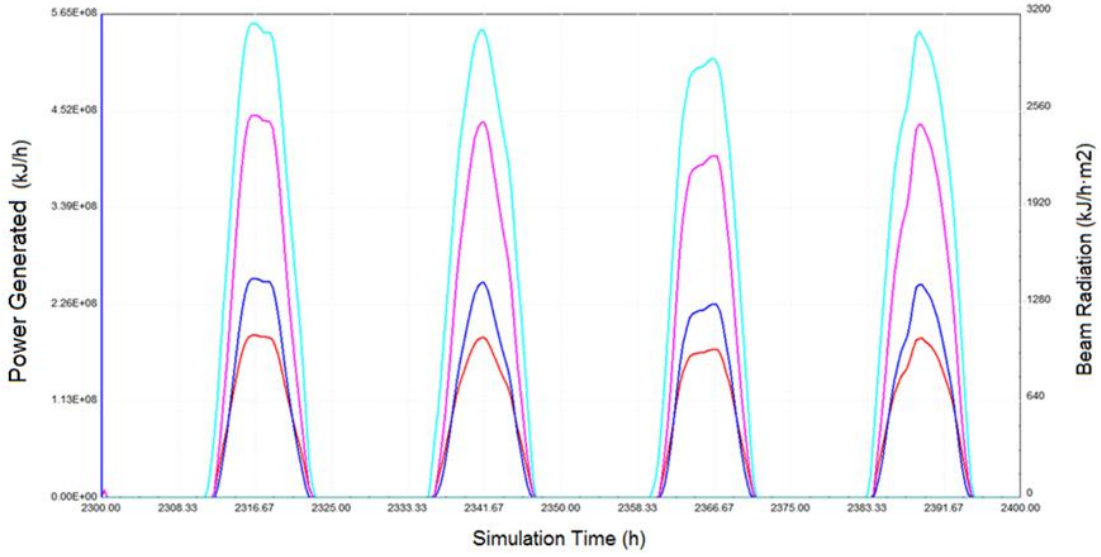


**Figure 58**: Turbine power generation [kJ/h] and beam radiation [kJ/m$^2$·h] (y-axis) vs. time [h] (x-axis)

The time span chosen was from the hour 2300 to the hour 2400. In turquoise is the beam radiation [kJ/m$^2$·h] from the sun, referenced to the right vertical axis. In dark blue is the first stage turbine power generation [kJ/h], in red is the second stage turbine power generation [kJ/h]

and in pink is the total turbine power as the addition of both powers [kJ/h]. Given the uninterrupted irradiation throughout these four days, the results are not bad. The total power obtained for these days doesn't quite reach our peak demand of **162MW**, but at its maximum we obtain approximately $4{,}5 \cdot 10^8$kJ/h, or **123MW** of power, which is already more that 20% more than the daytime average power demand (99,05MW).

The main problem occurs when the solar irradiation that reaches the solar field is too low. We can see an example of this in the following graph. We chose a very cloudy day followed by a very sunny one. One can clearly appreciate the drastic differences:

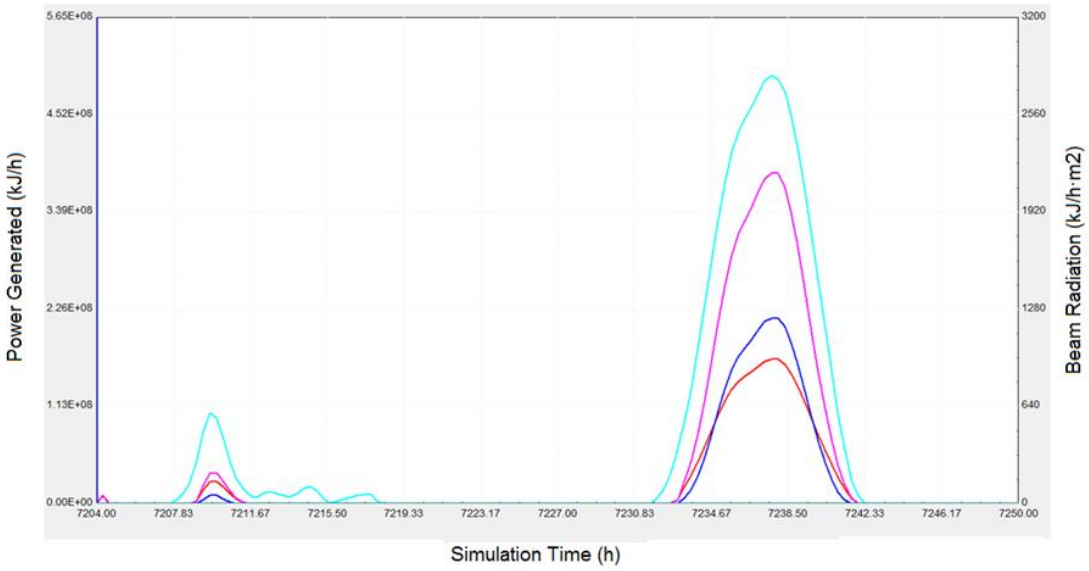


**Figure 59**: Turbine power generation [kJ/h] and beam radiation [kJ/m$^2$·h] (y-axis) vs. time [h] (x-axis)

The legend is the same as for the previous graph. The obvious correlation between solar irradiation and power generation is captured here, thus being clear that in order to truly have an autarkic solar power system it will be of imminent necessity to overcome the difficulty of not having constant solar irradiation 24 hours a day, consequently leading one to consider the implementation of an energy storage system.

### 6.5.4 Rankine cycle plus solar field and heat storage

As it was discussed in the previous section, we now include a storage system to the Rankine Power plant plus solar field. The reason is to achieve a 24 hours a day operability. The basic idea is simple: the storage system is charged when it receives solar irradiation during the day and then, either when because of the weather the beam radiation is reduced or because it is night time, the stored energy is discharged towards the Rankine cycle in order to allow the power plant to continue running.

As mentioned in section 2.2, there are various possibilities to try to carry out a successful energy storage system. Depending on the size and demands of the specific system we wish to supply, the choice will turn out to be more or less fitting.

For our actual system, using TRNSYS as we are, we are conditioned by the libraries it offers. Currently, the only storage possibilities available are "concrete storage" or "rock bed storage". They are both very similar. We choose the "**concrete storage**".

#### 6.5.4.1 TRNSYS type430 "concrete storage"

This type we will be using represents concrete thermal storage for single phase fluid (HTF oil, water, air). It consists of parallel equally spaced tubes in concrete with HTF flowing through in two possible directions: flow down (normally charge flow entering hot) and flow up (normally discharge flow entering cold). The main difference to standard type Rockbed is the three node temperature model: fluid temperature - concrete temperature - ambient temperature.

The model includes thermal capacity of concrete mass, thermal capacity of HTF and thermal loss of concrete to environment. It does not include however thermal capacity of (steel) pipe in concrete. It considers convective and conductive heat transfer perpendicular to flow direction. No axial conduction is contemplated.

The number of nodes in flow direction can be chosen deliberately (10 nodes are normally sufficient).

Input values are:

-Temperature and flow rate entering the storage on top or bottom.
-Ambient temperature
Output values are:

-Temperature and flow rate leaving the storage on top or bottom.
-Concrete temperature at top, middle and bottom bode.
-Effective heat rates in storage
-Net stored energy

Parameters are:

-Dimensions of storage
-cp and density of HTF
-cp and total mass of concrete
-Overall heat loss coefficient
-Overall heat transfer coefficient from HTF to concrete at reference flow rate
-Reference HTF flow rate
-number of axial nodes
-5 Parameters for scaling of heat transfer coefficient as:
kA/kA_ref = a0 + a1*flow/flow_ref + a2*(flow/flow_ref)**2 + a3*(flow/flow_ref)**3 + a4*(flow/flow_ref)**4 + a5*(flow/flow_ref)**5

#### 6.5.4.2 Schematics

In this system layout two solar fields are included: one (above) destined to supply the Rankine directly with HTF from the solar troughs, as in the previous installation (6.4.3) and the other, newly incorporated, is dedicated to store thermal energy in the concrete storage bloc (below). This thermal stored energy is meant to be used when there is a shortage of received solar radiation. The key piece to the new system layout is this therefore the "concrete storage" together with a regulating system formed by pumps and input commands given by Type "Equation 2" and applied to both solar fields. This regulation is basically a charge/discharge system which decides if the heated HTF will be coming from the concrete thermal storage or from the "standard" solar field above.

In this model, the Rankine cycle is the same one that has previously been proven to work. Attached are the solar fields, to serve as a source of energy. The regulation system works as following (the schematics are included in the next figure): "Equation 2" icon receives beam radiation as an input from the weather file. It has then two different comparators: "OnOffSolar" and "OnOffStorage". The "OnOffSolar"comparator gives an output signal when the beam radiation received is greater than 500kJ/m2·h. The second, "OnOffStorage" gives an output signal when 500kJ/m2·h is greater than the beam radiation received. The value 500kJ/m2·h was the one chosen to describe the absence of sufficient beam radiation. These two outputs are connected to specific pumps' control signal input. When the control output signal is given from "Ecuation 2" to a certain pump, the latter is activated. Therefore, when the beam radiation received is greater than 500kJ/m2·h, "Pump3" and "Pump4"are activated. This means that the

solar field above is pumping heated thermal oil to the Rankine cycle while in the solar field below, the HTF in being pumped only into the concrete storage; it is being charged. The concrete storage system is charged by the HTF slowly flowing through parallel pipes in a certain flow direction, heating the surrounding concrete material. While charging, the hot temperature front moves slowly with the flow direction along the storage.

When the beam radiation decreases due to overcast weather or to night time, “Pump4” and “Pump3” stop, and “Pump2” and “Pump” commence to operate. “Pump2” makes the HTF circulate from the heated concrete storage to the Rankine cycle, and “Pump” makes it flow back around, closing the cycle.

Through the concrete storage flow various pipes; at the top enters the hot HTF direct from the solar field (troughs) and at the bottom the cold HTF from the Rankine.

There is a “T-valve” included in the system where both HTF conducts from the two solar fields meet. This is necessary because there is only one input for the HTF in the Rankine cycle.
In a similar matter, there is a splitter at the exit of the hot fluid conduct of the Rankine cycle, that either recirculates it the HTF to the above solar field above or to the one below. “Pump” and “Pump2” are synchronized so the amount of HTF held by each solar system remains constant.

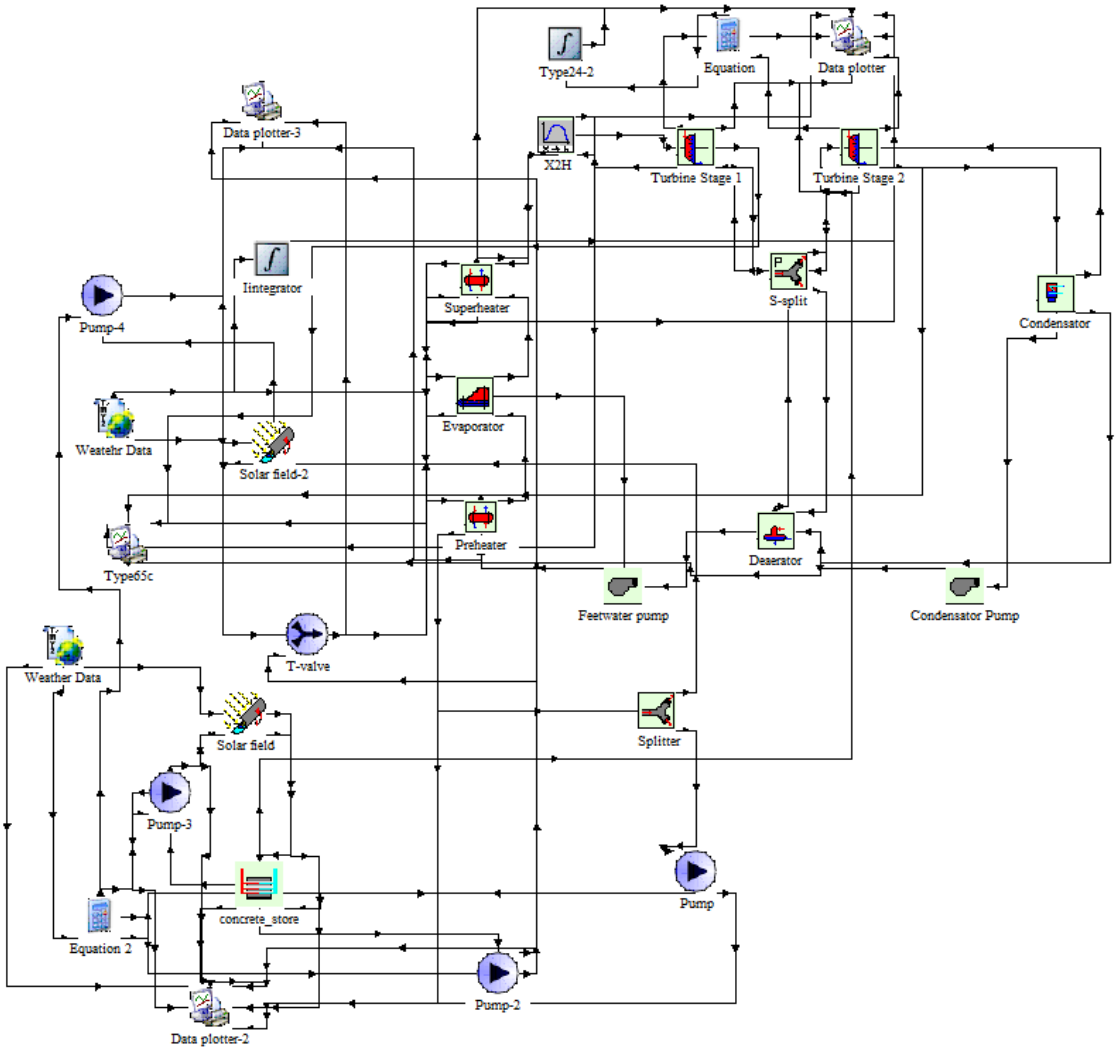


**Figure 60**: Schematics of the Rankine power plant plus solar field plus concrete storage system, in TRNSYS

#### 6.5.4.3 Concrete storage dimensioning

The size of the concrete storage must be dimensioned for our needs. We calculate the energy needed to run the Rankine cycle:

$$\dot{Q} = \dot{m}_{water}\, Cp_{water}\, (T_{out,preheater} - T_{in,preheater}) +$$

$$+\dot{m}_{water} \cdot (h_9 - h_8) + \dot{m}_{steam}\, Cp_{steam}\, (T_{out,superheater} - T_{in,superheater}) \qquad (6.30)$$

Where:

$$\dot{m}_{water} = \dot{m}_{steam} = 223\frac{kg}{s}$$

$$Cp_{water} = 4{,}18\frac{kJ}{kg \cdot K}$$

$$(T_{out,preheater} - T_{in,preheater}) = 311 - 231{,}95 = 79{,}05K$$

$$h_9 - h_8 = 2725 - 1407{,}8 = 1317{,}2\ \text{kJ/kg}$$

$Cp_{steam} = 2{,}05 \frac{kJ}{kg \cdot K}$

$\left(T_{out\,,super\ heater} - T_{in,super\ heater}\right) = 390 - 311 = 79K$

$$\dot{Q} = 441060\ kJ/s \tag{6.31}$$

The demands at night are approximately 40% of the maximum demand (6.31), so we will consider that during this time the power needed will only be

$$\dot{Q}night = 40\%\ of\ 441060 \frac{kJ}{s} = 176424 \frac{kJ}{s} \tag{6.32}$$

Considering that the night (absence of sun) has on average 14 hours duration, the energy needed to be stored to supply the system at night would be

$$Q_{TOTAL} = 176424\ \frac{kJ}{s} \cdot 13\ h \cdot 3600 \frac{s}{h} = 8{,}26 \cdot 10^9 kJ \tag{6.33}$$

From the following expression we can calculate the value of the concrete mass needed for such a system.

$$Q_{concrete} = m_{concrete}\ Cp_{concrete}\ (\Delta T) \tag{6.34}$$

Considering the $Cp_{concrete}$=2,33 kJ/kg·K, and a $\Delta T$ , temperature difference of no more than 25ºC (from 390ºC to 365ºC), making equal $Q_{TOTAL} = Q_{concrete}$ , we obtain:

$$m_{concrete} = \frac{Q_{concrete}}{Cp_{concrete}\ (\Delta T)} = 141{,}8 \cdot 10^6 kg = 141.802Tm \tag{6.35}$$

The density of thermal concrete is around ρ=2100 kg/m$^3$. Therefore, given the density and mass, we know we will need the following volume:

$$V = \frac{m}{\rho} = 67.524\text{m}^3 \tag{6.36}$$

Considering it is simply shaped like a cube, the side of the cube would be approximately 41 m long.

#### 6.5.4.4 Results and validation

The following graph includes 3 whole years of simulation of the Rankine cycle plus solar field and thermal storage. It is possible to see that the power generation never decreases to cero during shortage of beam radiation received. This means that the thermal energy storage system is indeed working. The problem is that there are great variations during day and night.

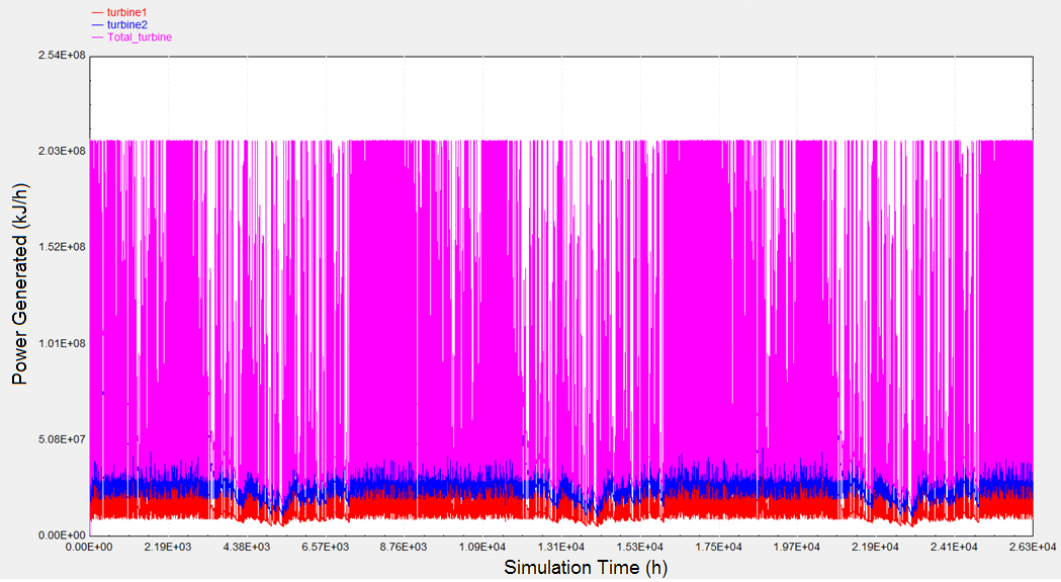


**Figure 61:** Behavior throughout 3 years of thermal storage in power plant

The pink curve is the total turbine power generated (sum of stage 1 turbine, dark blue, and stage 2 turbine, red). In the next figure, we zoom in to observe the behavior in a more detailed matter:

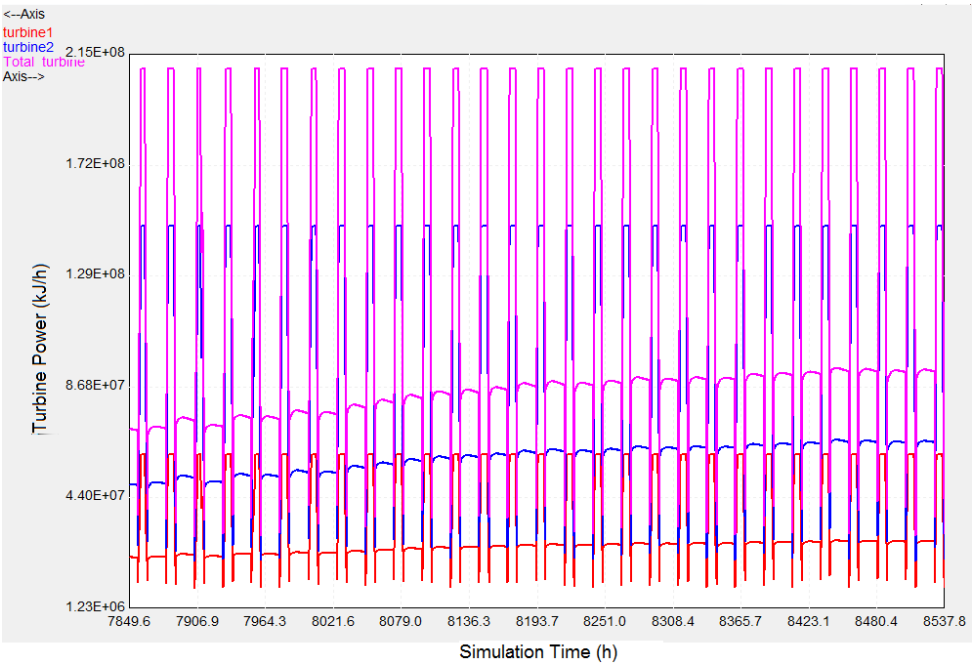


**Figure 62:** 24 hour a day electric generation

The pink line, total turbine power generation, reaches maximum values during the day. During the night, despite the continuous power generation, it decreases drastically over half of the average during the day. The entire system suffers from these drastic changes in load. The ideal would be to achieve a constant power generation value 24 hours a day. It can be noticed that the slope of the total power generated at night by the turbines slowly decreases during the night as the temperature of the storage also slowly decreases.

If the zoom-in is in a section where we have cloudy days, the results are worse. The maximum power generation is not reached at any time during various days. The system should be improved in order to overcome this insufficiency.

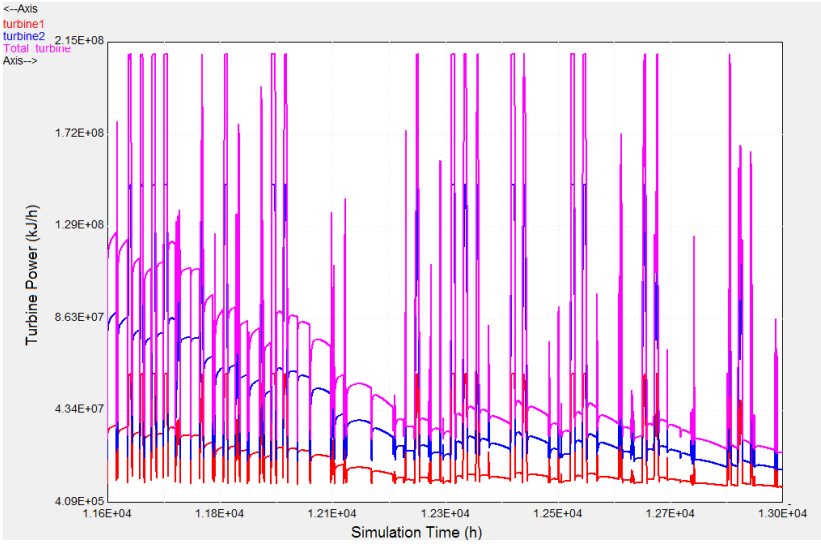


Figure 63: Zoom-in on previous graph

A global energy balance is calculated next. In it, the amount of energy stored during the day and the amount discharged during the night are compared. They should tend to an equal value. The procedure to calculate this balance is as follows:

The energy stored during the day can be based on the HTF temperature difference between the HTF temperature out of the solar trough and the HTF temperature at the outlet of the concrete storage (bottom).

$$\dot{Q}_{storage\ \_day} = \dot{m}_{HTF} \cdot C_p (T_{out,solar\ \ field} - T_{out,concrete\ \ storage\ \ bottom})$$

The energy discharged at night can be obtained based on the temperature difference between the HTF temperature at the outlet of the preheater and the HTF temperature at the outlet of the concrete storage (top).

$$\dot{Q}_{discharge\_night} = \dot{m}_{HTF} \cdot C_p (T_{out,preheater} - T_{out,concrete\ \ storage\ \ top})$$

The next figure shows a schematic of how the system is working and which temperatures are being used in each of the equations involved.

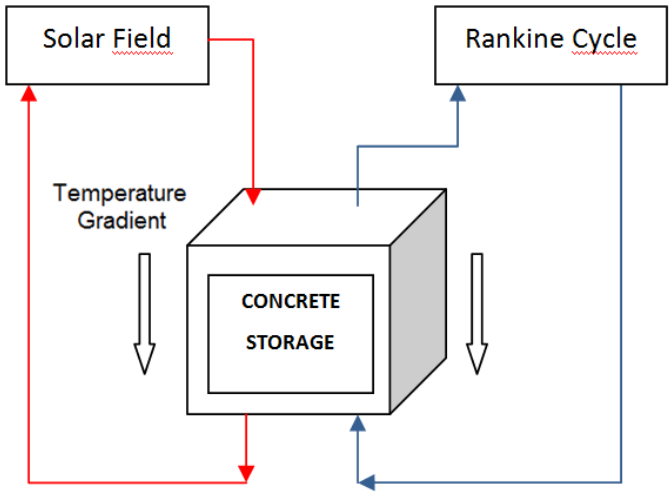


Figure 64: Schematics of HTF flows in and out of concrete storage.

From the total year, a series of sunny days are taken, and certain values are graphed out:

- HTF outlet solar field temperature (red)
- HTF outlet concrete storage temperature at bottom (blue)
- HTF outlet concrete storage temperature at top (pink)
- HTF outlet preheater temperature (orange)

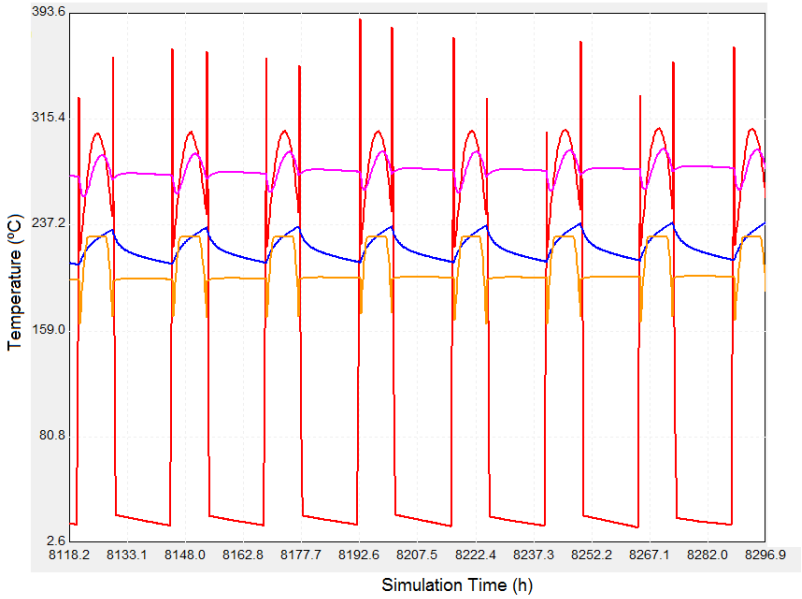


Figure 65: Various HTF temperatures (ºC) vs. time (h)

The HTF temperature in the Solar field (red line) rises to about 306ºC during the day at a period of sunny weather and then, at night, it behaves like the ambient temperature, slowly decreasing until the next time the sun rises. There is an impulse rise in the solar HTF temperature every day but this value is so short in time it is practically insignificant. It takes place between the change of systems, the regulation system changes from the solar field HTF to the storage HTF (in the instant before and after receiving 500 kJ/h·m2 from the sun). In this time, the HTF stops circulating and is heated when the solar field pump stops, while the solar troughs are discontinuing their operations. The ideal would be to first turn away from the sun the solar troughs and then disconnect the pump. In any case, the temperature never goes over 390ºC so the oil will not become degraded.

The HTF temperature at the bottom of the storage (blue) rises during the day and then, at night, when the HTF running through the Rankine cycle start to withdraw thermal energy from it, it decreases. It is the area of the storage concrete where the energy first starts to discharge. The HTF temperature at the top of the storage (pink) also rises during the day and remains practically constant at night (it also has a slight decreasing tendency). The reason is because the temperature gradient starts below and before it reaches the top, as to say, the sun rises again and again increases the temperatures.

As for the HTF temperature at the outlet of the preheater, it is higher during the day because the HTF used at this time is warmer, and at night time, it remains practically constant because there is not enough time for the HTF being used to discharge all the stored energy in the concrete block.

Now, as for the numerical results, the following are obtained on average:

$$\dot{Q}_{storage\ \_day} = 1500\frac{kg}{s} \cdot 2{,}6\ \frac{kJ}{kg \cdot k}(306{,}3 - 229{,}7) = 298.740kW$$

Note: the HTF temperature at the bottom of the storage is taken as the average during the day. The temperature rises in approximately a linear matter.

$$\dot{Q}_{discharge\ \_night} = 1500\frac{kg}{s} \cdot 2{,}6\ \frac{kJ}{kg \cdot k}(278{,}0 - 198{,}7) = 309.270kW$$

Between the two results, there is a difference of approximately 3,4%, as was expected. This proves then that the amount of energy stored during the day is the amount that is being withdrawn at night.

The simulation time used is far away from the beginning of the iteration. It is passed the 8000$^{th}$ hour, so any error due to the beginning of the calculations has been avoided. This behavior can be found in any case all throughout the simulation. In the following model we shall analyze the total energy stored during the day with the one discharged at night throughout the whole year for a more extensive energy balance calculation.

#### 6.5.4.5 Improvements and optimizations

With the following improvements on the storage system, the goal pursued is to achieve an always full storage in order to avoid such big fluctuations between night and day in the power generated by the turbines.

There are primarily four parameters with which we can achieve improvements in this direction, especially when varied in combination with one another:

- *Increase of solar field area:*

By increasing this surface, we increase the amount of energy we capture from the sun.

- *Increase in HTF mass flow from storage solar field to concrete storage.*

Greater amount of energy could be transferred to the concrete storage with the same temperature difference.

- *Increase of concrete total mass*

More energy could be stored.

- *Increase in temperature of HTF that flows from solar field to the concrete storage.*

This would also be a way to achieve greater amount of energy transfer from the solar field to the concrete storage maintaining the same HTF mass flow. The problem is that this option has only theoretical value because the thermal oils available in the market have a temperature limit of around 390ºC-400ºC maximum. If this temperature were to be exceeded, the oil would degrade itself thus losing all its properties and therefore becoming useless.

Given these variables, the parameters from the system are empirically modified until a practically constant power generation output from the turbines is achieved. This means that the variation during day and night is practically insignificant. The main strategy is to consider that the increase in solar field should be the last option why it results in the most expensive of modifications.

One of the solutions reached is the following:

- Increase of concrete mass to 2.646.000.000kg with a total cross section area of pipes of 15.000m$^2$ and a length of storage of 84m. The initial value was 141.800.000 kg, with a total cross section area of pipes of 1.658m$^2$ and a length of storage of 41m.

- Increase the solar fields to 925 collectors in series and 925 collectors in parallel, with a same aperture of 6m$^2$. The initial value was of 323x323 collectors, with 6m aperture.

- Increase the HTF from the solar field to the concrete storage to 1100kg/s. Initial value was of 223kg/s.

With these new parameter inputs we obtain the following behavior of the turbines:

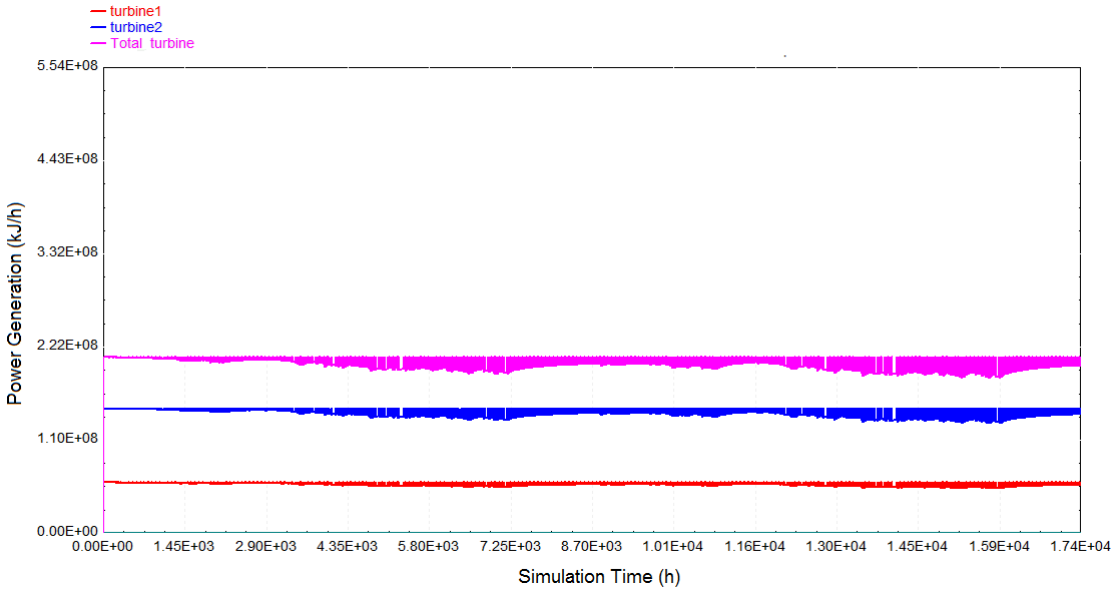


Figure 66: Power generation (kJ/h) vs. Time (h)

The pink line, as in earlier similar graphs, represents the total power generated by the two turbine stages. The criteria used to modify the system were to have a variation of power generation of from 5 to 10% during day and night. This means that the power generation is practically constant.

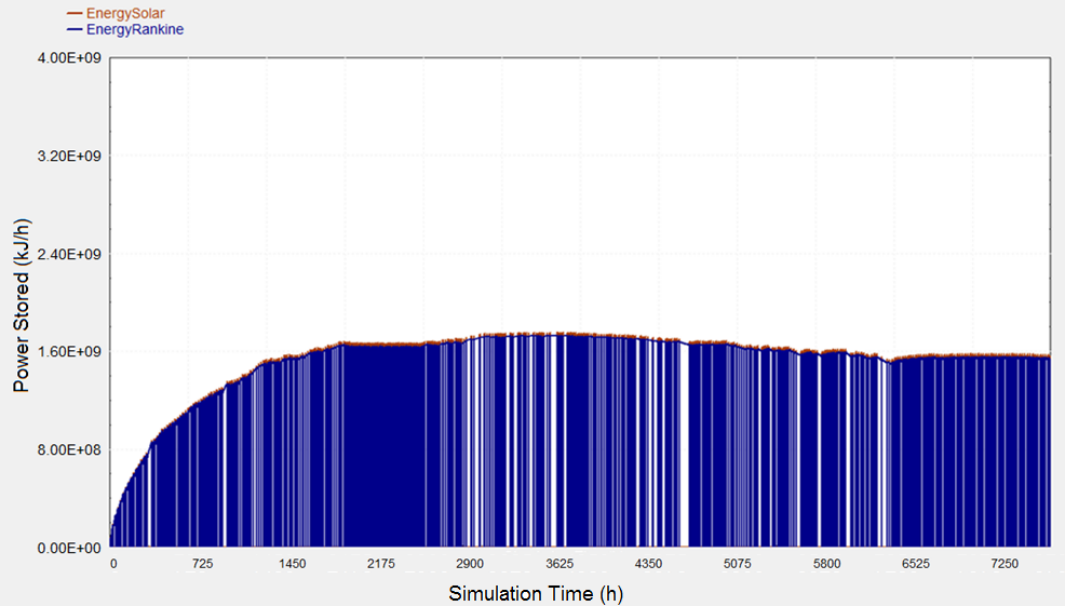


Figure 67: Energy stored during the day and energy discharged during the night

In this graph one can see that the energy stored during the day (brown) and the energy discharged at night (blue) are practically the same. Therefore, the balance is practically cero, as expected. The calculations have been done analogous to $\dot{Q}_{storag\ e\_day}$ and $\dot{Q}_{disc\,harge\_nig\,ht}$, previously displayed, but throughout a much longer amount of time, not just instantly.

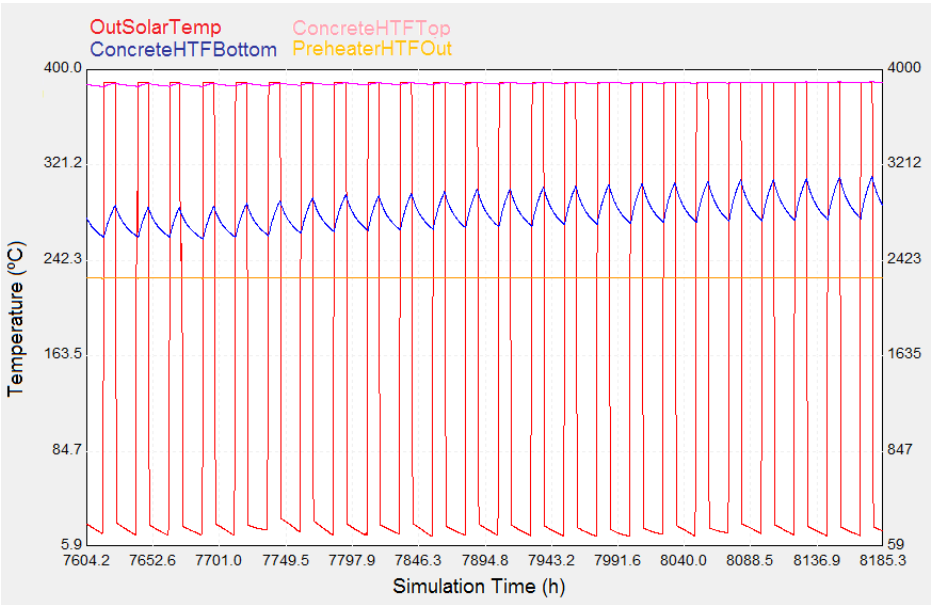


Figure 68: Various HTF temperatures (ºC) vs. time (h)

Analogous to Figure 65, we have a zoom-in of the behavior of the HTF temperatures on top (hot) and bottom (cold) of the concrete block, at the solar field of the storage system and preheater outlet. In this over-dimensioned model, the HTF exiting the solar field (red) is always 390ºC during the day, maximum temperature permitted for the oil to reach, and decreases to atmospheric temperature during the night. The temperature of the HTF at the top (pink) is practically a constant throughout day and night, at 390ºC, which indicates that the storage is full. The temperature of the HTF at the bottom (blue) oscillates; it grows during the day, of course, and decreases as the HTF from the Rankine cycle receives its heat transfer. As for the preheater HTF outlet temperature, it remains a constant because it always has enough heat to operate either from the daily system or the storage, night system.

In any case, the system modeled is clearly over-dimensioned. As reflected in Table 6, section 4.2.2, the electric demand esteemed during the night is approximately 35% lower on average than that one demanded during the day. Therefore, the aim will be to adjust the storage system to this specific demand.

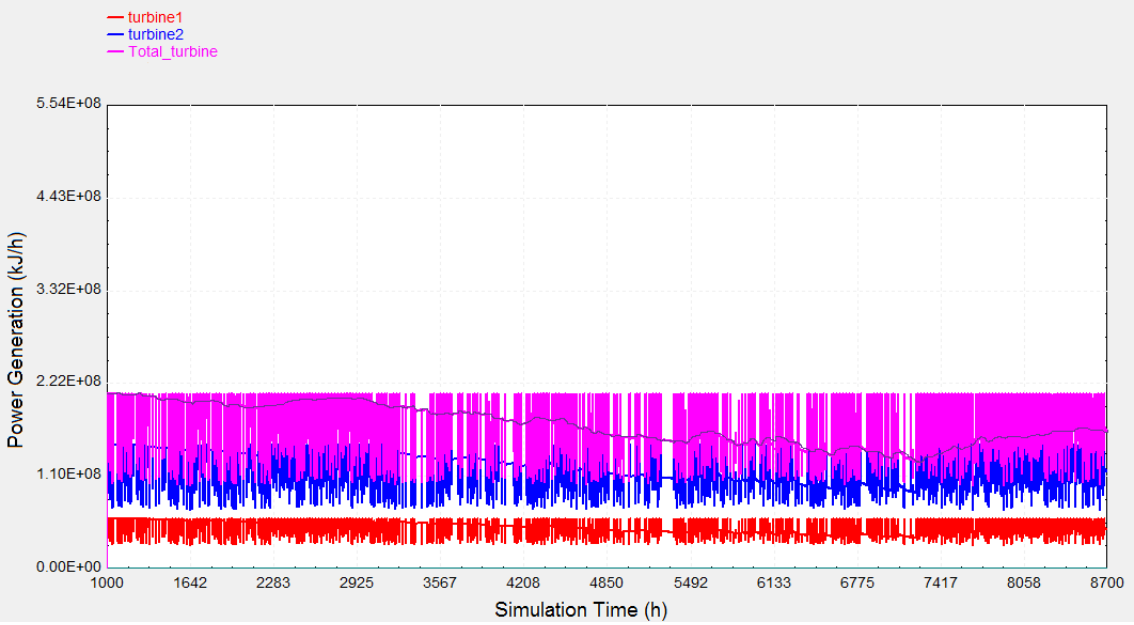


Figure 69: Power generation vs. time (h)

Once again, empirically modifying the key parameters in our system, we obtain a new model, ultimately more adjusted to the needs. The pink line once again represents the power generated by the two stage turbine. There is great oscillation when the system regulator switches from the direct solar field to the storage system, but these peaks in power generation are only impulses, and are not lasting sufficiently in time to represent a significant behavior. In fact, highlighted in purple there is a line that represents the steady power generated, aside from the oscillations. The maximum reached during the day is of $2{,}09 \cdot 10^8$ kJ/h and the minimum at night is of

$1{,}35 \cdot 10^8$ kJ/h. This means that there is a **35% reduction** in the power generated at night, which fits the demands previously mentioned.

In order to achieve the previous results, the following reductions were carried out in the amount of solar collectors:

Solar field collectors: 590 parallel x 590 in series at a $6m^2$ aperture (from a previous 1100x1100).

HTF flow from solar field to concrete storage: 695kg/s (from a previous 1500kg/s).

Concrete storage mass reduction of a 50% in relation to the previous design; this is 1.323.000.000kg ($85m^3$ cube).

As for the energy stored during the day in relation to the energy discharged during the night, the following results were obtained and reflected in the next figure.

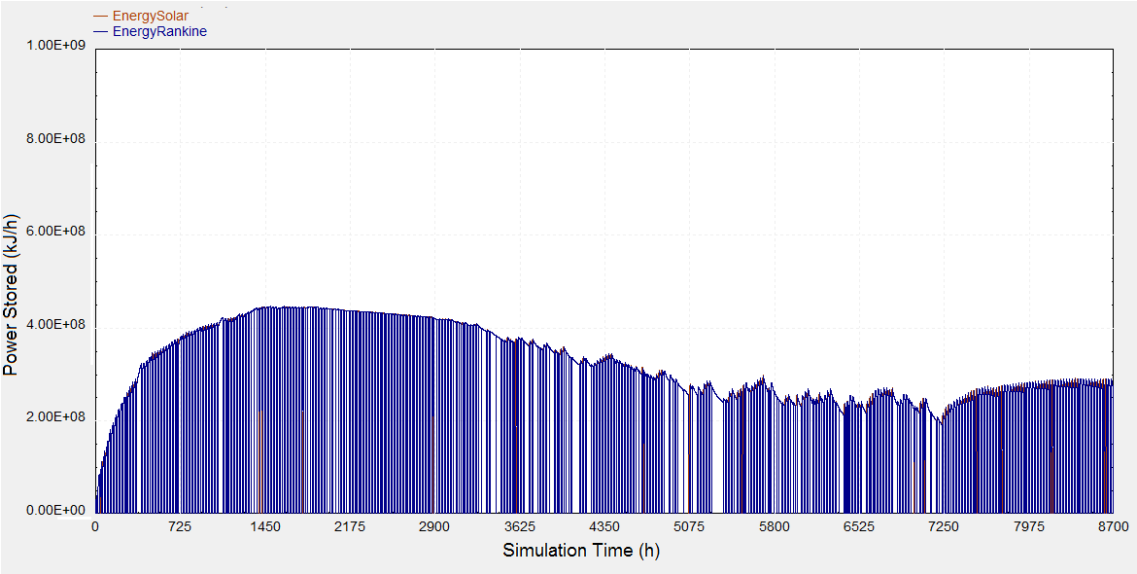


Figure 70: Energy stored during the day and discharged during the night

The power stored and discharged basically overlap. The net flux is practically cero.

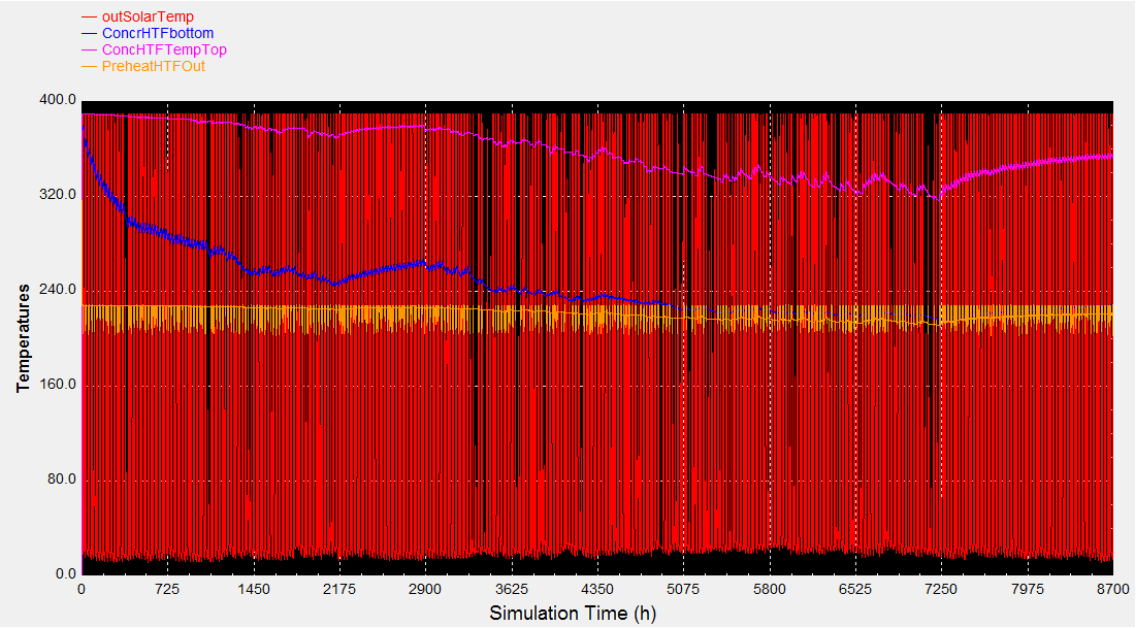


Figure 71: Various HTF temperatures (ºC) vs. time (h)

Observing the temperature behavior throughout the year, one is able to observe that in this case the storage is once again not quite full; the bottom *and* top HTF temperatures from the concrete storage vary. In fact, the bottom one is practically at the preheater temperature. This is a critical point and the temperature at the bottom of the concrete storage should obviously never be below the preheater one. In this case they overlap for some time, but as observed before in the turbine behavior of figure 69, the power obtained by the turbine still fits to the needs to fulfill.

The system is now not so over dimensioned in relation to the initial estimations and is still better adjusted than the previous model in a way that the demands are met. During the day, the turbine generates maximum power and during the night it is reduced approximately a 35%.

## 6.6 ENERGETIC BYPASS

In systems of this nature, it is usually standard to include an energetic bypass which is meant ensure the continuity of electric generation. Usually the bypass is achieved through fossil fuels but, in any case, the politics applied to these energetic supplements limit them to an approximate 25% of the general electric generation production.

In our system, we avoid using this possibility. Aside from the concrete storage system, other ideas were being considered to ensure the 24 hour per day electric generation. If the thermal storage proved to be insufficient at any given point, excess electric energy could be generated during the night and sold to the electrical grid (sometimes directly for credit) and then, when needed, it could be directly rebought and used. In this case, even though the technical autarky would fail, at least the system would still maintain economical independence, also a very important factor to not be forgotten.

Further ideas actually would involve an energetic bypass, but instead of basing it on traditional fossil fuels, local biomass or even local waste could be contemplated as an energetic option, assuming always full viability and sustainability with the local environment, such as its economy (the idea would have to be discarded if the use of a local biomass would have price rise as a side-effect, especially if the biomass chosen is used as an essential part of local needs).

## 6.7 CONCLUSIONS

Starting from an independent Rankine power cycle with constant inputs, a solar field combined with a thermal concrete storage subsystem was attached to it in order to reproduce a model fed energetically by the sun radiation (transient) and able to operate 24 hours per day.

The first estimations showed that, despite generating electricity during the night, this amount was not enough to cover demands.

Thanks to the empirical manipulation of the key parameters in the designed model (number of solar collectors, HTF from solar field to storage, dimensions of storage), a constant power generation output was achieved. The problem with this solution was the over dimensioning of the system given in order to obtain such behavior. The energy stored during the day was roughly 4 times more than the energy discharged at night.

Conclusively, the dimensions of the system were decreased so the day demand and night demand (approximately 35% lower) could be both covered when needed.

## 6.8 SOLAR FIELD FLOW RATE REGULATION

In many existing solar power plants, the flow rate of the circulating heat transfer fluid is manually controlled by a plant operator. The plant operators typically increase the flow rate gradually through the solar field during start up, maintain a relatively constant flow through mid-day operation, and gradually lower the flow rate late in the day in preparation for power plant shut down. High flow rates improve the heat transfer coefficient in the HTF steam heat exchangers, but result in higher pumping parasitics and lower solar field outlet temperatures. Conversely, low flow rates will result in smaller pumping parasitics and higher solar field outlet temperatures, but reduce the heat transfer coefficient in the HTF steam heat exchangers. At very low flow rates, operators may further run the risk of degrading the heat transfer fluid, or creating thermal shock or HTF expansion in the solar field equipment great enough to break the receiver tubes. Plant operators rely on observation of temperatures in the solar trough field, observation of weather conditions (such as cloud cover), and their individual experience and best judgment to balance the competing temperature and flow rate requirements.

The efficiency of the solar field decreases with increasing outlet temperature. The efficiency of the power cycle increases with increasing outlet temperature. The magnitude of these competing trends is such that the net change in system efficiency with outlet temperature is small. Therefore, operation over a wide range of solar field temperatures and flow rates will produce little discernible difference in the electricity output.

# 7. DESALINATION PLANT

## 7.1 INTRODUCTION

This chapter is dedicated to the design and simulation of the desalination plant that will supply the housing estate with potable water. From the models displayed in section 2.3, we finally choose to design a *multi-stage flash* (MSF) desalination plant since it is the one that most fits to our needs and to the characteristics of our project (site placement, solar energy as a source of energy, comparative maturity of the desalination technology for this purpose).

The model presented here, developed in TRNSYS, is of a simplified MSF plant. Part of the components or of the structure of the real plants are not possible to model with the existing library in TRNSYS and would have to be either completely programmed or approximated with a successful combination of already existing types.

**Figure 72**: MSF power plant of a 23500ton/day production [44]

## 7.2 DIMENSIONING AND CALCULATIONS

In section 3.5, it was estimated that the water demand to be processed was of

$$Q_{daily\ \ demand} = 4.011.311 \frac{liters}{day} \quad (7.1)$$

In section 4.1.1 the energy demand needed to run the plant was calculated to be

$$ED_{desali\ nation} = 18094{,}12 \frac{kW\,h}{day} \quad (7.2)$$

One day is contemplates as 10 hours. In the following table, key parameters for our installation have been included. They are based on previous calculations (section 4.1.1) or from other bibliographical sources from other existing power plants (16),(17),(18),(19) In all sources, the electric demand is about a 6% (20) of the net energy heat input.

| | |
|---|---|
| Production | 4012 m3/day |
| Electric power required | 1809kW |
| Sea water flow | 401 m3/h (10 hours a day) |
| Heat imput | 30150kW |

Table 10: MSF plant operation parameters

### 7.2.1 Water inlet

The need is 4.012.000 l/day. If the day has 10 hours of direct sunlight on average, then 401.200 l/h are required of purified water. The percentage of inlet flow seawater that is distilled in the plant is 45% (16),(17),(18),(19). Therefore, we will need

$$Seawater\ flow = 891.555{,}6 \frac{\mathrm{l}}{\mathrm{h}} \quad (7.1)$$

### 7.2.2 Solar field surface

In order to calculate the solar field surface required, we must be aware of the amount of beam radiation received from the sun. Therefore we include the following graph, where the *beam radiation* (kJ/h·m$^2$) is represented by the pink line and the integrated value in time of the beam radiation is the red line. The x-axis is time (h), the left vertical axis is kJ/h and the vertical right one is kJ/h·m$^2$.

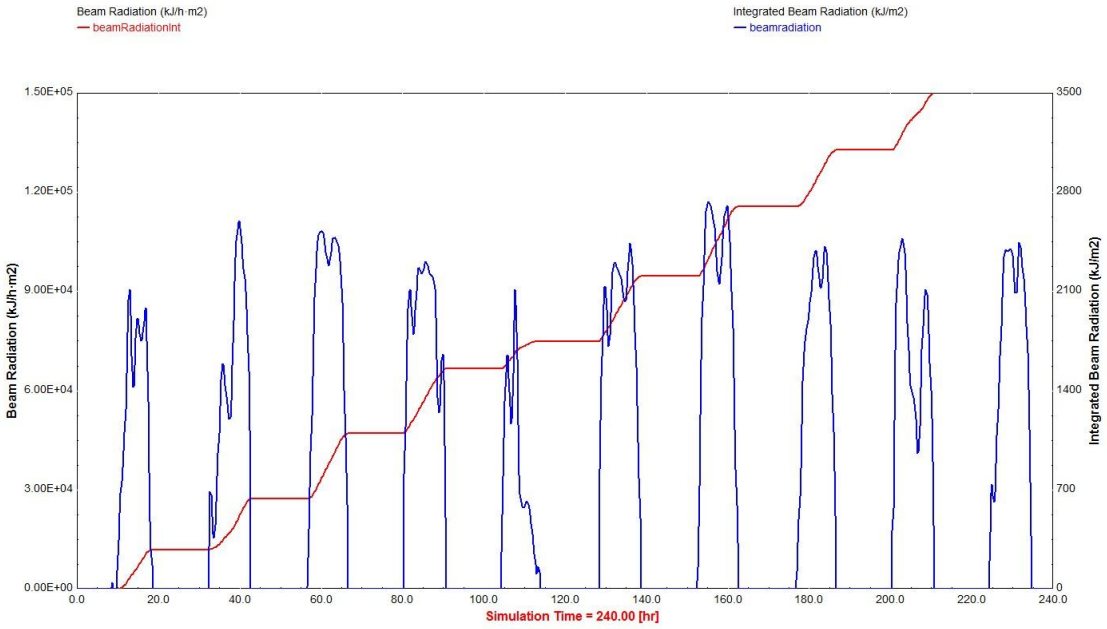


**Figure 73:** Beam radiation and integrated beam radiation

Based on an average sunny day, with almost complete absence of clouds, in winter, that receives a peak of 2500 kJ/h·m$^2$, integrated throughout the whole day, we obtain 19795 kJ/m$^2$. This amount of energy is received in 10 hours so we have:

$$1979{,}5\frac{\text{kJ}}{\text{m}^2\cdot\text{h}}\cdot\frac{1\text{h}}{3600s}=0{,}55\frac{kW}{m^2}$$

We contemplate the inner efficiencies of the plant, (40%).

Finally, we have:

$$Solar\ Field\ Area=\frac{Necessary\ \ heat\ imput}{solar\ \ power\ \ per\ \ m^2}=\frac{30150\,kW}{0{,}22\ kW/m^2}=137045m^2 \qquad (7.4)$$

Our solar field will have the following dimensions:

- Number of collectors in parallel: 151
- Number of collectors in series: 151
- Aperture area: 6 m$^2$

### 7.2.3 Electric demand

It is of course mostly used for the different pumps, although a small percentage is also meant to go to illumination or to valve control. In any case, this is a general estimation of how the electric demand is broken down. As we have already said, our electric demand is 1809 kW.

| Al Taweelah B breakdown of power requirements (in %) | |
|---|---|
| Seawater supply pump | 26 |
| Brine recirculation pump | 64 |
| Brine blowdown extraction | 3 |
| Distillate pump | 5 |
| Condensate extraction | 2 |

| UANE 4-5-6 breakdown of power requirements (in %) | |
|---|---|
| Seawater supply pump | 29 |
| Brine recirculation pump | 61 |
| Brine blowdown pump | 5 |
| Distillate pump | 4 |
| Condensate extraction | 1 |

Figure 74: MSF plant power requirement breakdown

### 7.2.4 Thermodynamic parameters

In this section are gathered the values of pressure, temperature and mass flows that correspond to each different stage. They are available in any water table although the parameter stages are based on real data (21).

| | | STAGE 1 | STAGE 2 | STAGE 3 |
|---|---|---|---|---|
| LIQUID | | $T_{1l}$=99,63ºC | $T_{2l}$=73,75ºC | $T_{3l}$=38,25ºC |
| | | $P_{1l}$=1bar | $P_{2l}$=0,37bar | $P_{3l}$=0,07bar |
| VAPOR | | $T_{1v}$=99,63ºC | $T_{2v}$=73,75ºC | $T_{3v}$=38,25ºC |
| | | $P_{1v}$=1bar | $P_{2v}$=0,37bar | $P_{3v}$=0,07bar |
| MASS FLOW | Liquid | $m_{l1}$=13373,3l/h | $m_{l2}$=133376,4l/h | $m_{l3}$=131058,7l/h |
| | Vapor | $m_{v1}$=75782l/h | $m_{v2}$=62408,9l/h | $m_{v3}$=49303,0l/h |

Table 11: MSF parameters in 3 stages

The inlet from the ocean is 891556l/h during 10 hours. In the 1st stage 155 is distilled, in the 2nd 17% and in the 3rd, 21% of the remaining seawater.

## 7.3 TRNSYS model. Components. Assumptions

### 7.3.1 TRNSYS model

The basic appearance of an MSF plant is represented in the following figure:

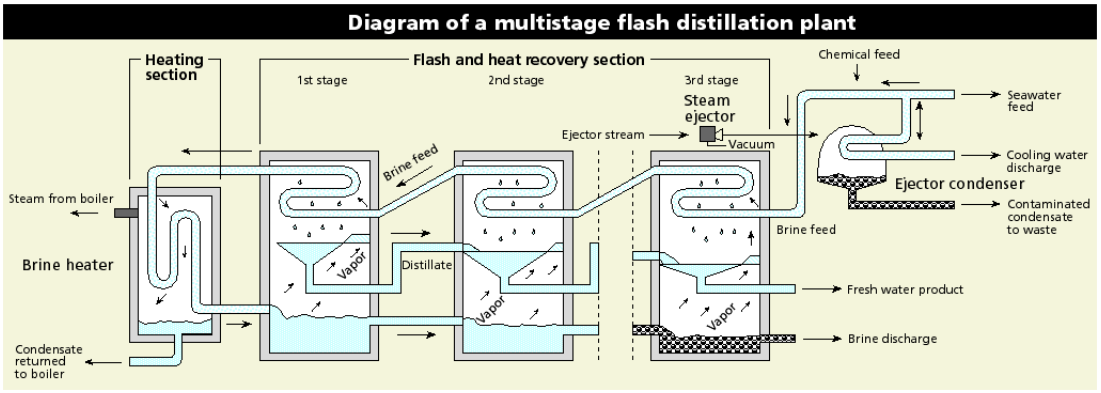


**Figure 75**: Diagram of MSF desalination process [45]

In the TRNSYS model that has been developed, we have designed only three stages. In reality there are usually between 12 and 24, although the concept is exactly the same.

The actual design of the MSF plant in TRNSYS is included below and is further explained. The length of it forces it to be divided into three pieces in order to appreciate the entire design.

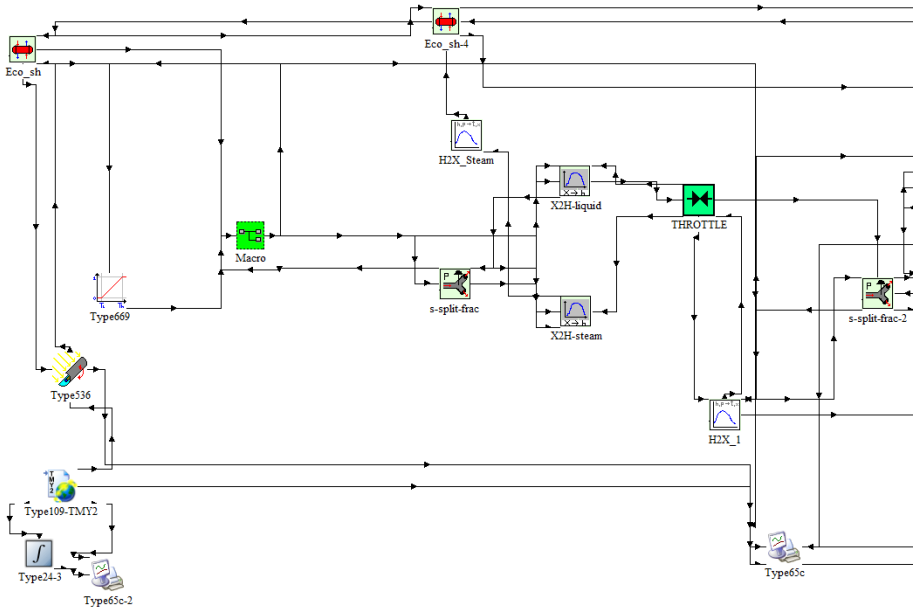


**Figure 76**: MSF plant in TRNSYS. Part 1 of 3

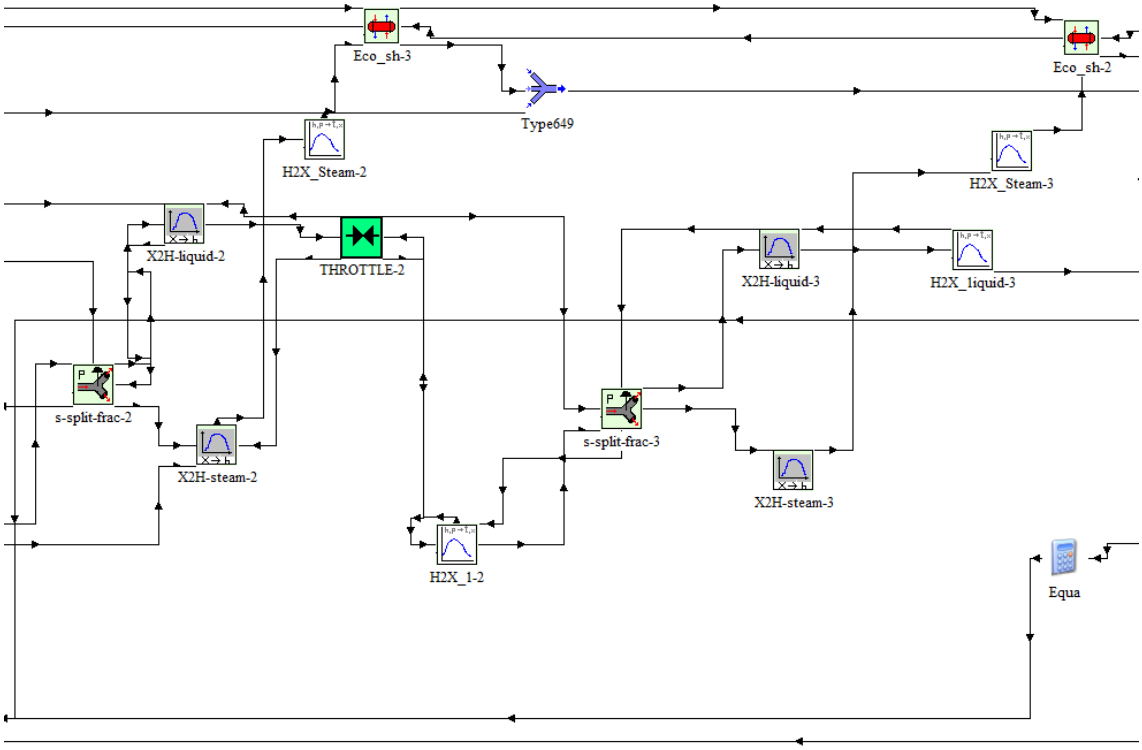


**Figure 77**: MSF plant in TRNSYS. Part 2 of 3

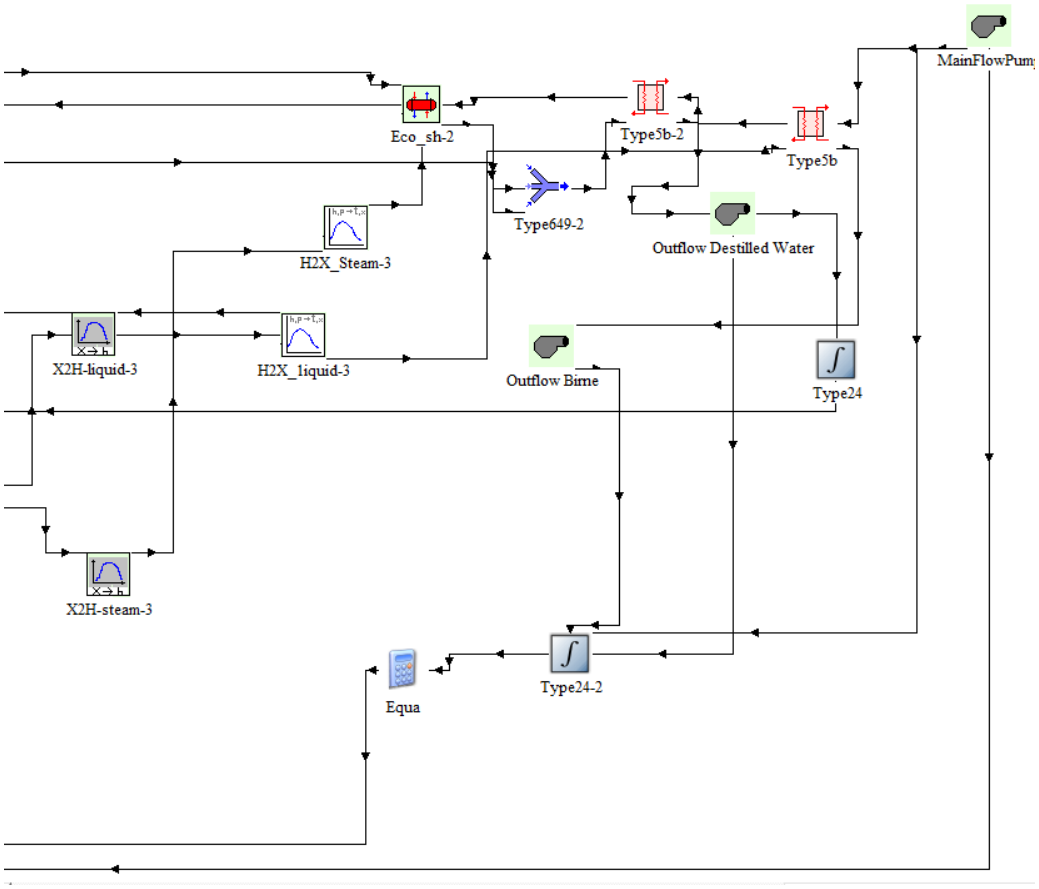


**Figure 78**: MSF plant in TRNSYS. Part 3 of 3

### 7.3.2 Components

- *Main flow pump (part 3 of 3)*

Seawater enters the system at a flow of $891.555{,}6\frac{l}{h}$.

- *Type5b type5b-2, counterflow heat exchangers*

The inlet seawater goes through the first heat exchanger and receives heat from the distilled water and the brine that are already exiting the plant.

- *Eco_sh-2, condenser*

In reality, they are condensers, but the TRNSYS component that was used is a preheater. The vapor that is released from below, from the brine evaporating, passes through this preheater as the hot fluid. It warms the sea water that enters it as a cold fluid. *Eco_sh-3*, *Eco_sh-4* and *Eco_sh* serve the same purpose. They use the residual heat in order to raise the efficiency of the whole process. The last condensator, *Eco_sh*, actually receives the heat from the solar field. Its hot fluid entrance is actually HTF (thermal oil) from the solar troughs.

- *Type 669, proportional controller*

It will regulate the water recirculation of the system. At the system start-up, the seawater doesn't have enough time to sufficiently heat up and reach the first evaporating temperature (aprox. 95ºC), so it has to be recirculated. The controller, what it does, is allow the water that has greater quality than 0 to go by. In other words, water already in liquid-vapor stage. If it is still 0, it is when it is recircled. It is contemplated that the amount of water that is recircled is subtracted from the amount of seawater being pumped in. If not, we would obviously have excess water in the system.

- *"Macro, s-split-frac, X2H-liquid, X2H-steam", separator*

The MSF plant works with different boxes or compartments. When the heated seawater enters one of these compartments, there is a flash evaporation due to the lower pressure conditions. The vapor rises and goes through the condenser, and the distilled water is then collected in a separate processed water conduct, and the brine down below continues to the next compartment, at a yet lower pressure, in which, despite the lower temperature, the process repeats itself. In TRNSYS we are not able to model such compartments, but we can design a sort of steam separator from the above mentioned components. Its result is to separate the proportion of steam from the liquid mix. Since we have three stages, in each stage there is 15% of the seawater

evaporated, adding the total of 45% at the end of the whole process. The vapor is separated (15%) and connected to the condenser above and the brine (85%) is connected to the *throttle.*

- *H2X_Steam*

It changes the parameters we work with to have temperature as an outlet parameter, so it is compatible with the condenser/preheater inlets.

- *Throttle*

It s a sort of valve that allows the upstream flow to have a different pressure as the downstream flow. This way, the pressure chamber difference is emulated. This is the division between the 1st and 2nd stage, and also from the 2nd and the 3rd further down.

- *Type64, mixing valve*

It mixes the first evaporated seawater with the one obtained from the condenser in the second stage. The *Type649_2* has the same function but between stage 2 and 3.

- *Outflow distilled water pump*

It pumps out the distilled potable water after it has already passed through the initial counterflow heat exchangers.

- *Outflow brine water pump*

It holds the same function as the above except for the residual salt water. It is also connected to the outflow of the initial counterflow heat exchanger.

- *Type 24, 24_2 and Equa*

They serve to have an account of the combined power that the pumps demand to work.

- *Type109-TMY2, weather file*

As described for the Rankine cycle, the weather file is connected to the solar troughs by beam radiation [kJ/h·$m^2$] and atmospheric temperature [ºC].

- *Type24-3, integrator*

It integrates the solar beam radiation in the time variable.

- *Type65c, type65c-2*

They are data plotters.

### 7.3.3 Assumptions

Normally, a MSF desalination plant has from 12 to 24 different stages where the seawater gradually becomes distilled. In our model, just 3 stages have been designed, because the concept is totally analogous and repetitious. Obviously then, the percentage of water that evaporates in each stage is higher than usual in order to achieve the same outlet distilled flow.

In MSF process, the different chambers of each stage are carefully designed, following specific geometric constructions and techniques. In our design, this must be substituted by a more simple design due to the unavailability of such components in the TRNSYS library.

The chemical processes that the distilled water should go through to ensure a correct quality have been excluded from the design for similar reasons, aside from the fact that our design is more centered in the more thermodynamic behavior of the plant.

## 7.4 MODEL VALIDATION

### 7.4.1 Distilled flows, heat transfer

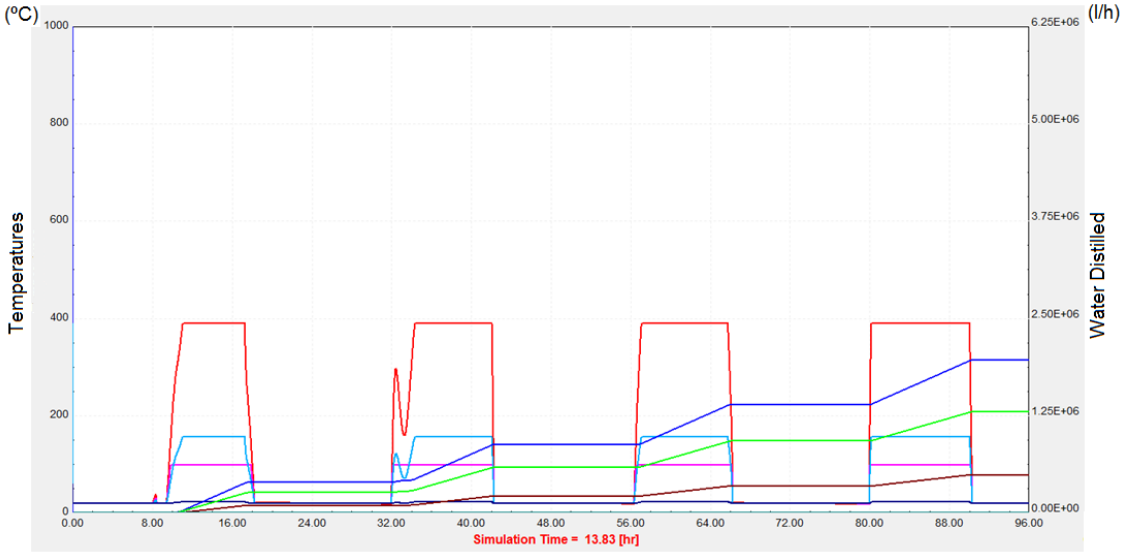


**Figure 79:** Desalination plant parameters and behavior

In the previous graph, there are various variables represented:

The *distilled flows* are the ascending lines that have horizontal sections. The distilled flow obtained in each stage is represented: the brown line is for the distilled water from stage 1, the green from stage 2 (added to the previous stage) and the dark blue is for stage 3 plus the two previous stages, thus constituting the entire distilled water flow. The vertical axis to the right is where this variable is referenced; it is in l/h. One can see that the total quantities coincide with what was dimensioned. Every day approximately 4.012.000 l are obtained. The horizontal stretches of the lines indicate nighttime, when the plant is not operating.

The *heat transfer* from the HTF to the inlet seawater can also be appreciated in this graph. The red line indicates the outlet temperature of the HTF from the troughs; in other words, the thermal oil that has been heated and is leaving the solar field at maximum temperature. Its temperature during the day reaches 390ºC. The turquoise line is for the hot side outlet flow from the preheater from stage 1. In other words, the thermal oil after it has heated the incoming seawater. It is noticeable lower than at the entrance (approximately 157.5ºC at maximum point). This temperature difference can be translated as the heat transfer between the HTF (oil) and the incoming seawater.

### 7.4.2 Electric pump demand

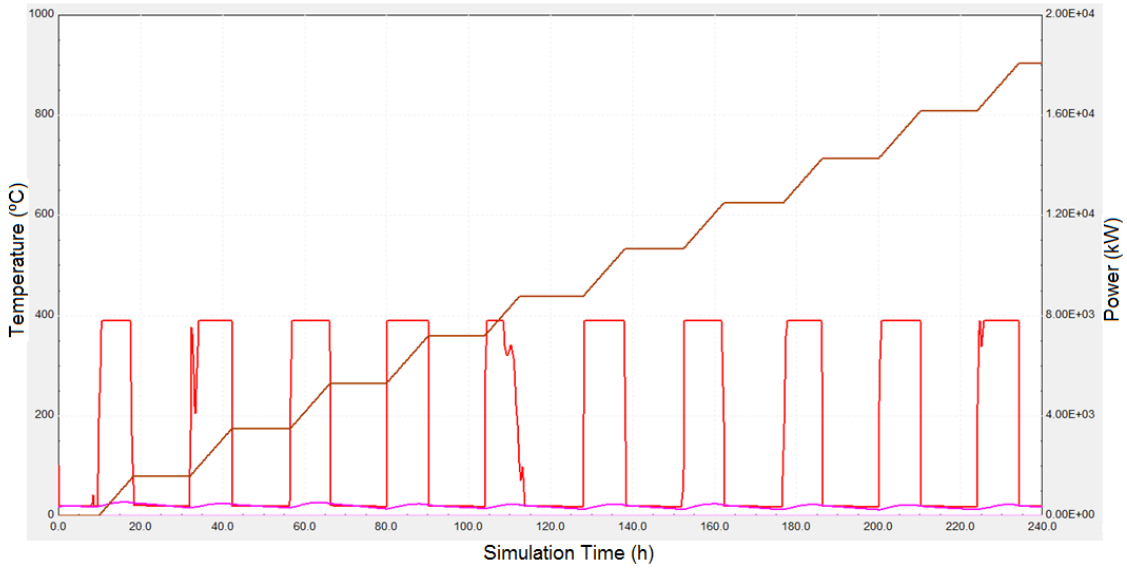


**Figure 80:** Desalination plant electric pump demand

In this graph, the sum of powers that the pumps consume is plotted out as a brown line. The vertical right axis indicates the value in kW. The x-axis is for time (hours) and the left vertical one is in ºC. It is for the red line, which indicates the HTF's temperature. It is an indicator of day and night. We can observe that the average power is between 1700kW and 1900kW, coherent with what explained above. The stretches where the line is horizontal indicates that the pumps are not working because there is no sun anymore.

### 7.4.3 Recirculation

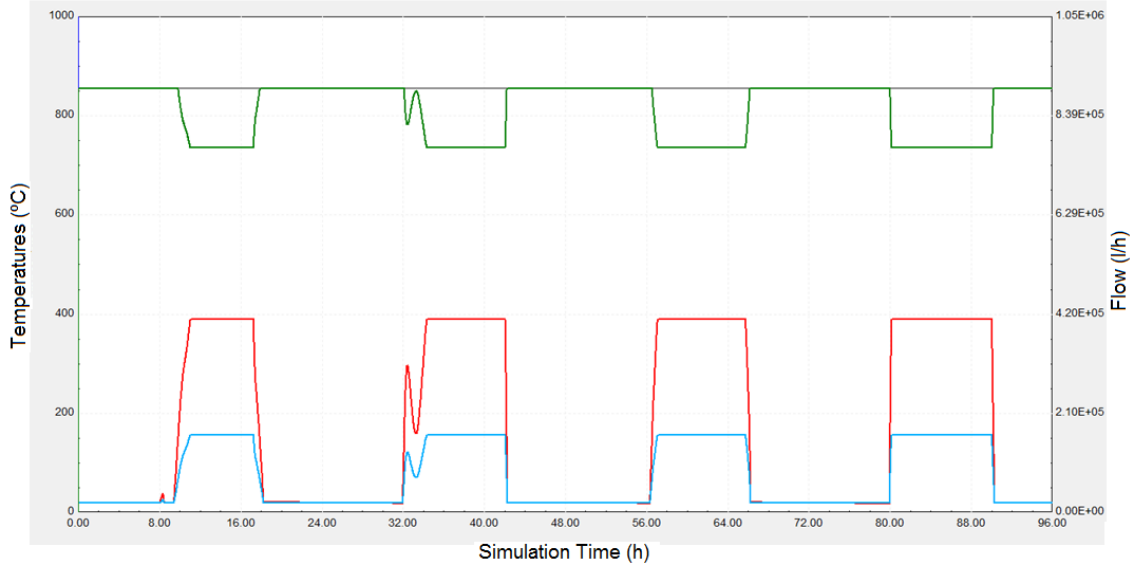


**Figure 81:** Desalination recirculation flow

In the previous graph, the new addition is the symbolization of the recirculation process. It is represented by the dark green line and the grey line above. As we have mentioned, the proportional controller only permits passing the inlet flow with a greater than 0 quality. The rest of the flow is recirculated to achieve further heating of it. This recirculation flow must be subtracted from the incoming seawater flow moved by the "main flow pump" in order to not have excess water in forced into the system circuits. So, the grey line represents the total flow of seawater that is circulating in the system, and the green line indicates the inlet seawater that the main flow pump impulses in from the ocean. Therefore, when there is recirculation, the amount of recirculated flow coincides with the amount that is subtracted from this inlet flow. When the green line decreases is when it is taking place. The right vertical axis is the one these values are referenced to. The units are l/h. The total flow is $891.555\,\frac{l}{h}$, calculated in section 3.2.1.

### 7.4.4 Thermodynamic parameters

In the following graph, key thermodynamic parameters previously discussed are included. In the upper section of the graph there is a legend included:

-tempVap1: it is the temperature of the vapor created in stage 1. It is 99,63ºC.
-tempVap2: it is the temperature of the vapor created in stage 2. It is 73,86ºC.
-tempVap3: it is the temperature of the vapor created in stage 1. It is 38,86ºC.

-LiqTempIn: it is the temperature of the seawater flow in the beginning of the distillation process. It is 99,63ºC. The temperature during the night obviously shows a decrease. It indicates it reaches approximately 19ºC. It is directly correlated with the ambient temperature.
-LiqTempOut: it is the temperature of the seawater flow at the end of the process. It is 38,86ºC.

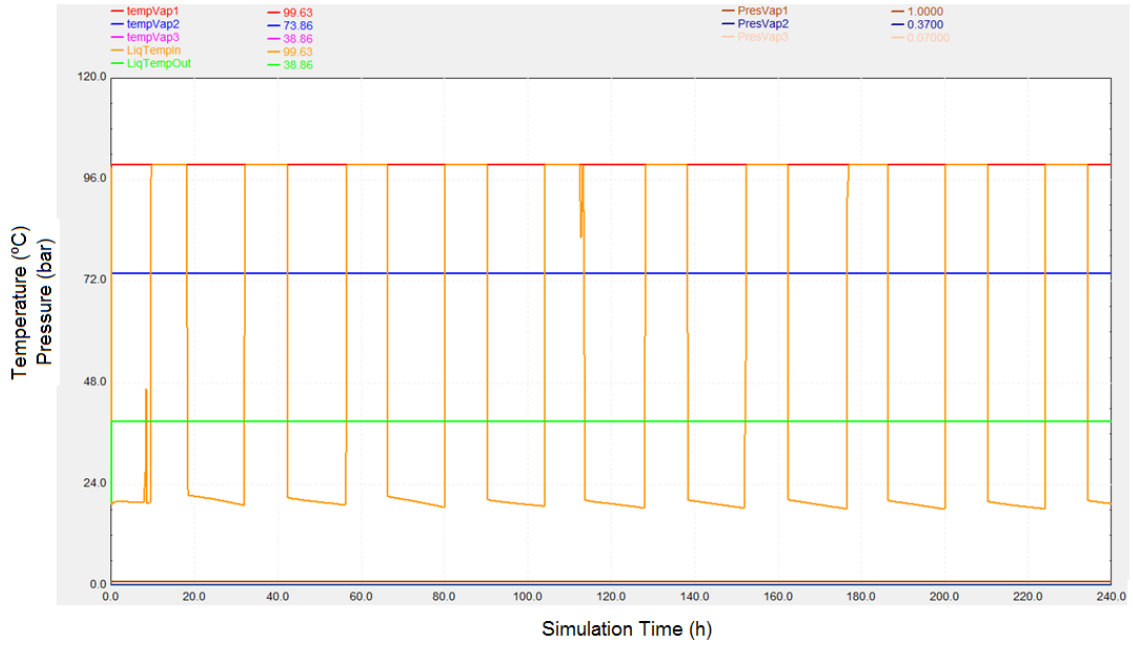


**Figure 82:** Desalination plant parameters

-PresVap1: It indicates the pressure the destilled water has in stage 1. It is of 1bar.

-PresVap2: It indicates the pressure the destilled water has in stage 1. It is of 0,37bar.

-PresVap3: It indicates the pressure the destilled water has in stage 1. It is of 0,07bar.

These pressure values serve in a way to observe how the different chambers (at different pressures) have been emulated.

## 7.5 STORAGE

The same as we designed a thermal storage sub-system for the Rankine cycle in order to work at night and in low beam radiation moments during the day, it is clear that some sort of storage for the MSF plant will be needed in order to face moments where the amount of processed seawater decreases due to adverse weather conditions. The advantage is that it is not necessary to implement an energy storage facility. It is much easier to simply store purified water instead of energy. For that, we should install the adequate water tanks.

The key parameter of the tank, aside from the materials used and the placement, is of course the volume capacity. In order to have an idea of which storage volume we will need, the following graph has been included where we can see the behavior of the MSF plant throughout the whole year:

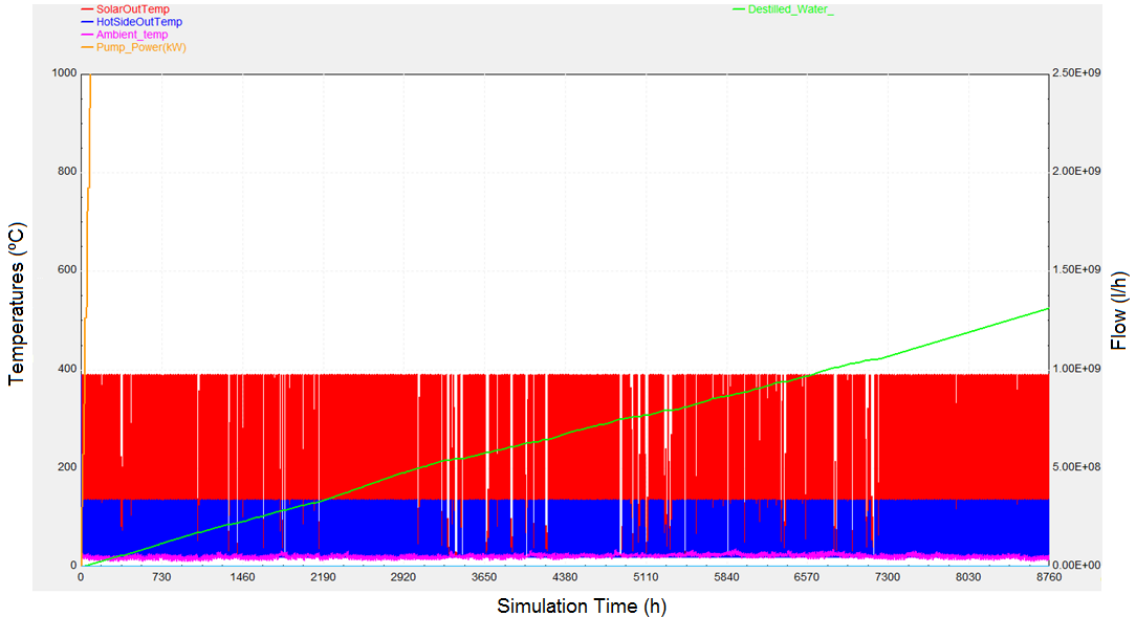


**Figure 83:** Yearly convergence of desalination plant simulation

One can appreciate that there are moments throughout the year where the solar beam radiation is lower, thus limiting the distillation process. The worst case is represented in the following zoom-in:

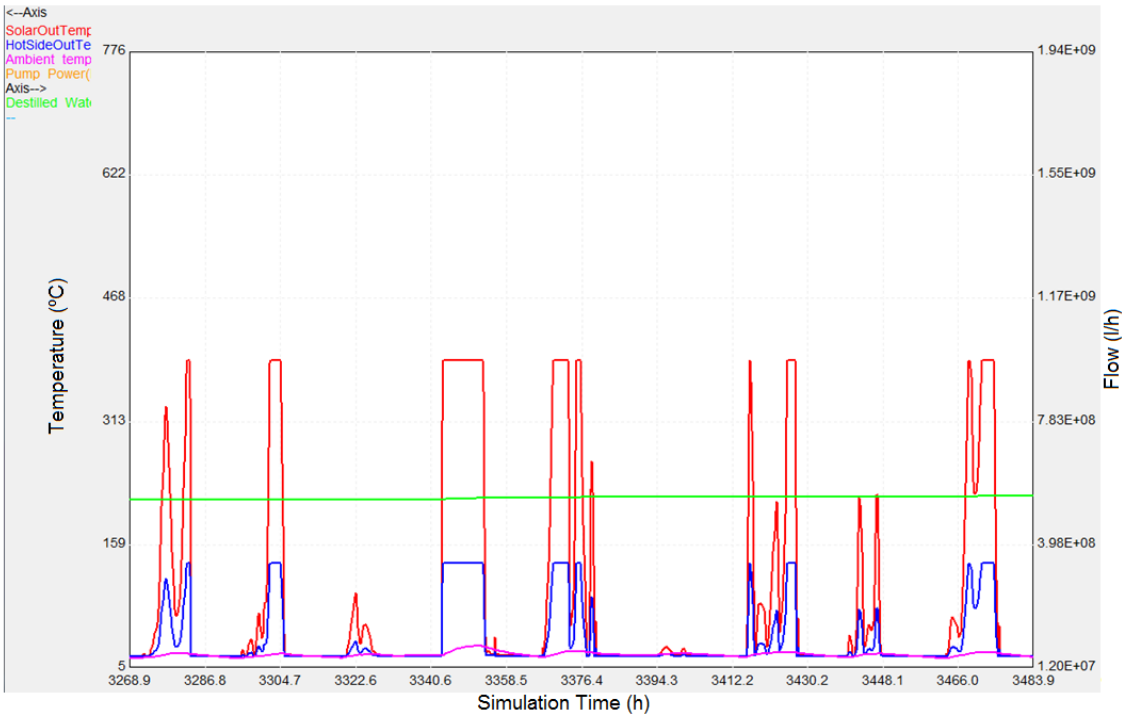


**Figure 84:** Bad weather week

The green line refers to distilled water. The red to HTF outlet temperature (directly related to the beam radiation received). The human consumption per day was estimated as 3.000.000 l/day.

It is a 9 day period in which $13{,}54 \cdot 10^6$ l are gathered. This means that on average we distill only 1,504,444 l/day. From the $3 \cdot 10^6$l needed, we will need 1.495.556 l/day more. This in the 9 day period adds up to $13{,}46 \cdot 10^3 m^3$. This volume, if to be contained in a spherical tank, would mean that the radius of the tank would be:

$$R = \sqrt[3]{13{,}46 \cdot 10^3 m^3 \cdot \frac{3}{4}\pi} = 14{,}76m \approx 15m \qquad (7.5)$$

## 7.6 COGENERATION

In order to minimize cost and to augment the global system efficiency, the MSF process can be coupled to the power plant, which can supply low grade steam. In any case, the steam used by a MSF plant could be used to generate more electrical power. By tapping of this steam at a higher temperature than necessary, the power output of the power station is reduced. Therefore, the need for detailed thermodynamic analysis is thus quite evident in order to get a detailed understanding of the process and search for optimal process irreversibility.

Coupling of MSF process with power generation system has greatly contributed in reducing energy requirement by about 50% or more compared to single purpose desalination plants using the same kind of energy source, but it is still considered as an energy intensive process.

In any case, another possibility to be contemplated is using the heat extracted in the condenser of the Rankine cycle to preheat the inlet seawater from the MSF plant. Currently, the condenser is cooled directly with the ocean water nearby, considered a constant cold temperature reservoir (T≈20ºC).

$$\dot{Q}_{condenser} = \dot{m}_{(1-y)}(h_3 - h_4) = 336MW \quad (7.6)$$

## 7.7 CONCLUSION

The model developed in TRNSYS is a simplification of what the complete real MSF plant would be. In any case, it serves to achieve a general idea and gain an orientation of what values we are working with. The main key parameters are displayed, and the theoretical technical viability of the solar MSF desalination plant is proven. The site chosen to implement the system is the ideal to achieve success; beside the ocean and in a highly solar irradiated area.

In any case, solar MSF (as well as solar MED) are not mature technologies and especially with the large water demand our system requires, it cannot yet be considered fully proven technologies (22).

Once again, to develop a more steady simulation of an MSF, specific programming is required. A team of people should design each separate component individually, based on the complete MSF detailed process, and assure that all interconnections between these components are compatible, thus achieving successful compilations.

# 8. CONCLUSIONS

After displaying all the different existing technologies available that could be used to carry out the project of energy and water supply of the specific housing estate, the most efficient combination of options was selected in order to try to ensure maximum performance. The idea behind the choices taken is to ensure an autarkic system as much as possible, a system that is able to run independently and exclusively on solar energy. This would reinforce the use of technologies that permit a more sustainable development and would also comply with the "*Kyoto Protocol*" and the *cero emission* politics.

For the electric generation, a *solar energy generation system* (SEGS) was selected. The model developed consists of a solar trough field connected to a standard *Rankine cycle power plant*. The heat transfer fluid (thermal oil) that runs through the troughs heats the Rankine working fluid thus generating steam which will propel the turbine blades. Linked to this system is a *thermal concrete storage* sub-system that stores heat in order to ensure 24 hours per day operability of the power cycle despite low or non-existent solar radiation. The result of this model is that during the day, maximum power is obtained from the 2-stage turbine and during the night, there is a power generation decreases in approximately 35%, which is apt considering that this is the difference between average electric demand during the day and during the night.

For the supply of water, it has been chosen to build a desalination plant; more specifically, a *solar multi-stage flash* desalination plant. The main energy source that is required for the plant to function is thermal energy, which will be obtained also from a *solar trough field*. A water storage tank will serve as a solution to low radiation problems and/or nocturnal water consumption. The system is able to distill 4.012.000 l/day using a solar surface of 136.806$m^2$.

The TRNSYS simulation models developed to analyze the behavior of such layout have been successful on a general level. They have proven the theoretical technical viability on a first approach. In any case, greater detail and precision would be required to settle these system choices and particular designs as truly legitimate ones. In order to do so, more in depth knowledge of the simulation program, more time and a greater work force would be needed. Programming of specific components to be used in the systems would be highly advisable, thus using the unique and powerful open source option available in TRNSYS.

# BIBLIOGRAPHY


(1) **[Online]**http://stable.toolserver.org/geohack/geohack.php?pagename=Dakhla&language=fr&params=23_43_N_15_57_W_

(2) **[Online] World Health Organization. URL:** http://www.who.int/water_sanitation_health/

(3) **[Online]** http://www.eapv.org/ordena.terri.golf.general.htm

(4) Wilf, Mark: "Economics of Desalination", 1991.

(5) **[Online] ENCODEX 2008 URL:** www.encodex.com

(6) Daikin Product Manual: "TXR42E URURUSARARA: 1,05Kw. Saunvier Duval SDH 12-050 NW: 1,51kW"

(7) **[Online]** Núñez-Cacho del Águila, Juan: "Energy Management in Hotels" (Gestión Energética en Hoteles), Madrid, 2005. **URL:** www.madrid.org/caeem

(8) **[Online]** Peñarroya Real Estate Company. **URL:**http://www.hosteltur.com/noticias/7281_espana-inmobiliaria-penarroya-comienza-construir-costa-sol-mayor-complejo-hotelero-dotado-10255-camas.html)

(9) Duffie, J.A., and W.A. Beckman; Solar Engineering of Thermal Processes; J. Wiley and Sons, 1991.

(10) De Winter, Francis:"Solar Collectors, Energy Storage and Materials", Massachusetts: The MIT Press 1990.

(11) TRNSYS v.16.1 User Documentation

(12) **[Online]** Patnode, Angela: "Simulation and Performance Evaluation of Parabolic Trough Solar Power Plants", University of Wisconsin, Madison, 2006. **URL:** http://minds.wisconsin.edu/handle/1793/7590

(13) **[Online]** Scott A. Jones: "TRNSYS Modeling of the SEGS VI Parabolic Trough Solar Electric Generating System", Sandia national Laboratories, 2001. **URL:** http://sel.me.wisc.edu/trnsys/trnlib/stec/jones_et_al.pdf

(14) Incropera, DeWitt: "Fundamentals of Heat and Mass Transfer", 6th edition, 2004

(15) **[Online]** Roberto Borsani, Silvio Rebagliati: "Fundamentals and Costing of MSF Desalination Plants and Comparison with Other Technologies", European Desalination Society, 2005.**URL:** http://www.sciencedirect.com/science?_ob=ArticleURL&_udi=B6TFX-4HGS940-6&_user=103677&_rdoc=1&_fmt=&_orig=search&_sort=d&view=c&_acct=C000007978&_version=1&_urlVersion=0&_userid=103677&md5=f195cc5a69565df74ecdae48006fb2f8

(16) **[Online]** http://www.brighthub.com/engineering/mechanical/articles/29621.aspx

(17) **[Online] California Energy Comission. URL:** http://www.owue.water.ca.gov/recycle/desal/Docs/UnitCostDesalination.pdf

(18) **[Online]** Darwish, M.A: "On electric power and desalted water production in Kuwait", Department of Mechanical Engineering, Kuwait University, 2001.**URL:** http://www.sciencedirect.com/science?_ob=ArticleURL&_udi=B6TFX-44BNGN9-Y&_user=103677&_rdoc=1&_fmt=&_orig=search&_sort=d&view=c&_acct=C000007978&_version=1&_urlVersion=0&_userid=103677&md5=2bcd101b670bfb94fb5ca85750a0bf9b

(19) [**Online**] Sommariva,C; Borsani,R.:"Reduction of power requirements for MSF desalination plants: The example of Al Taweelah", Annual Meeting of the European Desalination Society Nº2, .Genova, Italy, 1997. **URL:**http://www.sciencedirect.com/science?_ob=MImg&_imagekey=B6TFX-3VXRTDN-5-1&_cdi=5238&_user=103677&_orig=search&_coverDate=02%2F28%2F1997&_sk=998919998&view=c&wchp=dGLzVtz-zSkWz&md5=b0ac53b60fcf58ec587349914505a6ca&ie=/sdarticle.pdf

(20) **[Online]** Gambier, Adrian:"Dynamic Modeling of a Single-Stage MSF Plant for Advanced Control Purposes", IEEE Conference on Control Applications, 2005. **URL:**http://ieeexplore.ieee.org/stamp/stamp.jsp?arnumber=01507206

(21) **[Online]** Hazim Mohameed Qiblawey, Fawzi Banat: "Solar Thermal Desalination Technologies", European Desalination Society Congress, 2007. **URL :** http://www.desline.com/articoli/8947.pdf

(22) Huang, Francis F:"Engineering Thermodynamics. Fundamentals and Applications", Macmillan Publishing Co., Inc., New York, 1976.

(23) Moran, J., Shapiro, N.M: "Fundamentals of Engineering Thermodynamics",5th ed., Wiley, 2006.

(24) "A TRNSYS Model Library for Solar Thermal Electric Components (STEC) Reference Manual Release 3.0 November 2006. Last Update: November 2007.

(25) Patel, Mukund: "Wind and solar power systems", Boca Raton London New York Washington, D.C.: CRC Press. ISBN 0-8493-1605-7. (1999), **URL:** http://books.google.com/books?id=8aQDw14fQnkC

(26) "Environmental Impact Assessment Process Proposed Concentrating Solar Power (Csp) Plant and Associated Infrastructure in the Northern Cape Area", Briefing Paper, March 2006". **URL:** http://www.docstoc.com/docs/3571288/ENVIRONMENTAL-IMPACT-ASSESSMENT-PROCESS-PROPOSED-CONCENTRATING-SOLAR-POWER-CSP-PLANT

(27) **[Online]** TWIKI E302 web (future knowledge base of the Institute for Thermodynamics and Energy Conversion, Technical University of Wien). **URL**:

http://e302peac1.ite.tuwien.ac.at/twiki/bin/view/E302/SeminarITEWS2007
http://e302peac1.ite.tuwien.ac.at/twiki/bin/view/E302/SeminarITESS2008

(28) **[Online]** Journal of Solar Engineering and American Society. **URL:** http://scitation.aip.org/getabs/servlet/GetabsServlet?prog=normal&id=JSEEDO000124000002000153000001&idtype=cvips&gifs=yes

(29) **[Online]** Solar Millenium AG. **URL:** http://www.solarmillennium.de/upload/pdf/PM_SMAG_AS1_Salzspeicher_en_finalVersion.pdf

(30) **[Online]** Osman A. Hamed, Mohammad AK. Al-Sofi, Monazir Imam, G. M. Mustafa, Khalid Bamardouf and Hamad Al-Washmi**: "**Simulation of Multistage Flash Desalination Process", Saline Water Conversion Corporation. **URL:** http://www.swcc.gov.sa/files%5Cassets%5CResearch%5CTechnical%20Papers%5CThermal/SIMULATION%20OF%20MULTISTAGE%20FLASH%20DESALINATION%20PROCESS.....10.pdf

(31) **[Online]** D. Alarcón, J. Blanco, E. Zarza, S. Malato, J. León: **"**Comparación Económica de Procesos de Desalación de Agua de Mar: El Reto de la Destilación Multi-Efecto con Energía Solar", CIEMAT – PSA. **URL:** http://www.psa.es/webeng/aquasol/files/Congresos/Alarcon%20-%20Congreso%20Iberico%20(04.11.2002).pdf

(32) **[Online]** Elrod, Scott:**"**Solar Concentrators", Palo Alto Research Center. **URL:** http://e302peac1.ite.tuwien.ac.at/twiki/bin/viewfile/E302/ParabolicTrough?rev=1;filename=Solar_Concentrators.pdf

(33) **[Online]** Shaobo Hou, Zhongjin Zhang, Zhongzhou Huang, Aixia Xie:"Performance Optimization of Solar Multi-Stage Flash Desalination Process Using Pinch Technology", College of Engineering, Guangdong Ocean University, China,School of Aeroengine and Thermal Power Engineering, Northwestern Polytechnical University,China, 2007. **URL:** http://www.desline.com/articoli/8934.pdf

(34) **[Online]** "Seawater and Brackish Water Desalination in the Middle East, North Africa and Central Asia. A Review of Key issues and Experience in Six Countries", 2004. **URL:** http://web.worldbank.org/external/projects/main?pagePK=64817132&piPK=64817141&theSitePK=40941&menuPK=51521783&%09&conceptattcode=Cyprus~82634&pathtreeid=COUNT&displayOrder=DOCNA,DOCDT,REPNB,DOCTY&sortattcode=REPNB%20Asc&showattributesDOCNA,DOCDT,REPNB,DOCTY&startPoint=1&pageSize=50

(35) **[Online]** Narmine H. Aly, Adel K. El-Fiqi **:"**Mechanical Vapor Compression Desalination Systems – a Case Study", 2003. **URL:** http://www.desline.com/articoli/5175.pdf

(36) **[Online]** Department of Energy, Energy efficiency and Renewable Energy. URL: http://www.eere.energy.gov/
http://www1.eere.energy.gov/solar/sh_basics_collectors.html#flatplate
http://www1.eere.energy.gov/solar/sh_basics_collectors.html#evacuatedtube

http://www1.eere.energy.gov/solar/sh_basics_collectors.html#evacuatedtube
http://www1.eere.energy.gov/solar/dish_engine_rnd.html
http://www1.eere.energy.gov/solar/photoelectric_effect.html
http://www1.eere.energy.gov/solar/thermal_storage.html
http://www1.eere.energy.gov/solar/power_towers.html

(37) **[Online]** National Renewable Energy Laboratory. URL: http://www.nrel.gov/csp/troughnet/thermal_energy_storage.html

(38) **[Online]** http://www.livingstone.qld.gov.au/commser/watersupply/8.pdf

(39) **[Online]** http://solar1.mech.unsw.edu.au/glm/papers/Morrison_Aus_China2006.pdf

(40) **[Online]** http://www.newsociety.com/titleimages/pv_ch1.pdf

(41) **[Online]** http://www.flasolar.com/active_dhw_flat_plate.htm

(42) **[Online]** http://www.clairvoyantenergy.com/energy-works.html

(43) **[Online]** http://e302peac1.ite.tuwien.ac.at/twiki/bin/view/E302/DishStirling

(44) **[Online]** http://www.greenoptimistic.com/2009/02/22/how-to-use-solar-energy-at-night-or-during-rainy-days/

(45) **[Online]** http://technology4life.wordpress.com/

(46) **[Online]** http://www.greentechgazette.com/

(47) **[Online]** http://en.wikipedia.org/wiki/Vapor-compression_desalination

(48) **[Online]** http://en.wikipedia.org/wiki/Desalination

(49) **[Online]** http://en.wikipedia.org/wiki/Parabolic_trough

(50) **[Online]** http://en.wikipedia.org/wiki/Photovoltaics#Disadvantages

(51) **[Online]** http://en.wikipedia.org/wiki/User:Adacore/Solar_Energy

(52) **[Online]** http://en.wikipedia.org/wiki/Vapor-compression_desalination

(53) **[Online]** http://en.wikipedia.org/wiki/Reverse_osmosis#Drinking_water_purification

(54) **[Online]** http://en.wikipedia.org/wiki/Electrodialysis

(55) **[Online]** http://www.hosteltur.com/noticias/7281_espana-inmobiliaria-penarroya-comienza-construir-costa-sol-mayor-complejo-hotelero-dotado-10255-camas.htmlhttp://en.wikipedia.org/wiki/Thermal_energy_storage#Molten_salt_technology

(56) **[Online]** http://www.entropie.com/en/services/desalination/MED/

(57) **[Online]** http://www.oas.org/dsd/publications/Unit/oea59e/ch20.htm

(58) **[Online]** http://www.trec-uk.org.uk/images/kramer-junction_large.jpg

(59) **[Online]** http://ludb.clui.org/ex/i/CA9679/

(60) **[Online]** http://www.docstoc.com/docs/4992331/concentrated-solar

(61) **[Online]** http://www.sasakura.co.jp/e/products/water/106.html

(62) **[Online]** http://www.brighthub.com/engineering/mechanical/articles/29621.aspx

(63) **[Online]** http://www.owue.water.ca.gov/recycle/desal/Docs/UnitCostDesalination.pdf

(64) **[Online]** http://www.sciencedirect.com/science?_ob=MImg&_imagekey=B6TFX-3VXRTDN-5-1&_cdi=5238&_user=103677&_orig=search&_coverDate=02%2F28%2F1997&_sk=998919998&view=c&wchp=dGLzVtz-zSkWz&md5=b0ac53b60fcf58ec587349914505a6ca&ie=/sdarticle.pdf

(65) **[Online]** http://ieeexplore.ieee.org/stamp/stamp.jsp?arnumber=01507206

# BIBLIOGRAPHY OF FIGURES AND IMAGES:


[1] **[Online]** http://www.powerfromthesun.net/Chapter6/Chapter6.htm

[2] **[Online]** U.S. Department of Energy. URL: http://www1.eere.energy.gov/solar/sh_basics_collectors.html#flatplate

[3] **[Online]** http://www.viessmann.es/es/products/Solar-Systeme/Vitosol_200.html

[4] **[Online]** http://www.daviddarling.info/encyclopedia/BAE_batch_heater.html

[5] **[Online]** http://beyondzeroemissions.org/files/tech/trough_diagram.gif

[6] **[Online]**http://thefraserdomain.typepad.com/photos/uncategorized/solargenix_trough_frame .jpg

[7] http://www.clairvoyantenergy.com/images/Parabolic-Concentrators.jpg

[8] Photo Source: Solol UVAC, 2004

[9] **[Online]** http://www.greenoptimistic.com/wp-content/uploads/2009/02/power-tower2-300x300.jpg

[10]**[Online]** http://www1.eere.energy.gov/solar/power_towers.html

[11]**[Online]**Twiki. URL: http://e302peac1.ite.tuwien.ac.at/twiki/bin/view/E302/DishStirling

[12]**[Online]** US Department of Energy. URL: http://www1.eere.energy.gov/solar/dish_engines.html

[13]**[Online]** TWiki http://e302peac1.ite.tuwien.ac.at/twiki/bin/view/E302/FresnellMirrorConcentrator

[14]**[Online]** TWiki. URL: http://e302peac1.ite.tuwien.ac.at/twiki/bin/view/E302/FresnellMirrorConcentrator

[15]http://farm4.static.flickr.com/3289/2922575338_aaf36e96ba.jpg

[16]**[Online]** TWiki. URL: http://e302peac1.ite.tuwien.ac.at/twiki/bin/view/E302/FresnellMirrorConcentrator#LiteratureSources

[17]**[Online]** Wikipedia. URL: http://upload.wikimedia.org/wikipedia/commons/thumb/4/45/Giant_photovoltaic_array.jpg/300px-Giant_photovoltaic_array.jpg

[18]http://technology4life.wordpress.com/

[19]http://www.greentechgazette.com/

[20]National Renewable Energy Laboratory

[21]Flagsol. URL: http://www.nrel.gov/csp/troughnet/thermal_energy_storage.html

[22]National Renewable Energy Laboratory
URL:http://www.nrel.gov/csp/troughnet/thermal_energy_storage.html

[23] Sandia national Laboratories. URL:
http://www.nrel.gov/csp/troughnet/thermal_energy_storage.html?print

[24]National Renewable Energy Laboratory URL:
http://www.nrel.gov/csp/troughnet/thermal_energy_storage.html?print

[25]http://newenergydirection.com/blog/wp-content/uploads/2008/12/parabolic_trough_storage_png.png

[26]**[Online]** TWiki. URL:
http://e302peac1.ite.tuwien.ac.at/twiki/bin/view/E302/SeawaterDesalinationVerdampfung

[27]**[Online]** http://www.unep.or.jp/ietc/Publications/techpublications/TechPub-8d/F80122.gif

[28]**[Online]** http://www.unep.or.jp/ietc/Publications/techpublications/TechPub-8d/F80122.gif

[29]**[Online]** PDF: http://www.livingstone.qld.gov.au/commser/watersupply/8.pdf

[30]**[Online]** PDF: http://www.psa.es/webeng/aquasol/files/Congresos/Alarcon%20-%20Congreso%20Iberico%20(04.11.2002).pdf

[31]**[Online]** PDF:
http://e302peac1.ite.tuwien.ac.at/twiki/pub/E302/SeawaterDesalinationVerdampfung/Desal_mainreport-Final2.pdf

[32]**[Online]** TWiki. PDF:
http://e302peac1.ite.tuwien.ac.at/twiki/pub/E302/SeawaterDesalinationVerdampfung/Desal_mainreport-Final2.pdf

[33] **[Online]** Wikipedia URL:
http://en.wikipedia.org/wiki/File:Reverse_osmosis_membrane_coil.jpg

[34]**[Online]** PDF: http://www.livingstone.qld.gov.au/commser/watersupply/8.pdf

[35]**[Online]** http://en.wikipedia.org/wiki/File:Edprinc.jpg

[36] Red Eléctrica de España. URL: http://www.ree.es/operacion/curvas_demanda.asp

[37]**[Online]** http://www.trec-uk.org.uk/images/kramer-junction_large.jpg

[38]PDF: “Simulation and Performance Evaluation of Parabolic Trough Solar Power Plants”, Patnode, Angela, 2006

[39]TRNSYS v.16.1 User Documentation

[40]Modified from “Fundamentals of Engineering Thermodynamics”, Moran, J., Shapiro, N.M., -5th ed. -2006 – Wiley

[41]“Fundamentals of Heat and Mass Transfer”, Incropera, DeWitt, 6th edition, 2004.

[42]**[Online]** http://www.docstoc.com/docs/4992331/concentrated-solar

[43]Example taken from “A TRNSYS Model Library for Solar Thermal Electric Components (STEC) Reference Manual Release 3.0 November 2006. Last Update: November 2007.”

[44]**[Online]** http://www.sasakura.co.jp/e/products/water/106.html

[45]**[Online]** http://www.ehponline.org/docs/2000/108-2/innovationsfig2B.GIF

# APPENDIX A

Calculations of UA [W/K]

### 9. *Steam Generator* (from point 8 to 9):

$$\dot{Q}_{steam} = \dot{m}_{steam} \cdot \left(h_{in,steam} - h_{out,steam}\right) = 253\frac{kg}{s} \cdot (2725{,}51 - 1407{,}81) = 333{,}38MW$$

$$\dot{Q}_{HTF} = \dot{m}_{HTF} \cdot C_{HTF} \cdot \left(T_{in,HTF} - T_{out,HTF}\right) = 2286\frac{kg}{s} \cdot 2{,}6 \cdot (377 - 311) = 392{,}18MW$$

We consider $\dot{m}_{HTF} = 2286\frac{kg}{s}$ [5]

$C_C \to \infty$

$$C_H = \dot{m}_{HTF} \cdot C_{HTF} = 2286\frac{kg}{s} \cdot \frac{2{,}6kJ}{kg \cdot K} = 5943{,}6\ kW/K$$

$$C_{min} = MIN(C_C, C_H) = C_H$$

$$\dot{Q}_{max} = C_{min}\left(T_{HTF,in} - T_{steam,in}\right) = 5943{,}6 \cdot (377 - 311) = 392{,}21kW$$

$$\varepsilon_{steam} = \frac{\dot{Q}_{steam}}{\dot{Q}_{max}} = \frac{333{,}38}{392{,}21} = 0{,}85$$

$$C_r = \frac{C_{min}}{C_{max}} = 0$$

$$\varepsilon_{steam} = 1 - \exp(-NTU_{steam}) \rightarrow NTU_{steam} = 1{,}89$$

$UA_{steam\ generator}$=11230 kW/K

### 10. *Preheater* (from point 7 to 8):

$$\dot{Q}_{steam} = \dot{m}_{steam} \cdot \left(h_{in,steam} - h_{out,steam}\right) = 75141kW$$

$$\dot{Q}_{HTF} = \dot{m}_{HTF} \cdot \left(T_{in,HTF} - T_{out,HTF}\right) = 2286\frac{kg}{s} \cdot (377 - 311) = 308984kW$$

$$C_C = 1366{,}2\frac{kW}{K}$$

[5] According to the data obtained from different existing SEGS (ex. SEGS VI, Kramer Junction), the HTF (thermal oil) is slightly less than ten times more than the water flow.

$$C_H = \dot{m}_{HTF} \cdot C_{HTF} = 5943{,}6\ kW/K$$

$$C_r = \frac{C_{min}}{C_{max}} = 0{,}23$$

$$\dot{Q}_{max} = C_{min}\left(T_{HTF,in} - T_{steam\ ,in}\right) = 84692kW$$

$$\varepsilon_{steam} = \frac{\dot{Q}_{steam}}{\dot{Q}_{max}} = 0{,}89$$

With $\begin{cases} \varepsilon_{steam} = 0{,}89 \\ C_r = 0{,}23 \end{cases}$, we go into the following graph and obtain NTU:

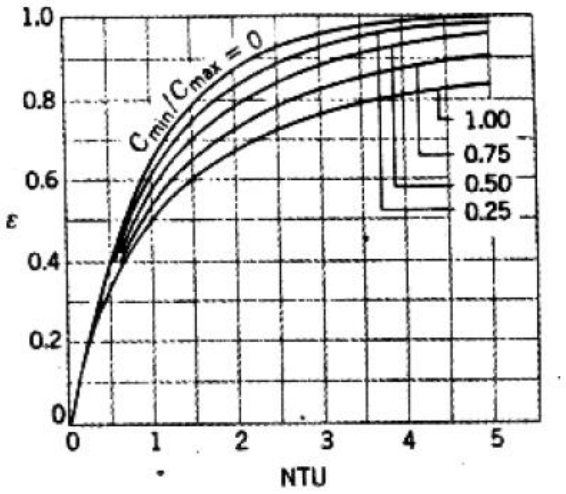


**Figure 59: Effectiveness for cross-flow heat exchangers [41]**

Also, we can work the value out from this expression:

$$\varepsilon = \frac{1-\exp\left[-NTU\cdot\left(1-C_r\right)\right]}{1-C_r\cdot\exp\left[-NTU\cdot\left(1-C_r\right)\right]}$$

$NTU_{steam}$=4

$UA_{preheater}$=5464 kW/K

***11. Superheater* (from point 9 to 1):**

$$\dot{Q}_{steam} = \dot{m}_{steam} \cdot \left(h_{in,steam} - h_{out\ ,steam}\right) = 85241\frac{kW}{K}$$

$$C_C = 1077 \frac{kW}{K}$$

$$C_H = 5943{,}6\ kW/K$$

$$C_r = \frac{C_{min}}{C_{max}} = 0{,}18$$

$$\dot{Q}_{max} = 85311{,}6\ kW$$

$$\varepsilon_{steam} = \frac{\dot{Q}_{steam}}{\dot{Q}_{max}} = 0{,}98$$

With $\begin{cases} \varepsilon_{steam} = 0{,}98 \\ C_r = 0{,}18 \end{cases}$, we go into the following graph and obtain NTU:

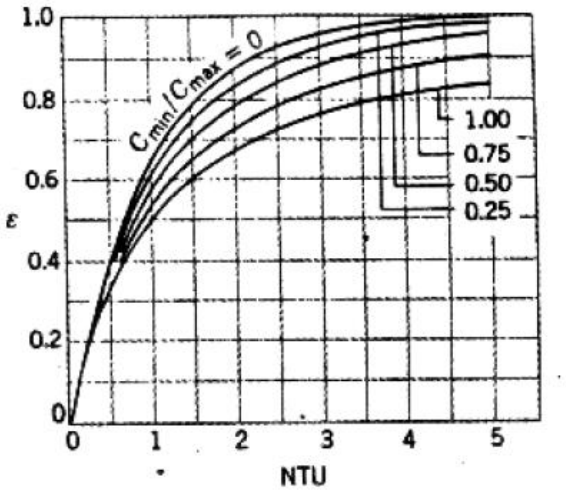


**Figure 60: Effectiveness for cross-flow heat exchangers [41]**

$NTU_{steam}$=4,8

$UA_{superheater}$=5169,6 kW/K

# APPENDIX B

The TRNSYS types used in the Rankine power cycle used are included in this appendix.
They are available in the following .pdf file, “A TRNSYS Model Library for Solar Thermal Electric Components (STEC)”

http://sel.me.wisc.edu/trnsys/trnlib/stec/stec_refguide_v3.0.pdf